Development of a Thermal Regulation Response Simulation Model for Human Infants

by
Alida Fanfoni

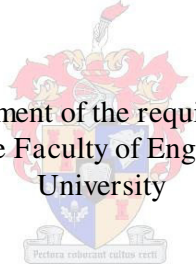

Thesis presented in fulfilment of the requirements for the degree of Master of Science in the Faculty of Engineering at Stellenbosch University

Supervisor: Mr Robert T Dobson

Department of Mechanical and Mechatronic Engineering

December 2014

Declaration

By submitting this thesis electronically, I declare that the entirety of the work contained therein is my own, original work, that I am the sole author thereof (save to the extent explicitly otherwise stated), that reproduction and publication thereof by Stellenbosch University will not infringe any third party rights and that I have not previously in its entirety or in part submitted it for obtaining any qualification.

December 2014

Abstract

The thermal regulation response of a neonate has to maintain temperature homeostasis, thus resisting the changes to core temperature caused by the unstable external environment. In this thesis a theoretical thermal regulation response model for human infants subject to a well-defined environment is presented. This model will aid in understanding the influences of environmental effects on core and skin temperature. The respiratory system was also included in the thermal regulation response model.

A literature study was undertaken emphasising thermal regulation of neonates. The blood circulation system, skin tissue physiology and the respiratory system physiology were reviewed and helped to provide a better understanding of the thermal regulation mechanisms and how heat transfer theory can be used to analyse heat loss in neonates. The thermal heat transfer properties of skin tissue was specified and used in the development of the theoretical simulation model. The bioheat equation developed by Pennes was reviewed as well as a mathematical model developed by Fiala et al.

The theoretical model was developed by applying the conservation of energy and the applicable properties to one dimensional layers to generate a set of time dependent differential equations. The set of equations was solved using an explicit numerical finite difference method, given the initial conditions. The mathematical model included heat loss through the skin, heat loss through the respiratory system, as well as the effect of environments (in incubator or in a bassinette) with different temperatures, relative humidity's and air velocities. Clothing was also incorporated.

A clinical trial was conducted to facilitate a better understanding of thermal stability in neonates. The data acquired during the clinical trial was also used to verify/validate the theoretical simulation model. The results from the simulation temperatures were compared with the average outer skin layer temperature measured during the clinical trial and an average deviation of only 0.22 °C was found, thereby proving that the simulation model gives realistic results.

An experimental respiratory model was designed to simulate the respiratory system and illustrate the functioning thereof with regards to heat transfer. This was done by designing an experimental mechanical lung apparatus. The apparatus was tested and successfully imitated the respiratory system with regards to heat transfer. The results obtained from this experiment indicated that the trachea must be moistened continuously in order to condition inhaled air.

The outcome of this project identified two possible applications. For the first application it can be used as a test tool for quickly evaluating the influence of different environmental conditions in the transient temperature distribution of neonates. The second application would be to enable medical professionals to monitor the influence of the thermal environment, including the temperature, relative humidity and air velocity, on the neonate's temperature change to allow for a speedier thermal intervention strategy.

Uittreksel

Die hitte regulering reaksie van 'n pasgebore baba moet temperatuur homeostase handhaaf, en sodoende die veranderinge aan die kern temperatuur weerstaan wat veroorsaak word deur ‘n onstabiele eksterne omgewing. In hierdie tesis word 'n teoretiese hitte regulerings reaksie model vir menslike babas, onderhewig aan 'n goed-gedefinieerde omgewing, aangebied. Hierdie model sal help met die verstaan van die invloed wat omgewings effekte het op die kern en vel temperatuur. Die respiratoriese sisteem is ook ingesluit in die hitte regulering reaksie model.

'n Literatuurstudie is onderneem met die klem op hitte regulering van pasgebore babas. Die bloed sirkulasie sisteem, vel weefsel fisiologie en die respiratoriese sisteem fisiologie is hersien en help met beter begrip van die hitte regulering meganismes en hoe hitte-oordrag teorie kan gebruik word om hitte verlies in pasgebore babas te analiseer. Die hitte-oordrag eienskappe van vel weefsel is gespesifiseer en word gebruik in die ontwikkeling van die teoretiese simulasie model. Die ‘bioheat’ vergelyking ontwikkel deur Pennes is hersien asook 'n wiskundige model wat ontwikkel is deur Fiala et al.

Die teoretiese model is ontwikkel deur die toepassing van die behoud van energie tesame met die gebruik van toepaslike eienskappe en een dimensionele lae om 'n stel tyd afhanklike differensiaalvergelykings op te wek. Die stel vergelykings is opgelos met behulp van 'n eksplisiete numeriese eindige verskil metode, gegewe die aanvanklike toestande. Die wiskundige model sluit in die hitte verlies deur die vel, hitte verlies deur die respiratoriese stelsel, sowel as die effek van die omgewing (broeikas of in 'n bassinette) met verskillende temperature, relatiewe humiditeit en lug snelhede. Klere is ook in ag geneem.

'n Kliniese proef is gedoen om 'n beter begrip van termiese stabiliteit in pasgebore babas te fasiliteer. Die data wat tydens die kliniese proef verhaal is, is ook gebruik om die die teoretiese simulasie model te verifieer. Die resultate van die simulasie temperature is vergelyk met die gemiddelde buitenste vel laag temperatuur gemeet tydens die kliniese proef en 'n gemiddelde afwyking van slegs 0.22 °C is gevind, wat dus bewys dat die simulasie model realistiese resultate gee.

'n Eksperimentele respiratoriese model is ontwerp om die respiratoriese stelsel te simuleer en die funksionering daarvan te illustreer met betrekking tot hitte-oordrag. Dit is gedoen deur die ontwerp van 'n eksperimentele meganiese long apparaat. Die apparaat is getoets en slaag daarin om die respiratoriese stelsel suksesvol na te boots met betrekking tot hitte-oordrag. Die resultate verkry uit hierdie eksperiment het aangedui dat die tragea kostant klam gemaak moet word om ingeasemde lug te kondisioneer.

Die uitkoms van hierdie projek het twee moontlike toepassings geïdentifiseer. Die eerste is dat dit as 'n toets instrument vir die vinnige evaluering van die invloed van verskillende omgewingsfaktore in die temperatuur verspreiding van pasgebore babas gebruik kan word. Die tweede toepassing sal wees om medici in staat te stel om die invloed van die termiese omgewing te monitor, insluitend die temperatuur, relatiewe humiditeit en lug snelheid, om die neonaat se temperatuur verandering te monitor en voorsiening te maak vir 'n vinniger verwarmings intervensiestrategie.

Acknowledgements

I want to raise acknowledgement here to my support system. It would not have been possible to complete this thesis without the help and support of the kind people around me.

Above all, I would like to thank my supervisor Mr RT Dobson for his unsurpassed knowledge, guidance and great amount of patience. I am extremely thankful for the advice and life guidelines that have been invaluable on a personal and academic level. I am also grateful for the financial support provided for the duration of my thesis.

I would also like to thank Professor J Smith, for his knowledge and medical expertise. I am grateful for the time he made available to assist me in the medical trial that had to be completed.

I would further like to acknowledge and thank the technical support provided by the personel from the Mechanical and Mechatronic Engineering Workshop.

I would like to thank Ryno Marais for his eternal personal support, great amount of patience and extended helping hand, which was never far away.

I would like to thank my mother Petro Fanfoni for the great support system that she has provided throughout the duration of my studies, always listening to my problems and providing me with motivation and encouragement during the tough times and inspiration during the good times.

I would like to acknowledge and thank my father Adolf Fanfoni for the financial support provided for the past years which allowed me to further my education at the university of my choice and never doubting in my capabilities.

TABLE OF CONTENTS

LIST OF FIGURES

LIST OF TABLES

NOMENCLATURE

A	area, m^2
BR	breathing rate, breaths/min
c	specific heat constant, J/kgK
D	diameter, m
D_{AB}	diffusion coefficient
E	energy, J
$\dot{E}$	energy, W
F	form factor
f	clothing factor
g	gravitational acceleration, m/s^2
h	latent heat of vaporization or heat convection coefficient, J/kg
I	intrinsic clothing insulation, W/m^2K
i	moisture permeability index
k	thermal conductivity, W/mK
KE	kinetic energy, J
L	length, m
M	metabolism, W
m	mass, kg
$\dot{m}$	mass flow rate, kg/s
n	decimal percentage value
Nu	nusselt number
P	pressure, Pa
PE	potential energy, J
Pr	prantl number
$\dot{Q}$	heat transfer rate, W
R	thermal resistance, °C/W
Ra	rayleigh number, $Ra = g\beta\, Pr(T_1 - T_2)\, L^3/(\mu/\rho)^2$
Re	reynolds number, $Re = V_a L/(\mu/\rho)$
Sc	schmidt number, $Sc = (\mu/\rho)/D_{AB}$
St	stanton number, $St_{mass} = St_{heat} Pr^{0.67}/Sc_a^{0.67}$, $St_{heat} = Nu_a/Re_a Pr$

t	time, s
T	temperature, °C/K
TV	tidal volume, ml/kg
U	internal energy, J
V	velocity, m/s
W	weight, kg
$\dot{W}$	work energy, W
x	thickness, m

Greek Symbols

β	volume expansivity, 1/K
Δ	change
ε	emissivity
μ	dynamic viscosity, kg/ms
υ	kinematic viscosity (μ/ρ), m^2/s
ρ	density, m^3/kg
σ	Stefan-Boltzmann's constant
ϕ	relative humidity
ω	specific humidity, kg H_2O/kg dry air

Subscripts and Superscripts

a	air
act	actual
art	artery
atm	atmosphere
b, bl	blood
c	convection
$\_c$	cross section
cl	clothing
e	evaporation
f	fluid, fat layer, forced
g	gas, vapour
h	heat

i	incubator
in	direction of flow
inh	inhale
s	skin surface
isl	inner skin layer
m	mass
n	natural
osl	outer skin layer
out	direction of flow
r	room, radiation
tis	tissue
tr	trachea
w	wall

Abbreviations

$NICU$	Neonatal Intensive Care Unit
IC	Indirect Calirometry
ITC	Indirect Thermographic Calirometry

Glossary

Term	Definition
Extrauterine environment	located or occurring outside the uterus
Hypothermia	a condition in which the temperature of your body is very low
Infant	Human infant of 0 to 1 year of age
Intrauterine environment	situated or occurring within the uterus
In vivo	In the living body
In vitro	Outside the living body and in an artificial environment
Neonate	Human infant of 0 to 28 days of age
Preoptic	situated in front of an optic part or region (preoptic tracts in the brain)
Sudomotor	nerve fibers controlling the activity of sweat glands
Vasomotor	nerves or centers controlling the size of blood vessels

(all definitions obtained from Merriam-Webster online dictionary (**Merriam Webster, 2014**))

1 INTRODUCTION

This thesis entails the development of a thermal regulation response simulation model for human infants subject to the instantaneous environment. Thermal regulation response has to be accomplished to maintain homeostasis, in order to resist the effect of changes caused by the external environment. The introduction to this thesis includes some interesting information regarding thermal regulation. The respiratory system is often neglected when analysing thermal response although it also contributes to heat loss. The background on research within this respective field, started during the 1930s, and is briefly reviewed.

The motivation for this project was to help enable doctors to predict skin temperatures in order to better predict the medical outcome of a neonate. The objectives discussed in Section 1.4 are set out to comply with the motivation and support further research in the field of thermal regulation. An outline of the thesis project is given in Section 1.5 which summarises the work done for this project.

1.1 Interesting Information

Homeostasis can be defined as the dynamic consistency of the internal environment and refers to the physiological control processes that must fight the changes, caused by external factors, in order to maintain relatively constant conditions within our body. Core body temperature is a variable that is precisely controlled via thermal regulation and is the most important parameter for maintaining homeostasis within the body (Fox, 2009). The external factors that influence changes in the skin/core temperature include clothing resistance and environmental factors such as temperature, relative humidity and air velocity.

Normal body temperature represents the optimal thermal condition needed to support internal functions, such as the digestive system, respiratory system, blood circulation system etc. (Fox, 2009). Thermoregulatory responses are generated in the hypothalamus and balance heat production through metabolism, to maintain normal core body temperature, which is counterbalanced by heat loss via convection, conduction, radiation and evaporation.

Another aspect of this thesis focuses on the respiratory system of which the lung is the most important organ. The surface area of human lungs is in the order of 70 m^2 and consists of a moist surface. Lungs are significant in that they enable the gas exchange between air and blood, which is induced by the diffusion of oxygen and carbon dioxide across the walls of the alveoli. Inhaled air is conditioned to have exact properties of 37 °C and 100% relative humidity when it reaches the lungs for gas exchange to take place. This system is therefor also an important factor when considering the thermoregulatory system in a human, because of the heat transfer that takes place during inhalation. The part played by the respiratory system in thermal regulation of the body is important when evaluating body homeostasis, especially in neonates.

1.2 Background

During the birth procedure, the infant leaves the constant temperature intrauterine environment, to enter the extrauterine environment. In the extrauterine environment, the thermoregulatory capabilities of the infant must provide for maximum restriction of heat loss to prevent cooling, which can result in hypothermia or death in severe cases. History in the studying of body temperature started during the 1930s to 1940s when physicians said that low body temperature was caused by the incomplete development of the thermoregulatory mechanisms of an infant. Little attention was given to the environmental conditions surrounding the infant (Sinclair, 1978).

Eckstein (1926) and Mordhorst (1932) both came to the same conclusion that thriving infants exhibited two important defects in their physiological responses. These infants were capable of elevating their metabolism when exposed to colder environments. Blackfan (1933) and Yaglou (1933) found an association between the stability of body temperature and lowered mortality in an environment temperature of 25 °C and relative humidity of 65%. They claimed that body temperature was a characteristic of immaturity. Richard Day undertook a landmark calorimetric study during 1943 on infants older than one week and weighing more than 2 kg. The results of his study were dismissed as unimportant because the infants were not small enough. Ignoring low temperatures in infants continued.

At the end of World War II infant incubators were introduced (naked infants placed in transparent boxes) and caretakers noticed how often infants went into respiratory distress. In 1950 the consequences for infants resulting from change in environment (influence of oxygen) started to raise questions, which resulted in clinical trials. By 1958 a clinical trial was completed which indicated that infants placed in incubators at 32 °C had a higher survival rate than infants placed in incubators at 29 °C (Silverman, et al., 1595).

During that same year, Mount (1951) demonstrated the response of the new-born piglet to a cooling environment resulting in a marked increase in heat production. Brűck (1957) published studies concerning humans and expanded Day's conclusion: infants weighing as little as 830 g exhibited appropriate defensive responses to thermal stimulus beginning from birth. By 1978 an enormous amount of information had been collected concerning thermoregulation and energy metabolism during the neonatal period, and the thermal environment would come to be considered an important variable in the caretaking of infants.

1.3 Motivation

The human body may be seen as a relatively complex thermodynamic machine in which energy stored in the food we eat is converted into work (and heat), which helps maintain thermal homeostasis by counter balancing heat loss. For a neonate there are many complexities after birth which includes under-development of the

lungs as well as not having the ability to shiver for heat generation when the environment is too cold. In Neonatal Intensive Care Unit's (NICU's) the temperature is monitored by the room air-conditioning and the nurses manually take the temperature of the infants, placed in bassinettes, with a thermometer. This provides room for human error and variable thermal discomfort for the infants.

Mathematical models have a role in both treatment and diagnoses. Mathematical models can aid in predicting the time course of temperatures or in giving information on the temperature where thermometry is lacking. These roles serve as the motivation for this project which is to develop a theoretical mathematical prediction model that broadens the understanding of how thermal stability is influenced and may help provide a model that can be used to improve the thermal stability of the infant in its now extrauterine environment.

1.4 Research Objective

The theme of this thesis project is focused on thermal regulation of the human body. The first objective of this project is to complete a literature study covering the topics of the thermal regulation system as well as the respiratory system in order to better understand the physiology of the human body. The objective is to define the thermal regulation control system of the human body, with the system dependencies, influences and results that are obtained when the infant is exposed to different environments. The effect of the respiratory system on the thermoregulation system must also be described and the functioning of the respiratory system must be understood.

The second and main objective of this thesis project is to attempt to define a theoretical thermal regulating system of a neonate. This project thus requires the development of a theoretical model to simulate the thermal regulation system of the human. This will be done by simulating the thermal regulating system theoretically by means of seeing the body as an energy conversion system in an unstable environment. The theoretical model must introduce a mathematical methodology using constitutive equations and equations of change to explain the heat transfer mechanisms. The theoretical model must indicate the behaviour, in terms of thermal regulation control strategies, of a human body with respect to different environments.

The third objective requires the development of a practical experimental model that simulates the respiratory system and illustrates the functioning of this system. This model should indicate the heat transfer in the respiratory system and show that inhaled air is conditioned to approximately 37 °C and 100% relative humidity by the time that it is exhaled. Further objectives include emphasizing the use of typical mechanical engineering theory and technology, rather than the bio-physical point of view. The model has to be designed such that the temperature and humidity of the air in an incubator may be simulated, with respect to different system inputs and environmental changes.

1.5 Thesis Outline

This thesis begins with a literature study in Section 2 focussing on physiological background. The physiological background places emphasis on the lung, blood and skin physiology with reverence to heat transfer. The literature study then follows to investigate the thermal regulation in a human, with focus on neonates. Topics discussed with regards to thermal regulation include a definition of the thermal environment as well as methods used for maintaining constant core temperature. Additionally, the literature study undertakes to determine the thermal heat transfer properties of the skin. Previously developed mathematical models are summarised and the literature study concludes with a brief discussion on practical methods used for determining body temperature and heat loss.

The largest part of this thesis is the mathematical modelling of thermal regulation mechanism in the human body and is discussed in Section 3. The derivation of heat transfer equations based on energy conservation is done. A theoretical model is developed to simulate the heat loss from the skin and heat loss during the respiratory process, respectively. These two theoretical models are then combined in order to develop the theoretical model for the neonate in a distinctly defined thermal environment.

A clinical trial is conducted and discussed in Section 4. The clinical trial was conducted in order to assist in the understanding of thermal stability in neonates. The results obtained from the clinical trial will be used to verify the developed theoretical simulation model (Section 3). The protocol used to gain the necessary data is discussed and the protocol information form is also presented. The protocol synopsis, consent form and letter providing ethical approval are filed in Addendum B.

In Section 5 the attempt to experimentally model the respiratory process is discussed. This section introduces the experimental lung apparatus designed and used to mimic the respiratory process with regards to heat transfer. Instrumentation used for operating the lung apparatus as well as the instrumentation used to capture relevant data such as temperature and relative humidity changes is discussed in this section. The heat transfer design of the experimental mechanical lung apparatus entails calculations needed for operation of the experiment and are discussed in Section 5 as well. The start-up, operation and shut-down procedures are listed, and safety as well as storage instructions are discussed.

Section 6 discusses the results obtained upon completion of this thesis project. This section looks at the results obtained from the theoretical heat transfer simulation model (model for heat loss through the skin and the respiratory system). Thermal response of a neonate in the delivery room is determined, followed by the thermal response of the neonate in the post natal ward. This section then validates the theoretical simulation results by comparing them to temperature measurements obtained practically during medical in-hospital trials.

Section 6 is concluded by discussing the success of the experimental respiratory model developed in Section 4.

Section 7 discusses the completion and success of the thesis with respect to the results obtained by completing the research objectives given in Section 1.4. Conclusions are also made based on the expected outcome and actual results of the developed theoretical simulation model. The verification and validity of the developed theoretical simulation model are discussed and an overall conclusion is presented in this section. Section 8 discusses the suggested recommendations as well as opportunities for future work in this field of research.

2 LITERATURE STUDY

The transition for a neonate, from an intrauterine to an extrauterine environment, requires rapid and on-going physiologic and anatomic changes in multiple organ systems. An understanding of these transitional events and the physiological adaptations that the neonate must make is essential for the medical professionals assisting the infants in maintaining thermal stability. The literature study focused mainly on infants, although the theory is applicable to adults as well.

The literature study starts with the physiological background on the respiratory system, the blood circulation system and skin tissue, with the focus on heat transfer. Thermal regulation is then discussed in some detail with focus on the physiological thermal regulation process. Methods for temperature regulation regarding heat gain and heat loss are explained leading to the definition of what a thermal neutral environment entails. Further, tissue properties are discussed which determine the degree to which energy is transferred or employed to maintain constant core temperature. These skin tissue properties will be used in the development of the theoretical simulation model, in Section 3.

In addition to the physiological background, the literature study also presents a review on research done on presently developed mathematical models used for prediction of skin temperatures and heat losses. A blood flow heat transfer model, developed by Pennes (Pennes, 1998) is discussed in this section. His model was used to predict skin tissue temperatures as a result of blood flow. An extensively detailed dynamic model predicting human thermal responses in different thermal environments was developed by Fiala et al (Fiala, et al., 1999). A contribution was made to research efforts in order to formulate a more precise, flexible and universal model of the human thermal regulation system. There exists a number of practical models, such as indirect calorimetry (IC) and infrared thermographic calorimetry (ITC), used for predicting heat gain and heat loss, which are also briefly discussed toward the end of the literature study.

2.1 Physiological Background

A physiological background on the lung, blood and skin physiology in relation to heat transfer is discussed in detail in this section. First, blood physiology is discussed with focus on the heat transfer characteristics. Blood physiology describes the human circulatory system which transports blood to all body tissues through an intrinsic network of blood vessels. Second, skin physiology and heat transfer are discussed, where the skin is one of the most vital organs of the human body and plays an important role in thermal regulation (heat loss). Thirdly, lung physiology is discussed with respect to the important functions of each organ in the respiratory system. The lung development of infants is discussed as well as the defects that could arise during premature birth. Lung and airflow volumes are provided with a diagram that explains lung volumes and capacities.

2.1.1 Blood physiology, heat transfer, and bioheat transfer

Blood is the fluid that delivers necessary substances such as oxygen, nutrients and hormones to cells and transports metabolic wastes away from those same cells (Fox, 2009). Bioheat transfer processes in living tissues are influenced by the local temperature distribution and by blood perfusion through the vascular network (Valvano, 2006). Convective heat transfer will occur when there is a significant difference between the temperature of the blood and the tissue through which it flows, altering the temperature of both the blood and the tissue. Perfusion based convective heat transfer is critical to thermal regulation. The rate of perfusion of blood through different tissues depends on physical activity, physiological stimulus and environmental conditions (Valvano, 2006).

The thermal interaction between tissue and perfused blood was thoroughly studied, documented and published by Harry H. Pennes (Pennes, 1998). This thermal transport model is analogous to the process of mass transport between blood and tissue. The results of his work showed a temperature difference of three to four degrees between the skin and the interior of the arm. He attributed these effects to metabolic heat generation and heat transfer with arterial blood perfused through the microvasculature. It is assumed that the blood perfusion effect is homogeneous and isotropic and that thermal equilibration occurs only in the microcirculatory capillary bed.

Blood, at the temperature of arterial blood (assumed as 37 °C), enters the capillaries where heat exchange occurs to bring the blood temperature to that of the surrounding tissue. There is assumed to be no energy transfer either before or after the blood passes through the capillaries, so that the temperature at which it enters the venous circulation is that of the local tissue. The total energy exchange between the blood and tissue is directly proportional to the density and perfusion rate of blood through the tissue, and is described in terms of the change in sensible energy of the blood.

2.1.2 Skin physiology and heat transfer

The skin is a vital organ of the human body. It is self-maintaining, self-repairing and it has a sensory and protective function. The skin plays an important role in thermoregulation, water excretion, fat storage and insulation (Lund, et al., 1999). Skin acts as a chemical barrier in limiting penetration by foreign substances and also provides mechanical protection against physical penetration.

The main layers of the skin are the viable epidermis layer, dermis layer and the hypodermis layer (refer to Figure 2.1). All the skin layers contain microstructures like blood vessels, lymph vessels, nerve endings, sweat glands and hair follicles. The influence of these structures on the mechanical properties can be considered minimal in comparison to the bulk mechanical behaviour caused by the main layers of the skin layer (Geerligs, 2010). Mechanical properties of skin depend on the nature and organisation of dermal collagen and elastic fibre networks, and the

water proteins and macromolecules embedded in extracellular matrix, with less contribution toward these properties by the epidermis and stratum corneum.

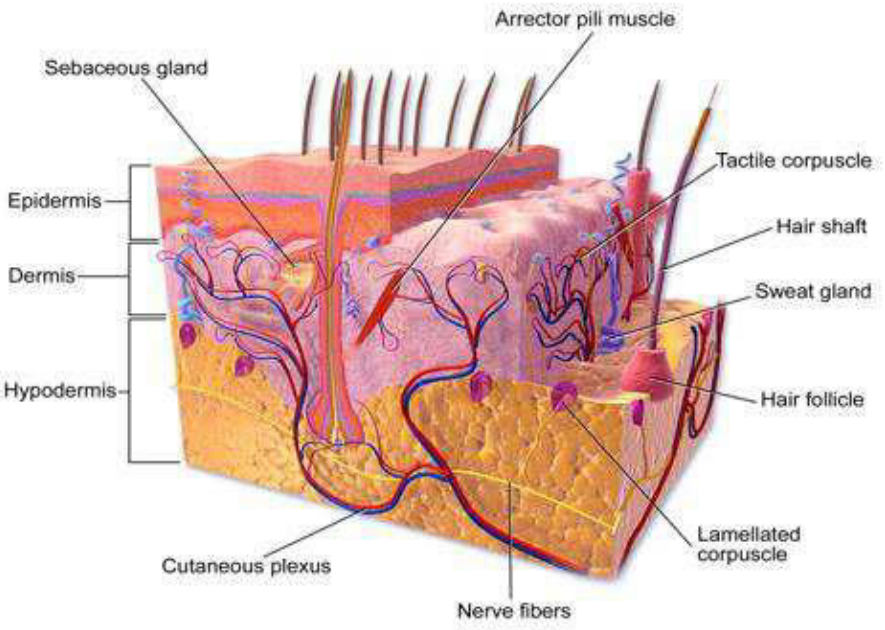

Figure 2.1: Skin physiology (Communications, 2014)

The outermost layer of the skin, the stratum corneum (upper half of the epidermis, see Figure 2.1) has a thickness of 10 to 25 µm (Geerligs, 2010). The stratum corneum layer retains metabolic functions such as infection whilst protecting against human and environmental insults. The most important function of the epidermis is retaining water and heat (Lund, et al., 1999). Total water content varies between 30 to 60%. The total thickness of the epidermis varies between 30 to 100 µm (Geerligs, 2010). The epidermis is influenced by environmental conditions such as relative humidity and temperature. Because of its non-vascular structure the epidermal cells are nourished from plasma that originates in the dermal blood vessels so that the nutrients are transported across the epidermal-dermal junction.

The basal layer of the epidermis is attached to the next layer in the skin physiology, the dermis (see Figure 2.1). The dermis thickness ranges from 1 to 4 mm (Geerligs, 2010) and cushions the body from stress and strain. The vascular volume content indicates physiological variations, which can alter the mechanical behaviour of the skin. The composition of the dermis provides the skin with mechanical strength and elasticity to withstand frictional stress and to extend over joints. The elastic fibre network ensures full recovery of tissue shape and architecture after deformation. Although the vascularization throughout the dermis appears relatively sparse, the supply of papillary loops is ensured by

arterioles irrigated from the deep dermis. The dermis also harbours the cutaneous nerve endings that provide senses of touch and heat.

The hypodermis, also known as the subcutaneous adipose layer (see Figure 2.1) is not a functional part of the skin. The purpose of this layer is to attach the skin to underlying bone and muscle as well as supplying it with blood vessels and nerves. The thickness of the hypodermis varies with anatomical site, age, sex, race and nutritional status of an individual. The functions of the hypodermis include heat insulation as well as serving as caloric reservoir where stored fat is the predominant component. Subcutaneous adipose tissue is structurally and functionally well integrated with the dermis through the nerve and vascular networks and the continuity of epidermal appendages such as hairs and nerve endings. The mechanical function of subcutaneous adipose tissue includes allowing the overlying skin to move as a whole and the attenuation and dispersion of externally applied pressure.

Two types of subcutaneous adipose tissue can be defined, namely brown adipose tissue and white adipose tissue. Brown adipose tissue (brown fat) differs morphologically and metabolically from ordinary white adipose tissue (white fat) in that it contains more capillaries than white fat because of its greater need for oxygen. Brown fat is of particular relevance to this study because of the role it plays in generating heat in infants.

Brown adipose tissue is located primarily in the subscapular, axillary, adrenal and mediastinal regions and can rapidly increase cellular metabolic rates and oxygen consumption, thereby generating heat (Thomas, 1994). Brown adipose tissue contains many mitochondria, numerous fat molecules, an abundant sympathetic innervation and an abundant blood supply (Asakura, 2004). Brown fat constitutes approximately 1.4% of the body mass of neonatal infants (Waldron & MacKinnon, 2007). Brown adipose tissue may account for as much as one third of the overall metabolic rate (Cinar & Filiz, 2006). Brown adipose tissue does not continue to develop after birth. The primary function is to generate body heat in infants.

Although neonatal and adult epidermis are similar with respect to thickness and lipid composition, skin development is not complete at birth. The full-term new-born's skin is well-developed, opaque with few veins visible, has limited pigmentation and wrinkles around joints, and is without edema (Lund, et al., 1999). Preserving skin integrity is an important aspect of nursing care across the life span of all patients, but is of particular significance in neonates, who are adapting from the uterine aquatic environment to aerobic environment.

2.1.3 Lung physiology and heat transfer

The primary purpose of the respiratory system is to provide an enormous surface area (70 m^2 in adults) for gas diffusion between air and blood. The diffusion of oxygen and carbon dioxide is accomplished by three components, namely

ventilation (airways and lung mechanics), lung perfusion by the pulmonary circulation, and gas exchange (Le Rolle, et al., 2008). A secondary aspect of the respiratory process involves the heat transfer that occurs during a respiratory cycle. A respiratory cycle is divided into the inhalation and the exhalation phases. During the inhalation phase the inhaled air is heated and humidified whilst during the exhalation phase the conditioned, oxygen depleted air leaves the lungs.

The physiology of the respiratory system can be divided into a conducting zone, Figure 2.2(a), and the respiratory zone, Figure 2.2(b). Air is inhaled through the conducting zone where it is heated and humidified. The air then moves through the respiratory zone where gas exchange transpires. The diaphragm is used to permit air movement into and out of the lungs, causing a respiratory cycle.

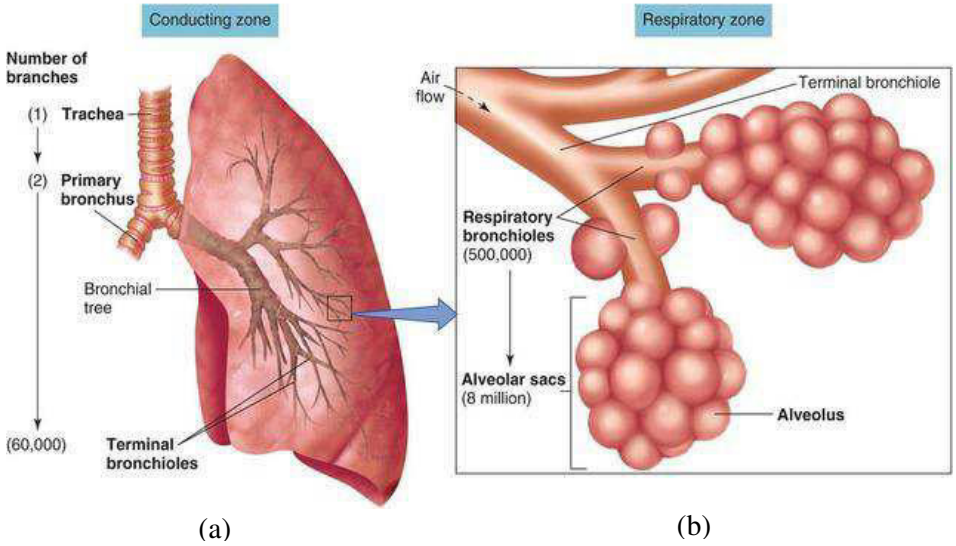

Figure 2.2: The (a) conducting and (b) respiratory zone of the respiratory system (Fox, 2009)

During normal inhalation air is inhaled via the nasal vestibule into the nasal cavity. Air can be inhaled via the oral cavity when the sinuses are blocked during sickness or during heavy exercise. Infants cannot inhale air through the oral cavity because the size of the tongue is too large (Wheeler, et al., 2007) . The inhaled air moves through the conducting zone from the nasal cavity. The nasal cavity is lined with cilia which filter the inhaled air in order to get rid of unwanted particles. The mucous membranes moisten the incoming air to 100% relative humidity and the surrounding blood capillaries warm the incoming air to core body temperature. During exhalation the mucous will take up some of the heat and water vapour from the expired air, to restore some of the moisture in the trachea.

The conditioning of air protects the alveoli and also reduces the loss of heat and water from the body during the respiratory process. If the inspired air was cold

and dry it would be conditioned to core body temperature and full humidity before it reaches the first bronchial branches. If the air is too dry when reaching the terminal bronchioles the dry cold air would parch and destroy the alveolar walls (Blakemore & Jennett, 2001).

The airway below the larynx (which contains the vocal folds) consists of the trachea, bronchi and bronchioles, see Figure 2.2. The trachea is a tube that extends almost to the middle of the chest connecting the bronchi and larynx. The bronchi are formed by the trachea splitting into two main branches and then each branch dividing again. The bronchioles are formed from the bronchi, which are thin and short distensible airways that again divide many times to form alveolar ducts.

The alveolar ducts contain blood capillaries and alveolar sacs which permit gas exchange through diffusion of oxygen and carbon dioxide. The network of blood capillaries and blood circulation that enables gas exchange is known as the pulmonary system. In a full grown adult there are about 300 million alveoli with diameters ranging from 0.1 to 0.3 mm diameter. The total alveolar surface area can range from 30 to 100 m^2 (Sharma, et al., 2011).

The neonatal period (which consists of the first 28 days of life) contains the most dramatic physiological changes seen in humans. One of these changes can be seen in the respiratory system. At full term birth the lungs are functionally adequate, but they are not fully developed. The lungs have fewer bronchial branches and far smaller alveolar surfaces than they eventually acquire (Blakemore & Jennett, 2001). Alveolar development continues after birth up to the age of 5 or 6, increasing to a number of 300 million alveoli.

The health of lungs is commonly evaluated by using a spirometer to measure lung volumes and capacities. Lung volumes and lung capacities refer to the volume of air associated with different phases of the respiratory cycle. Lung volumes are directly measured while lung capacities are inferred from lung volumes. The lung volumes and capacities are indicated in Figure 2.3, and the abbreviations are summarised in Table 2.1. The lung volumes and capacities, presented in Figure 2.3, are generally measured in millilitres or litres, but weight specific lung capacities and volumes are presented in Table 2.1 to accommodate the varying weights of neonates.

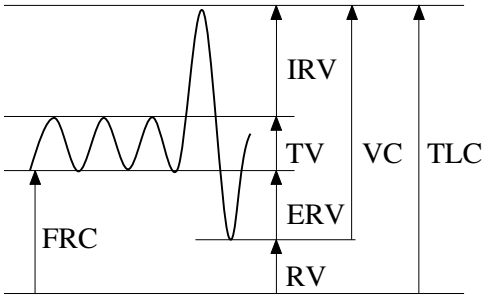

Figure 2.3: Lung volumes and capacities (see Table 2.1)

Table 2.1: Physiological lung variables and definitions with weight specific values measured in ml/kg

	Variable	Definition	Term Infant
TV	Tidal Volume	The volume of gas inspired or expired in an respiratory cycle	5-7
IRV	Inspiratory Reserve Volume	The maximum volume of gas that can be inspired during forced breathing in addition to tidal volume	–
ERV	Expiratory Reserve Volume	The maximum volume of gas that can be expired during forced breathing in addition to tidal volume	–
RV	Residual Volume	The volume of gas remaining in the lungs after a maximum expiration	–
TLC	Total Lung Capacities	The total amount of gas in the lungs after maximum inspiration	55-70
VC	Vital Capacity	The maximum amount of gas that can be expired after a maximum inspiration	35-40
IC	Inspiratory Capacity	The maximum amount of gas that can be inspired after normal expiration	
FRC	Functional Residual Capacity	The amount of gas remaining in the lungs after a normal tidal expiration	27-30
BR	Breathing Rate	Number of breaths taken per minute	30-50

2.2 Thermal Temperature Regulation and Heat Transfer

Physiological thermal temperature regulation is defined as the maintenance of the body's temperature within a restricted range under conditions involving variable internal and external heat loads (Bligh & Johnson, 1973). This section forms a review of the present understanding of the ways in which the new-born human infant transforms energy and regulates body temperature. The methods for temperature regulation regarding heat gain and heat loss are explained, which lead to the definition of what a thermal neutral environment entails and how it can be maintained to serve the thermal needs of the infant.

2.2.1 Physiological thermal regulation

Thermal regulation of the infant is the ability to balance heat production and heat loss in order to maintain the core body temperature in the normal range. Thermal regulation is also a critical physiological function related to the survival of the infant. Thermal regulation is controlled by the hypothalamus (Thomas, 1994). The physiological variable, controlled by the hypothalamus, is the core body temperature. Table 2.2 lists the start temperature (core temperature of the infant at birth) as well as the skin temperature ranges for an infant during the first 6 hours of life for different weight groups.

Table 2.2: Start temperature and skin temperature ranges for infants at 0 to 6 hours of age for different weight groups (Chatson, 2003)

	Temperature	
Weight (g)	**Start (°C)**	**Range (°C)**
<1 200	35.0	34.0-35.4
1 200 – 1 500	34.1	33.9-34.4
1501 – 2 500	33.4	32.8-33.8
> 2 500	32.9	32.0-33.8

The hypothalamus processes sensory information received from the thermal receptors, in the skin and the preoptic area of the hypothalamus, and compares it against the core temperature set point. Body temperature is modified by voluntary and involuntary reactions as indicated in the flow diagram for human thermoregulation control, Figure 2.4. Voluntary reaction includes only behavioural response whereas involuntary reactions include vasomotor and sudomotor response, motor tone and activity response, as well as metabolic response.

Vasomotor response relates to the vasoconstriction or vasodilation of arteries (smooth muscles) to regulate skin blood flow. Body temperature homeostasis is maintained by regulating the rate of blood flow through the skin. Cutaneous receptors in the skin sense temperature changes in the immediate environment. When the body temperature is high, cutaneous vasodilation increases blood flow through the skin. A decrease in body temperature causes cutaneous vasoconstriction which reduces blood flow through the skin.

Sudomotor response relates to sweat glands and erector pili. Sweat production is observed in infants older than 29 weeks gestation, although it is a slower response, less efficient and only occurs at high environmental temperatures. Motor tone and activity refer to the skeletal muscle contractions and the ability to adapt posture in order to reduce surface area for decreased heat loss. Heat production results from increased metabolic rate in response to cold stress. Shivering response is not well developed in infants and therefore heat production is primarily met through non shivering thermogenesis which leads to increased oxygen consumption.

Thermal response to a low temperature environment results in heat conservation stimulus in the hypothalamus. Ineffective ability to increase heat production leads to hypothermia (core temperature between 33 to 35 °C), and severe hypothermia at core body temperatures lower than 32 °C. Thermal response to high environmental temperature results in overheating of the infant. High environmental temperatures stimulate the heat loss centre in the hypothalamus. Long-term exposure to high temperature environments leads to heat exhaustion (core body temperature between 38 to 40 °C), and hyperthermia at 41 to 44 °C, which will result in death.

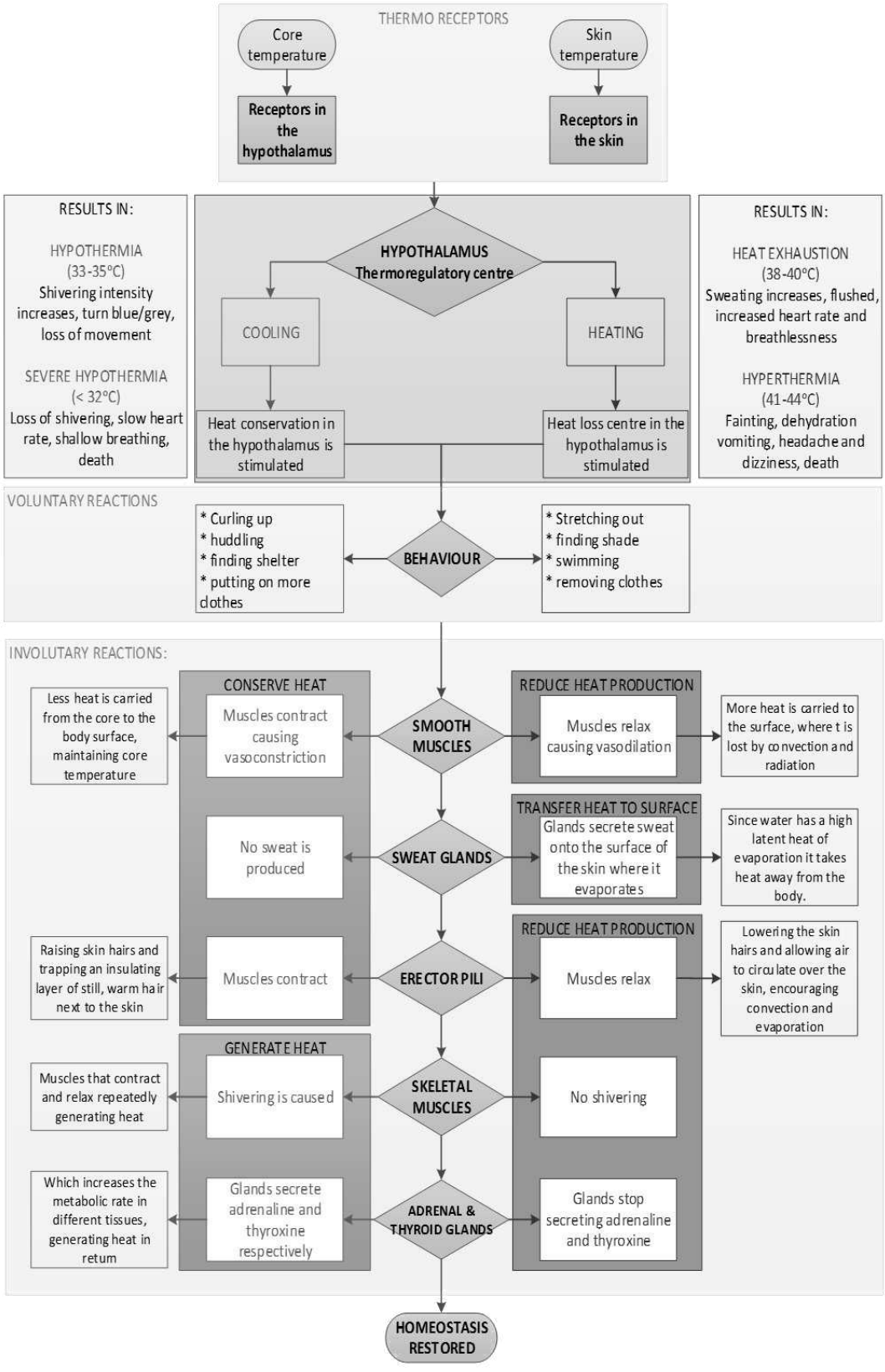

Figure 2.4: Flow diagram for human thermoregulation control

2.2.2 Methods of thermal regulation

Thermal stability is that property of a system which opposes variations in heat content under conditions allowing net thermal exchange between the object and its environment. Thermal stability is a function of body size, surface area, thermal insulation and the degree by which heat output can be altered (Adamsons, 1966). An understanding of these avenues for heat exchange provides the basis for modification of the environment.

Body heat is mainly produced by metabolism and non-shivering thermogenesis. Metabolism reflects the overall energy needs which support maintenance, repair and growth (Thomas, 1994). The heat produced must be precisely balanced against heat loss through conduction, convection, radiation and evaporation.

Heat is lost from the skin surface as well as the surface area in the respiratory tract. Surface area is directly related to heat exchange between the body and environment. The greater the surface area to mass ratio, the greater the imbalance between heat producing ability and heat loss. Infants have a large body surface area to mass ratio of between 2.5:1 to 3:1, which results in increased heat loss (Sharma, et al., 2011).

The first method of heat loss is conduction which occurs directly through body tissue from the internal heat producing organs to the skin surface and through the material, such as clothing or the matrass, in contact with the skin (Swyer, 1978). The temperature gradient between the skin and contacting surface has the largest influence on the rate of heat loss via the conduction mechanism.

There are three principle ways in which convection heat loss takes place (Swyer, 1978). The first method of heat loss via convection is when heat is convected to the skin surface from the blood stream. The second method of convection heat loss occurs when cold air moves across the skin surface. The third method of convection entails transfer of warmed inspired air to the environment during an exhalation phase; this is also called respiratory convective heat loss. Factors that influence heat loss by convection include air velocity, the temperature gradient and clothing insulation.

Heat loss via radiation occurs from the infant's skin to surrounding surfaces. Radiation heat loss is influenced by the emissivity of the radiating surfaces, temperature gradient between radiating surfaces, the surface areas and the distance between the radiating surfaces.

The last heat loss mechanism considered is heat loss via evaporation, which can also be accounted for by three methods (Swyer, 1978). The first method is insensible heat loss from the skin surface. The second method is the evaporation of sweat from the skin surface during heat exhaustion. The last method of evaporation heat loss occurs during the respiratory process with evaporation from the mucous of the respiratory tract into expired air. Premature infants have

increased evaporative heat losses as water diffuses across the permeable skin barrier and evaporates. Factors that influence the rate of evaporation are the air velocity, surface area and the vapour pressure (which is related to the temperature and relative humidity of the air).

2.2.3 Thermal neutral environment and thermal response

A thermal neutral environment is described by the Journal of Applied Physiology as "the range of ambient temperature within which the metabolic rate is at a minimum and within which temperature regulation is achieved by non-evaporative physical processes alone" (Bligh & Johnson, 1973). A thermal neutral environment is achieved when the infant is in thermal equilibrium with the environment.

The thermal environment is subject to the ambient air temperature, mean radiant temperature, relative humidity and the air velocity. Thermal responses resulting from changes in the environment require the adaptation of cardiovascular dynamics to maintain systemic perfusion pressure. Further, the thermal effects of body motion and air speed on clothing are so big that they must be accounted for (Havenith, et al., 2002). Effects on dry heat exchange are small for stationary bodies and light work at low air speed.

At raised environmental temperature or lowered body temperature the usual flow direction of heat from body core to exterior is reversed and heat storage rather than heat loss takes place causing a rise in body temperature. Such a rise must be temporary and reversible or death will result from overheating (Swyer, 1978). Overheating of the infant will result in increased fluid loss, increased respiratory rate and the metabolic rate will reach fatal levels. Infants have limited sweating ability and only develop the ability to sweat effectively 36 weeks after post conceptual age (Sharma, et al., 2011). Sweating is the only means of decreasing body temperature when the environmental temperature is greater than core body temperature. Relative humidity of the environment limits the sweating ability.

All infants, especially premature infants, are at high risk of heat loss, which lead to hypothermia and, thus need better temperature support. In order to treat hypothermic preterm babies more successfully the body temperature must be continuously regulated. The poor ability of the infant to regulate its own temperature is due to limited insulating capacity of subcutaneous fat and the inability of infants to generate heat by shivering until 3 months of age. Response to cold stress results in non-shivering thermogenesis for infants which utilises brown adipose tissue and in turn elevates the core body temperature. With continued cold stress the store of brown fat becomes depleted (Waldron & MacKinnon, 2007).

Heat loss in an infant can be divided into 34% convection, 3% conduction, 39% radiation and 24% evaporation (Sharma, et al., 2011). These heat losses can be prevented to some extent in the neonatal care facilities, but it is important to

understand the heat exchange mechanisms because these provide the basis for modification of the environment to suit the infant best.

Heat loss via radiation and conduction can be minimised by keeping the surrounding environment and objects at a higher temperature. This temperature must not be increased too much as this will cause heat gain. Convection heat loss can be minimised by increasing the surrounding air temperature and minimizing the air movement over the infant's skin. Evaporation heat loss is reduced by increasing the humidity and reducing the air movement across the infant's skin.

2.3 Thermal Heat Transfer Properties of Skin

The thermal properties of human skin play a vital role in determining the overall thermal energy balance within the body. The mechanical properties of skin vary considerably and depend on body site (e.g. arm, head, abdominal), age, race and gender. The degree to which this energy is transferred or employed to raise the skin temperature is determined by the various thermal properties of the skin. Energy reaches the skin by some transport mechanism: conduction, convection, radiation or evaporation. The skin properties discussed in this section include density, thermal conductivity, specific heat, emissivity and the skin wettedness factor (i.e. the proportion of the total skin surface area of the body covered with sweat).

Table 2.3 lists the tissue density values obtained for fat, dermis, and epidermis, as well as the density values obtained for blood for human skin. A variation of sources was used as indicated in the last column of Table 2.3. The density values obtained from Fiala et. al. (1999), listed in the second row of Table 2.3, will be used for the simulation developed in Section 3.

Table 2.3: Tissue density values measured in kg/m^3 for human skin layers

Fat	Dermis	Epidermis	Blood	Reference
850	1085	1085	1069	(Fiala, et al., 1999)
_	1110-1270	1110-1270	_	(CES 2013 EDUPACK, n.d.)

The thermal conductivity values for the fat, dermis, epidermis and blood for human skin are listed in Table 2.4. It is necessary to account for the effect of blood flow when measuring the conductivity of skin in vivo (Cohen, 1977). The thermal conductivity is also directly related to the water content of the skin. It is important to note that the thermal conductivity and the properties of the skin will vary according to the site of interest, due to different thicknesses and water content in the sites of interest.

From the values provided in Table 2.4 it is clear that the thermal conductivity values were constant over the different references. The thermal conductivity values obtained from Fiala et al., listed in the second row of Table 2.4, will be used for the simulation developed in Section 3. The thermal conductivity of blood

will be used as 0.492 W/mK with varying artery diameters of 0.01 to 0.000001 m (Valvano, 2006).

Table 2.4: Thermal conductivity values measured in W/mK for human skin layers

Fat	Dermis	Epidermis	Blood	Reference
0.16	0.47	0.47	_	(Fiala, et al., 1999)
0.201 to 0.217	0.293 to 0.322	0.209	0.492	(Holmes, n.d.)
_	_	_	0.493	(Bowman & Balasubramaniam, 1976)
0.205	0.293	0.209	_	(Cohen, 1977)

Table 2.5 lists the values obtained for the specific heat for fat, dermis, epidermis and blood tissue for human skin. A variation of sources was used as indicated in the last column of Table 2.5. The density values obtained from Fiala et al., listed in the second row of Table 2.5, will be used for the simulation developed in Section 3.

Table 2.5: Tissue specific heat values measured in J/kgK for human skin layers

Fat	Dermis	Epidermis	Blood	Reference
2300	3680	3680	650	(Fiala, et al., 1999)
_	3580	3580	_	(CES 2013 EDUPACK, n.d.)

Emissivity measurements made in excised skin samples during in vivo experiments indicate that skin radiates approximately as a black body in its emission wave band (Cohen, 1977). Cohen also reviewed that the emissivity's are in the order of 0.997, with no variation due to skin colour. This high value for emissivity is due to the surface roughness of the skin as well as the fact that the skin has such high water content.

Perspiration is a problem of mass transfer from a surface consisting of wet and dry areas. Moisture is always present in the cutaneous layer where sweat glands are located. The skin wettedness factor could be interpreted as the ratio of wet area to the total surface area of the human body; this skin wettedness cannot be measured directly from the human body surface but can be calculated by the ratio of actual evaporative heat loss to the maximum evaporative heat loss (Kuramae, et al., 2007). The simulations done by (Fiala, et al., 1999) indicated a skin basal wettedness factor of 0.06, which is the basic property used for human skin.

2.4 Mathematical Models

A number of mathematical models for human thermoregulation have been developed, (Fiala, et al., 1999), (Pennes, 1998), with variable accuracy, which contributed to the deeper understanding of regulatory processes. These models have not gained wide-spread use due to the lack of confidence in predictive abilities, limited range of applicability and poor modelling of heat exchange with the environment.

Blood flow and temperature models used in developments of mathematical models all refer to the work done by Pennes (Pennes, 1998). The most successful mathematical model developed to date, and used for tissue temperature prediction, was done by Fiala et al (Fiala, et al., 1999). Some practical methods have also been used to calculate or predict metabolic rate and heat loss such as indirect calorimetry and infrared thermographic thermometry, all of which are discussed in this section.

2.4.1 Blood flow and temperature models

In order to predict skin tissue temperatures, the influence of blood flow must be accounted for. Blood vessels have very high densities which make it difficult to compute a detailed temperature distribution for any amount of tissue surface. Previously developed models get increasingly sophisticated, although accurate predictions for individuals remain difficult due to many influencing factors. The bioheat equation, equation (2.1), for blood perfusion was developed by Pennes in 1948. The bioheat equation describes the heat transfer from blood to tissue as if the heat transfer only takes place in the capillaries (Pennes, 1998).

$$k_{tis}T - W_b c_b(T - T_{art}) + M = c_{tis}\rho_{tis}\partial T/\partial t \qquad (2.1)$$

The bioheat equation includes the heat transfer conduction coefficient k_{tis}, which includes the conduction heat transfer as a function of temperature T for the surface area (x and y direction) as well as the conduction moving to the surface of the tissue in the z direction. Equation (2.1) then includes heat transferred via blood perfusion W_b to the skin tissue which is calculated as a function of the specific heat of blood and the difference between artery temperature T_{art} and skin tissue temperature T. The bioheat equation also incorporates the metabolism M(measured in W/m^2). These heat transfer mechanisms are balanced against the stored heat within the tissue $c_{tis}\rho_{tis}\partial T/\partial t$.

The equation was developed based on the assumption that blood reaches the capillaries at the same temperature as the supply artery and in the returning veins heat transfer with the surrounding tissue is negligible. This bioheat equation has established itself as the most used continuum equation for tissue heat transfer, although significant temperature inhomogeneity is still unpredictable by any continuum model for large blood vessels.

2.4.2 Fiala model: The passive system

In the computer model of human thermoregulation developed, Fiala et al concluded that the heat exchange with the environment plays a key role in the thermal state of the human body (Fiala, et al., 1999). Further, the development of models for the passive system of human thermal regulation needs to reflect the importance and complexity of this phenomenon. The model accounts for geometric and anatomic characteristics of the human body and considers the physical, thermal, and basal physiological properties of tissue materials.

The Fiala model idealised the body construction as 15 spherical or cylindrical body elements which include the head, face, neck, shoulders, thorax, arms, hands, abdomen, legs and feet. The model consists of annular concentric tissue layers including brain, lung, bone, muscle, viscera, fat and skin tissue. Heat transfer within the tissue was based on the bioheat equation discussed in Section 2.4.1. The skin was modelled as two layers consisting of the inner skin and outer skin, both with an approximate thickness of 1 mm. The inner skin layer was modelled as the region where metabolic heat is generated and blood is perfused. In the outer skin layer there is no heat source or blood vessels; this layer only plays a role in evaporative heat loss.

Convective heat exchange between the skin surface and the air was modelled by considering both natural and forced convection by introducing a combined heat convection coefficient. The convection coefficient was developed as a function of the location on the body, the temperature difference at the specific node and the air velocity.

The concept of direction dependent average temperatures for the surrounding structures was adapted for the modelling of radiation heat loss. A mean temperature for the surroundings was used where the emissivity for indoor surrounding surfaces was 0.93. Further the emissivity of clothing and the human skin was 0.95 and 0.99 respectively. View factors, depending on the posture of the infant, were calculated for each of the individual body parts varying from 0.1 to 1.

The Fiala model made some effort to include clothing insulation factors by modelling different garment ensembles, which resulted in the overall insulation being 0.59 clo (where 1 clo is equal to 0.155 W/m^{2}K) with moisture permeability index of 0.34. Characteristics used in modelling heat transfer through garments include the intrinsic clothing insulation (I_{cl}), clothing area factor (f_{cl}) and the moisture permeability index (i_{cl}). The local effective heat transfer coefficient (U_{cl}, measured in W/ m^{2}K), calculated by equation (2.2), was developed as a function of the local heat resistance, type of clothing layer together with the local convective and radiative heat convection coefficients ($h_c$and h_r).

$$U_{cl} = \left[\sum_{j=1}^{n} I_{cl} + 1/f_{cl}(h_c + h_r)\right]^{-1} \qquad (2.2)$$

Further the corresponding evaporative coefficient ($U_{e,cl}$ measured in W/ m^{2}Pa), given by equation (2.3), was calculated as a function of local heat resistance (I_{cl}), local moisture permeability index (i_{cl}), type of clothing layer and the local convective heat transfer coefficient (h_c). Evaporative heat loss was calculated using the vapour pressure differences between the outer skin layer and the immediate air film, together with the clothing evaporative coefficient.

$$U_{e,cl} = \left[\sum_{j=1}^{n} I_{cl}/i_{cl} + 1/f_{cl}h_c\right]^{-1} \qquad (2.3)$$

The convective respiratory heat loss was expressed as a function of the pulmonary ventilation rate and the temperature and vapour pressure of the inhaled air, respectively. The evaporative respiratory heat loss was calculated as a function of the whole body metabolism, latent heat of vaporisation of water and the difference between the humidity ratio of the expired and inspired air.

The passive system model does not include thermoregulatory feedback mechanisms; they found it was not possible to validate the model by comparisons of field measurements. In order to verify the Fiala model, the model was compared to analytical solutions for heat flow over homogeneous cylinders and spheres. These comparisons indicated that the model was stable and capable of accurately predicting internal body temperatures

2.4.3 Practical prediction models and methods

Measurement of infant energy expenditure in the clinical setting is difficult and is rarely done. The objective of this study was to validate a newly developed method of determining energy expenditure in infants, viz. infrared thermographic calorimetry, against an established method, respiratory indirect calorimetry. (Adams, et al., 2000)

Direct calorimetry is the determination of energy expenditure from measurement of heat loss by the body. Indirect calorimetry (IC) is a method of indirectly calculating the heat produced by oxidative metabolism. These two methods provide similar results, but are rarely used in a clinical environment due to the long measurement times and frequent calibration required. Temperatures were measured with thermistor probes, and infant axillary temperature was used as the measurement of infant core temperature.

Infrared Thermographic Calorimetry (ITC) is the most accurate method of determining mean body skin temperature. When it is used in conjunction with heat transfer theory, mean body skin temperature can be used to calculate heat losses from the body from which the total heat loss can be determined. Infrared thermography was performed with an infrared camera that accurately and rapidly measures body temperature. ITC is an accurate measurement method for mean body surface temperature and interferes less with the immediate environment compared to IC.

The outcome of the clinical trial indicated that IC and ITC give similar results. The difference between ITC and IC for the heat loss was 1.3%. Physiological factors were most likely the primary cause of differences between the two methods at individual points in time. ITC may be less reliable for ascertaining the energy expenditure of individual infants; however, it should correctly assess changes in energy expenditure resulting from changes in the thermal environment. ITC is a portable and non-invasive method for measuring energy expenditure of infants in research and clinical settings. The results from this study will later be used to validate the simulation model developed for this thesis.

3 MATHEMATICAL MODDELING OF THERMAL REGULATION MECHANISMS IN THE HUMAN BODY

In this section a mathematical model is developed that simulates the thermal regulation response of the infant in a specified environment. This model is used to determine how the thermoregulatory system of the infant, at any premature age, adapts and functions to maintain thermal stability in a given environment (e.g. incubator or bassinette in a neonatal ward). Mathematical modelling of the human body thermal response is a valuable tool to understand the human body thermal behaviour under different environmental conditions and activity levels.

The thermoregulatory system maintains body temperature where body heat is produced by metabolism. This produced heat must be balanced against heat loss through conduction, convection, radiation, evaporation as well as heat loss via the respiratory system. This mathematical model includes analysis of heat loss from blood flow to the skin, conduction through the skin layers and heat loss from the skin surface, via convection, radiation and evaporation. The respiratory heat transfer is incorporated to analyse the importance of including heat lost via the respiratory process with respect to heat loss from the skin surface.

Section 3 starts with the derivation of heat transfer equations based on energy conservation, which allows the development of mathematical models. First the theoretical simulation model for heat loss through the skin is developed, focussing on the three different skin layers: the fat layer, inner skin layer, outer skin layer. Secondly, the theoretical simulation model for heat loss during the respiratory process is developed. Finally, the theoretical simulations for different thermal environments are developed.

3.1 Derivation of Heat Transfer Equations Based on Energy Conservation

For the mathematical models developed in this section it is necessary to solve a system of difference equations for each control volume associated with a temperature node. From the conservation of energy it follows that for a control volume the total energy expended is equal to the difference between the sum of the input energy and the sum of the output energy (Cengel & Boles, 2007) as shown in equation (3.1).

$$\Delta E/\Delta t = \sum \dot{E}_{in} - \sum \dot{E}_{out} \tag{3.1}$$

The energy that a system possesses ($\Delta E/\Delta t$) is calculated by taking the internal- (U), kinetic- (KE) and potential (PE) energy into account, as shown in equation (3.2), and multiplying the energies with the rate of mass flow ($\dot{m}$).

$$\Delta E/\Delta t = \Delta \sum \dot{m}(U + KE + PE) \tag{3.2}$$

The case studies in this theory are considered as stationary systems, thus it follows that the potential and kinetic energy can be neglected. The input and output energy can be calculated by taking into account the heat ($\dot{Q}$), work ($\dot{W}$) and mass transferred ($\dot{E}_m$), within the specified control volume, described by equation (3.3).

$$\Delta E/\Delta t = \Delta \sum \dot{Q} + \Delta \sum \dot{W} + \Delta \sum \dot{E}_m \tag{3.3}$$

The major focus in this theory is the internal energy as well as the heat and mass transferred. Equation (3.2) and equation (3.3) is used to develop equation (3.4), which relates the total internal energy of a system to the difference in total heat and mass transfer crossing the system boundaries.

$$\Delta \mathrm{U}/\Delta \mathrm{t} = \sum \dot{Q}_{in} - \sum \dot{Q}_{out} + \sum \dot{E}_{m,in} - \sum \dot{E}_{m,out} \tag{3.4}$$

The internal energy can be simplified as $U = mc\Delta T$ so that equation (3.4) is a function of mass (m), specific heat (c) and temperature (T).

$$\Delta(mcT)/\Delta t = \sum \dot{Q}_{in} - \sum \dot{Q}_{out} + \sum \dot{E}_{m,in} - \sum \dot{E}_{m,out} \tag{3.5}$$

An approximation for the specific heat constant is made, where $c_p \sim c_v = c$. Equation (3.5) may then be solved using an explicit transient numerical solution method such that equation (3.6) is developed, where h_g is the vapour enthalpy.

$$(mcT)^{t+\Delta t} = (mcT)^t + \Delta t\left(\sum \dot{Q}_{in} - \sum \dot{Q}_{out} - \dot{m}h_g\right)^t \tag{3.6}$$

Further, assume that properties such as specific heat and density are constant; It then follows that equation (3.6) can be reduced to form equation (3.7). The equation developed for calculating temperature according to the explicit finite difference method stated in equation (3.7) will be applied to predefined control volumes in the scope of the defined system, as set out in Section 3.2, Figure 3.1.

$$T^{t+\Delta t} = T^t + \Delta t/mc\left(\sum \dot{Q}_{in} - \sum \dot{Q}_{out} - \dot{m}h_g\right)^t \tag{3.7}$$

3.2 Theoretical Simulation Model for Heat Loss from the Skin

The theoretical simulation model for heat loss through the skin will focus on the heat loss from the blood through the skin to the surrounding environment. The formula for calculation of the temperature for the skin layers, as derived from the conservation of energy (see Section 3.1), are developed and expressed, based on a transient explicit numerical solution method (Cengel & Ghajar, 2011). This section discusses the separate control volumes starting with the fat layer (hypodermis) beneath the skin, followed by the inner skin layer (dermis). Section 3.2.3 discusses heat loss from the outer skin layer (epidermis) that is not covered by clothing, where Section 3.2.4 introduces the effect of clothing. A sketch of the heat transfer and control volumes with appropriate temperature nodes can be seen for an unclothed infant in Figure 3.1(a) and for a clothed infant in Figure 3.1(b).

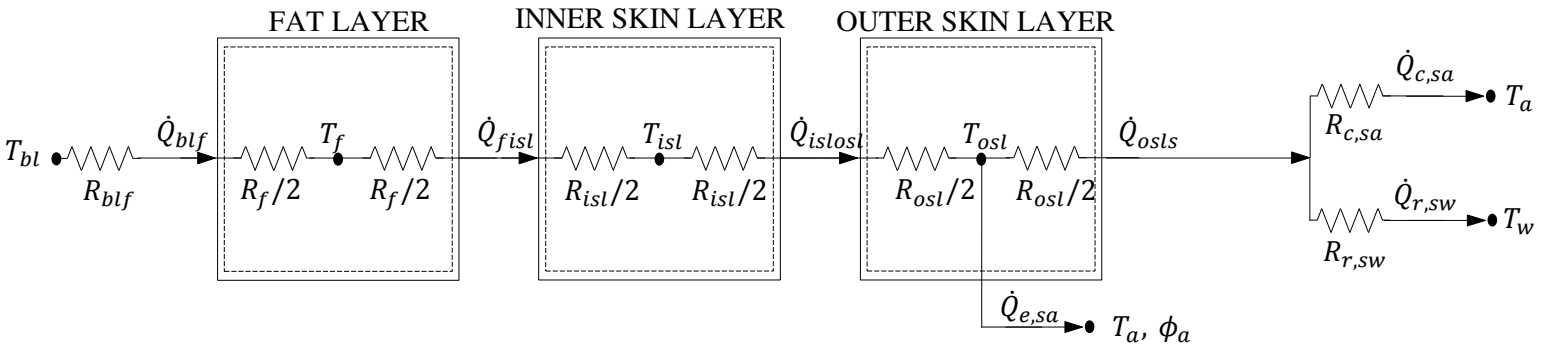

(a)

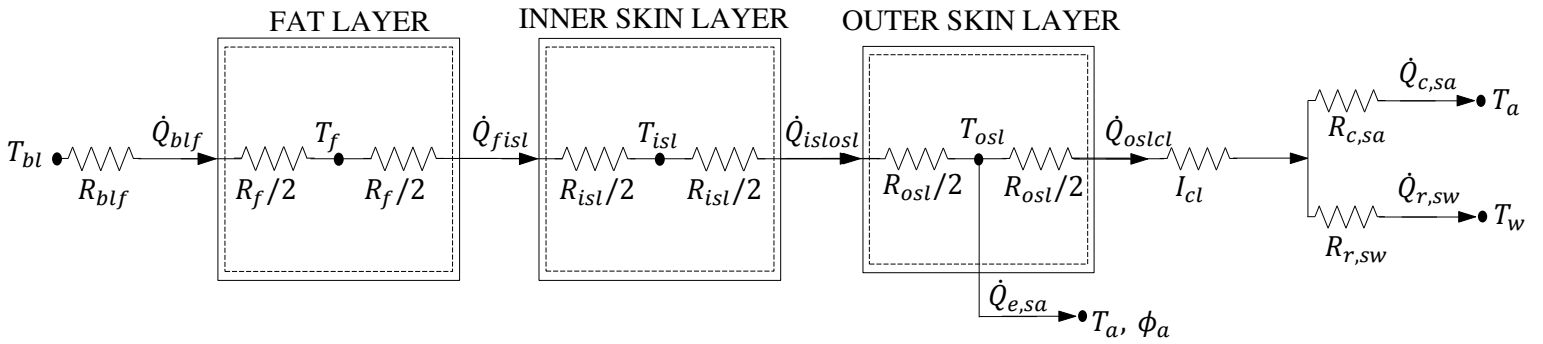

(b)

Figure 3.1: Combined thermal resistance diagrams for (a) the unclothed infant and (b) the clothed infant

3.2.1 The fat layer

The fat layer thermal resistance diagram as shown in Figure 3.1 (extracted below as Figure 3.2), introduces blood circulation into the fat layer and heat conduction to the inner skin layer (dermis).

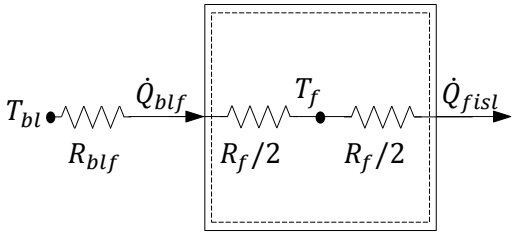

Figure 3.2: Thermal resistance diagram for the fat layer (hypodermis) beneath the skin

The temperature of the blood is a function of the metabolic heat produced and the heat transferred to the fat layer by means of convection. If the infant has fully functional metabolic heat production capability an assumption is made that the blood temperature stays constant at core body temperature throughout the simulation.

The blood temperature $T_{bl}^{t+\Delta t}$ is expressed by equation (3.8) according to the explicit finite difference method as stated in Section 3.2.

$$T_{bl}^{t+\Delta t} = T_{bl}^{t} - (\Delta t/(mc)_f)(\dot{Q}_{blf}^{t}) + \dot{Q}_{metabolic}^{t} \tag{3.8}$$

The heat transfer, via convection, from the blood to the fat $\dot{Q}_{blf}^{t}$ is given by equation (3.9), and the metabolic heat production capability is given by equation (3.10).

$$\dot{Q}_{blf}^{t} = (T_{bl} - T_{fat})/\left(R_{blf} + R_f/2\right) \tag{3.9}$$
$$\dot{Q}_{metabolic}^{t} = n(\Delta t/(mc)_f)(\dot{Q}_{blf}^{t}) \tag{3.10}$$

The efficacy of the metabolic heat production system is incorporated by n. Efficacy, in this case, being defined as the capability of producing metabolic heat to maintain constant core body temperature.

Convection R_{blf} and conduction R_f resistances for the blood and fat layer are defined respectively in equations (3.11) and (3.12). The fat layer conduction coefficient k_f is 0.16 W/mK.

$$R_{blf} = 1/h_{bl}A_f \tag{3.11}$$
$$R_f = \Delta x_f/k_f A_f \tag{3.12}$$

In order to determine the heat transfer coefficient of blood h_{bl}, assume that blood flow in arteries close to the skin is laminar because of the small artery diameters

(Valvano, 2006). Artery diameters near the skin ranges from 0.01 to 0.00001 mm. The Nusselt number for laminar flow in a tube is 3.6 (Cengel & Ghajar, 2011). The convection coefficient of the blood can now be calculated using equation (3.13), where the blood conduction coefficient k_{bl} is 0.492 W/mK.

$$h_{bl} = Nuk_{bl}/D_{artery} \tag{3.13}$$

The temperature for the fat layer $T_f^{t+\Delta t}$ is given by equation (3.14) and is developed according to the explicit finite difference method, as stated in Section 3.2.

$$T_f^{t+\Delta t} = T_f^t + (\Delta t/(mc)_f)(\dot{Q}_{blf}^t - \dot{Q}_{fisl}^t) \tag{3.14}$$

The conduction from the fat layer to the inner skin layer $\dot{Q}_{fisl}^t$ is described by equation (3.15).

$$\dot{Q}_{fisl}^t = (T_f - T_{isl})/(R_f/2 + R_{isl}/2) \tag{3.15}$$

Equation (3.16) can be used to calculate the inner skin layer conduction resistance R_{isl}, where the inner skin layer conduction coefficient k_{isl} is 0.470 W/mK.

$$R_{isl} = \Delta x_{isl}/k_{isl}A_{isl} \tag{3.16}$$

3.2.2 The inner skin layer

The inner skin layer (dermis) thermal resistance diagram is located between the fat layer and the outer skin layer (epidermis) as shown in Figure 3.1 (see extracted Figure 3.3). The equation developed for temperature of the inner skin layer $T_{isl}^{t+\Delta t}$ according to the explicit finite difference method, as stated in Section 3.2, is given by equation (3.17).

$$T_{isl}^{t+\Delta t} = T_{isl}^t + (\Delta t/(mc)_{isl})(\dot{Q}_{fisl}^t - \dot{Q}_{islosl}^t) \tag{3.17}$$

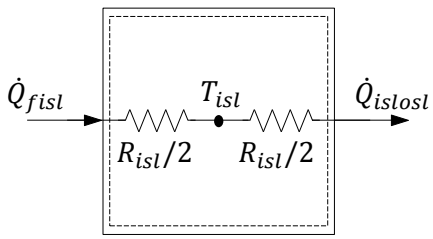

Figure 3.3: Thermal resistance diagram for the inner skin layer (dermis)

Heat is transferred from the fat layer to the outer skin layer by conduction as described by equation (3.18) and equation (3.19) respectively.

$$\dot{Q}^t_{fisl} = (T_f - T_{isl})/(R_f/2 + R_{isl}/2) \quad (3.18)$$

$$\dot{Q}^t_{islosl} = (T_{isl} - T_{osl})/(R_{isl}/2 + R_{osl}/2) \quad (3.19)$$

The conduction coefficient for the inner skin layer is given in Section 3.2.1, equation (3.16). The conduction resistance for the outer skin layer R_{osl} is defined by equation (3.20), where the outer skin layer conduction coefficient k_{osl} is 0.470 W/mK.

$$R_{osl} = \Delta x_{osl}/k_{osl}A_{osl} \quad (3.20)$$

3.2.3 The outer skin layer without clothing

The outer skin layer thermal resistance diagram as shown in Figure 3.1 (see extracted Figure 3.4) indicates how the skin temperature is affected by four heat transfer mechanisms. These heat transfer mechanisms include heat conduction through the outer skin layer $\dot{Q}^t_{islosl}$ and $\dot{Q}^t_{osls}$, convection to the air $\dot{Q}^t_{c,sa}$, radiation to the surrounding walls $\dot{Q}^t_{r,sw}$, and the evaporation of moisture from the skin surface to the air $\dot{Q}_{e,sa}$.

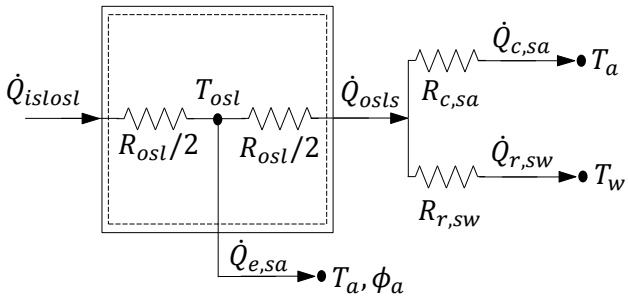

Figure 3.4: Thermal resistance diagram for the outer skin layer (epidermis) without clothing

The temperature of the unclothed outer skin layer $T^{t+\Delta t}_{osl}$ can be calculated by using equation (3.21), and is developed according to the explicit finite difference method as stated in section 3.2. Note that the convection from the air to the incubator wall is not included because it does not affect the skin temperature directly.

$$T^{t+\Delta t}_{osl} = T^t_{osl} + (\Delta t/(mc)_{osl})(\dot{Q}^t_{islosl} - \dot{Q}^t_{osls} - \dot{Q}^t_{c,sa} - \dot{Q}^t_{r,sw} - \dot{Q}_{e,sa}) \quad (3.21)$$

The conduction heat transfer into the outer skin layer $\dot{Q}^t_{islosl}$ is given by equation (3.22), where the conduction resistance R_{osl} is given in Section 3.2.2, equation (3.20). Equation (3.23) is used to calculate the conduction out of the outer skin layer $\dot{Q}^t_{osls}$.

$$\dot{Q}^t_{islosl} = (T_{isl} - T_{osl})/(R_{isl}/2 + R_{osl}/2) \quad (3.22)$$

$$\dot{Q}^t_{osls} = (T_{osl} - T_s)/(R_{osl}/2) \tag{3.23}$$

Radiation heat transfer $\dot{Q}^t_{r,sw}$ is calculated with equation (3.24), with temperature measured in Kelvin.

$$\dot{Q}^t_{r,sw} = \left(T^4_{osl} - T^4_w\right)R_{r,sw} \tag{3.24}$$

Only the convection from the outer skin layer to the surrounding air $\dot{Q}^t_{c,sa}$ is taken into account by using equation (3.25). The convection from the air to the incubator wall, indicated in Figure 3.4, is not included in calculating the outer skin layer temperature. This convection only has an effect on the incubator air and wall temperature and will be discussed in Section 3.4.

$$\dot{Q}^t_{c,sa} = (T_{osl} - T_a)/R_{c,sa} \tag{3.25}$$

Evaporation heat transfer $\dot{Q}^t_{e,sa}$ is calculated with equation (3.26) and will continue to take place until the surrounding air has saturated completely, reaching a relative humidity value of 100%.

$$\dot{Q}^t_{e,sa} = \dot{m}_{e,sa}h_{g@Tosl} \tag{3.26}$$

The calculated radiation resistance $R_{r,sw}$ must take into account the emissivity of both the skin surface ε_{osl} and the surrounding wall surface ε_w and is calculated with equation (3.27). Furthermore, a form factor must be incorporated to compensate for the amount of radiation leaving the skin and transmitting to the incubator wall surface. For the case under consideration the form factor $F_{osl,w}$ is 1, because all the radiation leaving the infant skin is assumed to transmit to the surrounding walls.

$$R_{r,sw} = \sigma/\left[\left(\frac{1-\varepsilon_{osl}}{\varepsilon_{osl}A_{osl}}\right) + \left(\frac{1}{F_{osl,w}A_{osl}}\right) + \left(\frac{1-\varepsilon_w}{\varepsilon_w A_w}\right)\right] \tag{3.27}$$

Further calculations discussed in this section revolve around the parallel development of the heat h_h and mass h_m transfer coefficients for convection and evaporation heat transfer. The convection resistance, given in equation (3.28), is dependent on the heat transfer coefficient.

$$R_{c,sa} = 1/h_h A_{osl} \tag{3.28}$$

The heat transfer coefficient is calculated by using the Nusselt number as given by equation (3.29). The Nusselt number incorporates the geometry and orientation of the infant. The body of the infant is approximated as a horizontal cylinder for the heat and mass transfer convection calculations in this section.

$$h_h = Nu_a k/L \tag{3.29}$$

The Nusselt number Nu_a used for convection consists of a combination of natural and forced convection as indicated by Equation (3.30).

$$Nu_a = (Nu_f^{1/3} + Nu_n^{1/3})^3 \tag{3.30}$$

Forced convection Nu_f is caused by air velocity in the vicinity of the infant's surroundings. An increase in the forced Nusselt number will cause an increase in the convection heat transfer. The forced convection Nusselt number for flow over a horizontal cylinder is given by equation (3.31).

$$Nu_f = 0.3 + \left[\frac{\left(0.62Re^{\frac{1}{2}}Pr^{\frac{1}{3}}\right)}{\left(1 + (0.4/Pr)^{\frac{2}{3}}\right)^{\frac{1}{4}}}\right]\left[1 + \left(\frac{Re_a}{282000}\right)^{\frac{5}{8}}\right]^{\frac{4}{5}} \tag{3.31}$$

The Reynolds number Re, given by equation (3.32), integrates the velocity as well as the dynamic viscosity and density of the surrounding air.

$$Re = V_a L/(\mu/\rho) \tag{3.32}$$

Natural convection takes place due to a temperature difference between the infant's skin and the surrounding air. The natural convection Nusselt number Nu_n is described by equation (3.33) for a horizontal cylinder.

$$Nu_n = \left(0.6 + \left[0.387Ra_a^{\frac{1}{6}}\right] / \left[1 + \left(\frac{0.559}{Pr}\right)^{\frac{9}{16}}\right]^{\frac{8}{27}}\right)^2 \tag{3.33}$$

The Rayleigh number Ra_a, calculated with equation (3.34), is used to incorporate the temperature difference between the infant's skin and the surrounding air.

$$Ra_a = g\beta\, Pr(T_{osl} - T_a)\, L^3/(\mu/\rho)^2 \tag{3.34}$$

The last heat transfer mechanism is evaporation, where the amount of water diffused from the exposed skin surface must be calculated to determine the evaporative heat loss. When the infant is born, the whole body is covered by a layer of amniotic fluid, which implicates large evaporative heat losses. When the infant is dried off and placed in an incubator or bassinette, water diffuses through the sweat glands only. The area used in equation (3.35) depends on the particular situation under consideration. Mass evaporation $\dot{m}_{e,sa}$ will continue until the air is sufficiently humidified (100% relative humidity).

$$\dot{m}_{e,sa} = h_m A_{infant} \rho(\omega_{osl} - \omega_a) \tag{3.35}$$

The mass convection coefficient h_m is calculated by equation (3.36). For a larger surrounding air velocity the mass convection coefficient will increase causing larger evaporative heat loss.

$$h_m = St_m V_a \tag{3.36}$$

For the approximations used in the development of the theoretical simulation model the dimensionless Stanton numbers, equation (3.37) for mass St_m and equation (3.38) for heat St_h, are used to relate the heat and mass convection.

$$St_m = St_h(Pr^{0.67}/Sc_a^{0.67}) \tag{3.37}$$

The Stanton numbers are used to relate mass convection to heat convection. The heat Stanton number is calculated by using the Reynolds and Nusselt numbers from Equation (3.32) and Equation (3.30).

$$St_h = Nu_a/Re_a Pr \tag{3.38}$$

The Schmidt number Sc_a, given by equation (3.39), is used to characterise the mass evaporation process and is dependent on the diffusion coefficient D_{AB}. The diffusion coefficient for evaporation from water vapour to air is $2.5x10^{-5}$.

$$Sc_a = (\mu/\rho)/D_{AB} \tag{3.39}$$

Evaporative heat transfer is dependent on the relative humidity of the surrounding air. The relative humidity is used to determine the amount of water vapour in the air using equation (3.40) and equation (3.41), where atmospheric pressure is defined as 101325 Pa.

$$P_{act,a} = \phi_a P_{sat@T_a} \tag{3.40}$$

$$\omega_a = 0.662 P_{act,a}/(P_{atm} - P_{act,a}) \tag{3.41}$$

Sections 3.2.1 to 3.2.3 constitute the theoretical model developed for the infant skin without clothing. This model is used in Section 3.4 where the infant is subject to different thermal environments.

The outer skin layer area used during simulation is dependent on the amount of skin exposed to the surrounding air layer. The exposed skin surface of the infant was calculated as a percentage value using the rule of Nines. The body of an infant is divided into the head (18%), left and right arm (9% each), chest and abdomen (18%), back (18%), right and left leg (14% each), and genitals (1%). Each of these sections make up nine present of the body's skin to cover it. Thus the percentage of area of skin exposed to the surrounding air layer was calculated as 60% and used accordingly. The remaining 40% included the back of the infant which is placed on a mattress where the assumption is made that the mattress served as perfect insulation and no heat is lost via conduction to the mattress.

3.2.4 The outer skin layer with clothing

The outer skin layer (epidermis) thermal resistance diagram is insulated with a layer of clothing as shown in Figure 3.1 (see extraction in Figure 3.5). For this diagram, heat is conducted from the outer skin layer directly to the clothing layer. An assumption is made that there is no air layer between the outer skin layer and the clothing layer, the effect of such a thin air layer has been proven to be negligibly small (Fiala, et al., 1999).

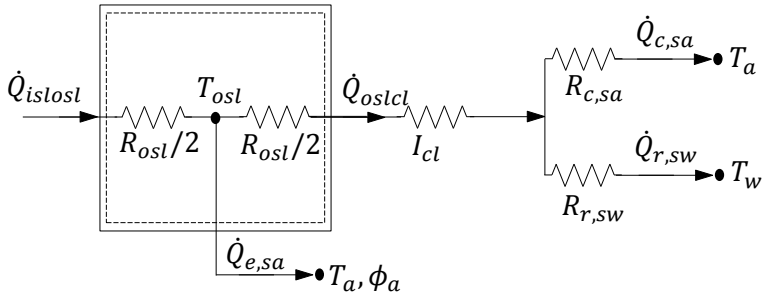

Figure 3.5: Thermal resistance diagram for the outer skin layer (epidermis) without clothing

Standard literature only provides clothing parameters not reflecting the real insulating properties, but rather providing characteristics of the particular clothing ensemble. The clothing were modelled as pure cotton, with the properties used in the development of this model being the intrinsic clothing insulation I_{cl} with a value of 0.155 W/m^{2}K and the clothing moisture permeability index of 0.34. The clothing surface factor incorporates the surface area ratio covered by clothing. For the body, the clothing factor f_{cl} value of 1 was used, because most infants are fully dressed and wrapped in a blanket when placed in the neonatal ward. A clothing factor value of 0.5 was used for the head, because it was covered with a cotton hat, leaving the face and ears exposed to heat loss from bare skin.

According to the explicit finite difference method, as stated in Section 3.2, the equation developed for temperature of the outer skin layer, with clothing, is given by equation (3.42).

$$T_{osl}^{t+\Delta t} = T_{osl}^{t} + (\Delta t/(mc)_{osl})(\dot{Q}_{islosl}^{t} - \dot{Q}_{c,cl}^{t} - \dot{Q}_{e,cl}^{t}) \tag{3.42}$$

Heat is transferred from the inner skin layer to the clothing layer, through conduction in the outer skin layer as described by equation (3.43).

$$\dot{Q}_{islosl}^{t} = (T_{isl} - T_{osl})/(R_{isl}/2 + R_{osl}/2) \tag{3.43}$$

Convection and radiation heat transfer $\dot{Q}_{c,cl}^{t}$ given in equation (3.44) is combined for this simulation model to incorporate the intrinsic clothing factor.

$$\dot{Q}_{c,cl}^{t} = (T_{osl} - T_a)/R_{c,cl} \tag{3.44}$$

Evaporation heat transfer $\dot{Q}_{e,sa}^{t}$ takes place due to a water vapour density difference between the outer skin layer and through clothing layer, influenced by the moisture permeability index. Evaporation heat transfer is described by equation (3.45).

$$\dot{Q}_{e,sa}^{t} = \dot{m}_{e,cl} h_{g@Tosl} \tag{3.45}$$

The conduction resistance $R_{c,cl}$ for the outer skin layer is defined by equation (3.46) where the heat convection coefficient h_h is calculated in the same manner as described in Section 3.2.3.

$$R_{c,cl} = [I_{cl} + 1/f_{cl}(h_h + h_r)]A_{osl} \tag{3.46}$$

The radiation coefficient h_r is calculated with equation (3.47) and the emissivity of clothing ε_{cl} is 0.93.

$$h_r = \sigma \varepsilon_{cl}\left(T_{osl}^2 + T_a^2\right)(T_{osl} + T_a) \tag{3.47}$$

Mass evaporation can be calculated in a similar manner as explained in Section 3.2.3, by using equation (3.48).

$$\dot{m}_{e,sa} = h_{m,cl} A_{infant} \rho(\omega_{osl} - \omega_a) \tag{3.48}$$

The mass convection coefficient has to be adjusted to incorporate the cotton permeability index and can be done using equation (3.49).

$$h_{m,cl} = 1/[(I_{cl}/i_{cl}) + 1/(f_{cl} h_m)] \tag{3.49}$$

To summarise it is seen that Section 3.2.1 to 3.2.3 together with Section 3.2.4 constitutes the theoretical mathematical model developed for the infant skin with clothing. This model is used in Section 3.4 where the infant is subjected to different thermal environments.

3.3 Theoretical Simulation Model for Heat Loss during the Respiratory Process

The theoretical simulation model for heat loss during the respiratory process is developed in order to determine whether the heat transferred during the respiratory process has an important effect with respect to thermal regulation of the human infant body. The literature study indicated that the conditioning of air was done in the nasal cavity and the conducting zone. Heat is transferred to the inhaled air only by convection and evaporation.

Taking the inhalation and exhalation cycles into account makes the heat transfer analysis for the respiratory system a bit more complex. For the inhalation cycle the heat is transferred from the blood to the nasal cavity and trachea walls which in turn transfer heat via convection and evaporation to the inhaled air. The core temperature varies from one person to another. For the purpose of this simulation model it is assumed that the exhalation cycle ends with exhaled air at 100% relative humidity and 37 °C. Figure 3.6 describes the control volume under consideration during the respiratory process.

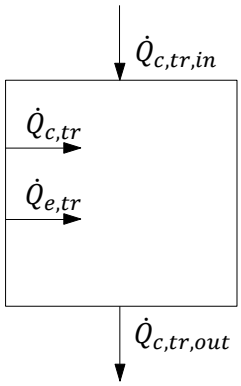

Figure 3.6: Detailed control volume developed for heat transfer during the respiratory process

The mass flow rate of the inhaled air $\dot{m}_{inh}$ is the varying property which, together with the temperature of the inhaled air, affects heat transfer during the respiratory process. The mass flow rate is directly dependent on the breathing rate (BR), tidal volume (TV) and weight (W) of the infant, and can be calculated using equation (3.50).

$$\dot{m}_{inh} = (BR/60)(TV/10^6)W\rho_a \tag{3.50}$$

A different approach to the previous sections is used to develop the theoretical heat loss model for the respiratory system. The area required for heat transfer A_{tr} has to be calculated. This is done because the air must reach 37 °C and 100% relative humidity before it reaches the alveoli in the lungs. Then the calculated area is used to determine the heat transfer by convection and evaporative mass transfer. The area required for complete conditioning of inhaled air can be calculated using equation (3.51).

$$A_{tr} = \frac{\dot{m}_{inh}(h_{tr,out} - h_{tr,in})}{h_{m,tr}\rho(\omega_{tr} - \omega_a)h_{f@T_{tr}} + h_{h,tr}(T_{tr} - T_a)} \tag{3.51}$$

Heat is transferred from the trachea wall to the inhaled air by convection $\dot{Q}_{c,tr}$. Due to a temperature difference between inhaled and exhaled air, heat is also transferred to the inhaled air, via convection, by air mixture specified heat convection coefficients as given by equation (3.52).

$$\dot{Q}_{c,tr} = h_{h,tr}A_{tr}(T_{tr} - T_a) + \dot{m}_{inh}(h_{tr,out} - h_{tr,in}) \quad (3.52)$$

The evaporation heat transferred $\dot{Q}_{e,tr}$ to the inhaled air is described by equation (3.53). The trachea wall is assumed to be completely moist. Equation (3.53) indicates that if the inhaled air is fully humidified, no evaporation heat transfer will take place during the respiratory process.

$$\dot{Q}_{e,tr} = h_{m,tr}A_{tr}\rho(\omega_{tr} - \omega_a)\, h_{f@T_{tr}} \quad (3.53)$$

The heat convection coefficient $h_{h,tr}$ for convection from the trachea wall is calculated using equation (3.54). The Nusselt number incorporates the geometry of the trachea which is simulated as a horizontal tube with a specified diameter.

$$h_{h,tr} = Nu_{f,tr}k/D_{tr} \quad (3.54)$$

The Nusselt number is dependent on the type of flow occurring within the trachea during a respiratory cycle. The flow can be laminar, transitional or turbulent and is determined by calculating the Reynolds number Re_{tr}, equation (3.55). For the small mass flow rates of inhaled air the Reynolds number is smaller than 2 300, which indicates that a Nusselt number of 3.66 can be used to calculate the heat convection coefficient.

$$Re_{tr} = V_{tr}D_{tr}/\upsilon_{tr} \quad (3.55)$$

The velocity V_{tr} used for calculation of the Reynolds number is calculated by using equation (3.56) and is dependent on the mass flow rate of the inhaled air and the cross sectional area A_{tr_c} of the trachea calculated by equation (3.57).

$$V_{tr} = \dot{m}_{inh}/(\rho_a A_{tr\_c}) \quad (3.56)$$

$$A_{tr\_c} = \pi(D_{tr}/2)^2 \quad (3.57)$$

Convection coefficients for the inhaled air $h_{tr,in}$, equation (3.58), and exhaled air $h_{tr,out}$, equation (3.59), are dependent on the moisture content and temperature of the inhaled and exhaled air respectively. It is assumed that exhaled air is at the trachea temperature and full humidity.

$$h_{tr,in} = c_p T_a + \omega_a(2501 + 1.89T_a) \quad (3.58)$$

$$h_{tr,out} = c_p T_{tr} + \omega_{tr}(2501 + 1.89T_{tr}) \quad (3.59)$$

Next the mass flow rate of evaporation from the trachea walls to the inhaled air $\dot{m}_{tr}$ is determined using equation (3.60). Mass evaporation from the trachea walls will continue until the inhaled air is fully humidified.

$$\dot{m}_{tr} = h_{m,tr}A_{tr}\rho(\omega_{tr} - \omega_a) \quad (3.60)$$

Mass convection coefficient $h_{m,tr}$ is calculated in a similar manner as discussed in Section 3.2.3. For faster breathing rates, the velocity of inhaled air will increase and thus cause the mass transfer convection coefficient to increase accordingly.

$$h_{m,tr} = St_{m,tr} V_{tr} \tag{3.61}$$

The mass and heat Stanton numbers, equation (3.62) for mass $St_{m,tr}$ and (3.63) for heat $St_{h,tr}$, are again used to relate the mass and heat convection coefficients.

$$St_{m,tr} = St_{h,tr} Pr^{0.67} / Sc_{tr}^{0.67} \tag{3.62}$$

$$St_{h,tr} = Nu_{f,tr} / (Re_{tr} Pr_{T_{tr}}) \tag{3.63}$$

The Schmidt number Sc_{tr} is used to characterise the mass evaporation process, provided that 0.7 < Sc < 160. The diffusion coefficient D_{AB} is defined as $2.5x10^{-5}$ for diffusion from water vapour to the inhaled air.

$$Sc_{tr} = (\mu/\rho)/D_{AB} \tag{3.64}$$

Evaporative heat transfer from the trachea walls is dependent on the relative humidity of the inhaled air. The relative humidity is used to determine the amount of water vapour in the air using equation (3.65) and equation (3.66), where atmospheric pressure P_{atm} is defined as 101325 Pa.

$$P_{act,tr} = \phi_{tr} P_{sat@T_{tr}} \tag{3.65}$$

$$\omega_{tr} = 0.662 P_{act,tr} / (P_{atm} - P_{act,tr}) \tag{3.66}$$

Section 3.3 constitutes the theoretical model developed for heat transferred during the respiratory process. This model, together with the theoretical model developed for heat transfer from the skin in Section 3.2, is used in Section 3.4, where the infant is subjected to different thermal environments.

3.4 Theoretical Simulation Model of the Thermal Environment

The theoretical simulation models for the thermal environments discussed in this section is developed using the simulation models discussed in Section 3.2 and Section 3.3 for heat loss through the skin and during the respiratory process, respectively. The thermal environment models will be used to analyse thermal stability of the infant in various thermal environments. “Thermal stability is that property of a system which opposes variations in heat content under conditions allowing net thermal exchange between object and environment” (Adamsons, 1966). Thermal stability is primarily a function of body size and surface area and is dependent on the degree to which heat output can be altered.

The first thermal environment to consider is in the delivery room where the infant is removed from a warm and constant thermal intrauterine environment to a colder extrauterine environment. The second thermal environment considered is the

closed temperature and relative humidity controlled incubator. Incubators provide an environment to maintain the body temperature of neonates by adjusting and maintaining suitable ambient conditions. Incubators are used for preterm infants as well as some ill full term infants. The third and last thermal environment to consider is the open radiant warmer type incubator. These theoretical simulation models of the three respective thermal environments will enable a clear understanding of heat loss and thermal regulation of the infant during the first days of life.

3.4.1 Thermal heat loss during the delivery procedure

After being in a relatively stable thermally neutral uterus, the neonate enters a cooler unstable environment resulting in significant heat loss which can cause hypothermia during the first minutes of life. The temperature of the delivery room stays constant but can vary from 18 °C to 25 °C depending on the doctor's preference. The thermal resistance diagram in Figure 3.7 depicts the relevant heat losses occurring during the delivery procedure.

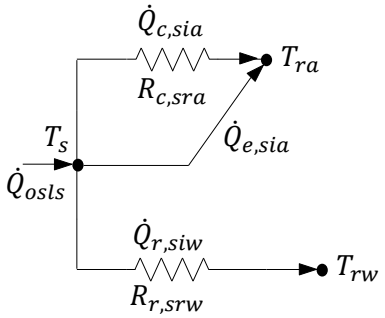

Figure 3.7: Thermal resistance diagram for heat loss from the skin during a delivery procedure

As soon as the infant is born it is still covered in a layer of amniotic fluid, which causes extremely high evaporative heat loss and results in fast temperature drops. Equation (3.67) is used to calculate the temperature drop accordingly.

$$T_s^{t+\Delta t} = T_s^t + (\Delta t/(mc)_{osl})(\dot{Q}_{osls}^t - \dot{Q}_{c,sra}^t - \dot{Q}_{r,srw}^t - \dot{Q}_{e,sra}) \quad (3.67)$$

The theoretical simulation model for this section can be used to compare conventional drying after birth to placing the infant in the incubator before drying.

3.4.2 The infant in a closed temperature and humidity controlled incubator environment

The heat output in a closed incubator is regulated by servo control to keep the skin temperature constant, where the skin temperature is regularly measured on the abdomen of the infant; air temperature and relative humidity can be controlled

separately. Increased humidity, heat shields and clothing are used to decrease heat losses.

The thermal resistance diagram depicted in Figure 3.8 indicates how the skin temperature T_s, is affected by various convection and radiation heat losses to the incubator environment when no temperature and humidity control is activated. Heat losses to the room also occur when it is assumed that the incubator is placed in an air conditioned room with constant air and wall temperatures.

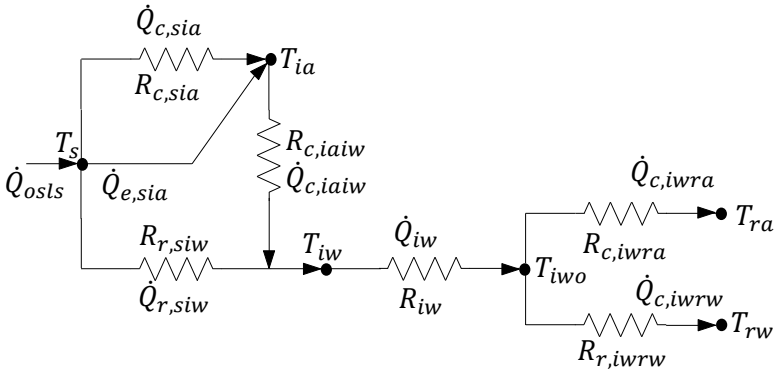

Figure 3.8: Thermal resistance diagram for heat loss from the skin in a closed incubator without temperature and humidity control

Heat is transferred from the infant's skin through the incubator wall into the air-conditioned room. The skin temperature will change according to equation (3.68) if the infant is placed in a closed incubator where no thermal control is applied to the air temperature and humidity within the incubator.

$$T_s^{t+\Delta t} = T_s^t + (\Delta t/(mc)_{osl})(\dot{Q}_{osls}^t - \dot{Q}_{c,sia}^t - \dot{Q}_{r,siw}^t - \dot{Q}_{e,sia}) \tag{3.68}$$

Air temperature and relative humidity in the incubator will increase with convective and evaporative heat losses from the infant's skin according to equation (3.69).

$$T_{ia}^{t+\Delta t} = T_{ia}^t + (\Delta t/(mc)_{ia})(\dot{Q}_{c,sia}^t + \dot{Q}_{e,sia} + \dot{Q}_{c,tr} + \dot{Q}_{e,tr} - \dot{Q}_{c,iaiw}^t) \tag{3.69}$$

The temperature of the incubator walls will also increase due to radiation heat loss from the infant's skin projected onto the incubator walls, equation (3.70). Heat will also transfer from the incubator walls to the room, equation (3.71).

$$T_{iw}^{t+\Delta t} = T_{iw}^t + (\Delta t/(mc)_{ia})(\dot{Q}_{c,iaiw}^t) + (\Delta t/(mc)_{iw})(\dot{Q}_{r,siw}^t - \dot{Q}_{iw}^t) \tag{3.70}$$

$$T_{iwo}^{t+\Delta t} = T_{iwo}^t + (\Delta t/(mc)_{iw})(\dot{Q}_{iw}^t - \dot{Q}_{c,iwra} - \dot{Q}_{r,iwrw}^t) \tag{3.71}$$

The thermal resistance diagram depicted in Figure 3.9 indicates how the skin temperature T_s, is affected by convection and radiation heat losses to the incubator

environment when temperature and relative humidity control is activated. Heat losses to the room are constant when it is assumed that the incubator is placed in an air conditioned room with constant air and wall temperatures.

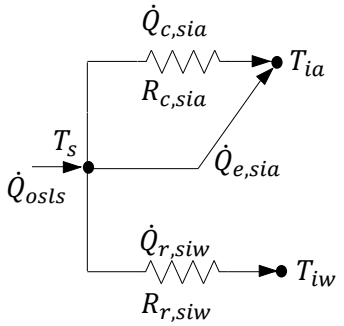

Figure 3.9: Thermal resistance diagram for heat transfer from the skin in a closed incubator with temperature and humidity control

Equation (3.72) is applicable for this thermal environment because the wall temperature of the incubator is constant and it is assumed that the incubator is placed in an air conditioned room with constant air and wall temperatures. Heat is conducted to the skin surface where it is lost by convection and evaporation to the air in the incubator, and radiation to the walls of the incubator, as indicated by equation (3.72).

$$T_s^{t+\Delta t} = T_s^t + (\Delta t/(mc)_{osl})(\dot{Q}_{osls}^t - \dot{Q}_{c,sia}^t - \dot{Q}_{e,sia} - \dot{Q}_{r,siw}^t) \tag{3.72}$$

3.4.3 The infant in an open radiant warmer environment

The use of radiant warmers increases convective and evaporative heat loss from the infant's skin, but radiative heat loss is eliminated. The biggest advantage of radiant warmers in comparison to closed servo controlled incubators is that radiant warmers provide easy access for the caretakers without disturbing the thermal environment.

The thermal resistance diagrams in Figure 3.10 depicts how heat is transferred from the infant's skin to the environment for a disabled radiant warmer (Figure 3.10(a)) and for an activated radiant warmer (Figure 3.10(b)). When the radiant warmer is activated the radiant heat transferred is adjusted by constant monitoring of the abdominal skin temperature.

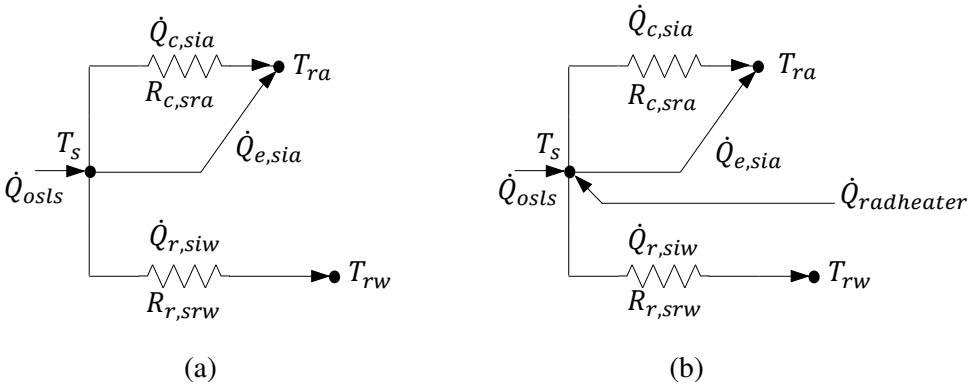

Figure 3.10: Thermal resistance diagram for heat transfer from the skin in an (a) disabled open radiant warmer and (b) activated open radiant warmer

Equation (3.73) indicates how the skin temperature (T_s), is affected by various convection and evaporation heat losses to the surrounding environment when no radiation control is activated. Heat losses occur directly to the air in the room when it is assumed that the radiant warmer is placed in an air conditioned room with constant air and wall temperatures.

$$T_s^{t+\Delta t} = T_s^t + (\Delta t/(mc)_{osl})(\dot{Q}_{osls}^t - \dot{Q}_{c,sra}^t - \dot{Q}_{r,srw}^t - \dot{Q}_{e,sra}) \tag{3.73}$$

Equation (3.74) is used to calculate radiative heat needed to keep the skin temperature constant. The radiation heat plus metabolic heat production must equal all the heat losses in order to maintain constant body temperature and can be used for heat gain by the infant in cases of decreased core body temperatures.

$$\dot{Q}_{radheater} = \dot{Q}_{c,sra}^t + \dot{Q}_{r,srw}^t + \dot{Q}_{e,sra} - \dot{Q}_{osls}^t \tag{3.74}$$

4 CLINICAL TRAIL AND DATA ACQUISITION

Thermal regulation is a critical physiological function that is closely related to the transition and survival of the neonate. An understanding of transitional events and the physiological adaptations that neonates must make is essential in helping the medical professionals provide an appropriate thermal neutral environment to assist the neonates in maintaining thermal stability. A clinical trial will be conducted to facilitate in understanding the maintaining of thermal stability in neonates. The clinical trial is used for data acquisition where the necessary data will be used to verify the developed theoretical mathematical simulation model for heat transfer in neonates.

For information regarding the Ethical procedures completed during the clinical trial refer to Addendum B. A summary of the protocol synopsis is provided in Addendum B.1 with the informed consent form presented in Addendum B.2. Ethical approval for this clinical trial was granted by the Health Research and Ethics Committee (Refer to Addendum B3)

4.1 Aims and Objectives

The hypothesis states that a term infant of 39 weeks gestation or older has an appropriate metabolism to thermally regulate the core temperature if the environment conditions are in a respectable range. This hypothesis will be tested with the developed computer simulation completed in the larger scope of this project. The validity of the developed simulation model will be established by comparison with information gleaned from the measurements stipulated in the summary of methodology.

4.2 Description of Subject Population

The data acquisition for the clinical trial includes a subject group of 15 boys and 15 girls with gestational age of 39 weeks. Race or ethnic group is of no relevance to the project. The infants must be regarded as “healthy” by the residing paediatrician or doctor. Healthy implies that the infant is not growth restricted or small for its gestational age. The method of birth is not of critical importance for this protocol.

4.3 Summary of Methodology

The methodology of this protocol is based on the standard procedures of data collection at birth, with the exception that the room temperatures will also be recorded for data simulation purposes. No invasive methods will be used to obtain the data needed for this protocol. Data that will be recorded for this protocol include the weight, length, head circumference and skin thickness of infant after delivery procedure as well as the skin and axillary temperatures.

The breathing rate, axillary and skin temperatures at various locations on the body of the infant will be recorded for 60 minutes, along with the corresponding room air temperature and relative humidity. The breathing rate will be taken once every hour. This information is recorded every 10 minutes while the infant is placed in a bassinette in the post natal ward. Temperatures will be recorded in the post natal ward at every measurement interval and noted on the protocol data collection form, Figure 4.1. It must also be indicated whether a measurement is taken whilst the mother is holding the infant.

The length of the infant will be measured using a sterilised plastic tape measure. The infant must be placed on a flat surface without a diaper to provide free movement of the legs. With the legs held flat the length is measured by placing the tape measure on the surface at the same position as the crown of the head and measuring the length to the ball of the foot. The measurement of the length is taken using the centimetre scale on the plastic tape measure. The accuracy is good enough for protocol data collection purposes. The head circumference is measured using the same plastic tape measure. A paper tape is not used because it has too much variability in printed measurement intervals. A metal tape would also not be used due to the increased risk of lacerations on the infant during the measurement procedure.

No pain or discomfort is associated with the measurements undertaken for the protocol data collection. The baby can be with the mother although this should be indicated in the protocol data form. Also feeding times can be indicated but will not have a great effect on the outcome of the research because the metabolic rate is not monitored or used as critical input to the simulation. Feeding times are non-relevant to the research project.

UNIVERSITY OF STELLENBOSCH
DEPARTMENT OF MECHANICAL AND MECHATRONIC ENGINEERING

PROTOCOL DATA

Age/Ouderdom:_____
Weight/Gewig: _____
Length/Lengte: _____
Head Circumference/Kop Omtrek: _____
Breathing Rate/Asemhalings Tempo: _____
Skin Thickness/Vel Dikte: _____

1	Head	7	Leg L
2	Neck	8	Leg R
3	Chest	9	Upper Arm L
4	Abdomen	10	Upper Arm R
5	Thigh L	11	Forearm L
6	Thigh R	12	Forearm R

		Room		Infant														
	Time	**Temperature**	**Relative Humidity**	**Breathing Rate**	**Axillary**	**1**	**2**	**3**	**4**	**5**	**6**	**7**	**8**	**9**	**10**	**11**	**12**	
1																		
2																		
3																		
4																		
5																		
6																		
7																		
8																		
9																		
10																		

Figure 4.1: Protocol data acquisition form

5 EXPERIMENTAL MODELLING OF THE RESPIRATORY PROCESS

Potentially life threatening respiratory problems is frequent in, although often restricted to, the neonatal period due to critical physiological changes necessary for adaptation to air breathing after birth. Constructing an experimental respiratory model is an excellent way to observe the basic concepts of the respiratory system and how it functions. This section discusses the ventilation component of the respiratory system, with focus on an experimental model which mimics the heat exchange that occurs during the respiratory process.

The first section will discuss the physical modelling of the respiratory process which includes the experimental mechanical lung apparatus, instrumentation and data capture as well as the heat transfer design of the experimental mechanical lung apparatus. Operational and safety procedures are briefly discussed with regards to the start-up and operation procedure, the shut-down procedure and the storage instructions.

5.1 Physical Modelling of the Respiratory Process

The physical modelling of the respiratory process is focused on mimicking the physiological respiratory process. The experimental mechanical lung apparatus is designed to imitate the naturally occurring heat transfer mechanisms in the conducting zone of the respiratory physiology. The experimental mechanical lung apparatus is based on the heat transfer model developed for the mathematical simulation model in Section 3.3. This experimental lung apparatus is also used to validate the mathematical modelling of the respiratory process.

The chosen design of the experimental mechanical lung apparatus along with the instrumentation used for data capture is discussed in this section. The control mechanisms used, and calculations needed for different breathing patterns and respiratory rates are also covered.

5.1.1 Experimental mechanical lung apparatus

The experimental mechanical lung apparatus, shown in Figure 5.1, closely mimics the mechanics of the respiratory system with respect to the respiratory rate and breathing pattern. This experiment was designed in order to imitate the naturally occurring heat transfer mechanisms in the conducting zone of the respiratory physiology.

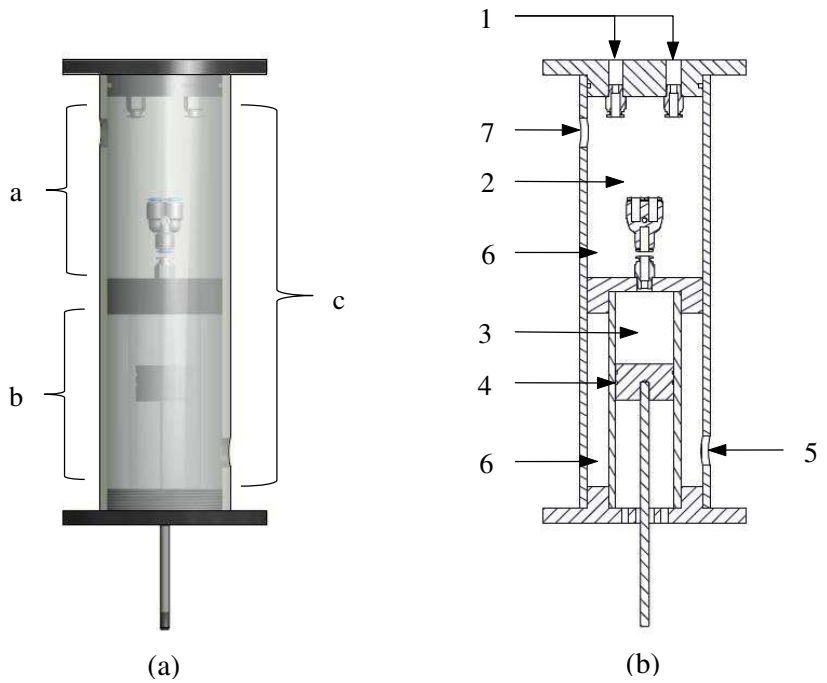

Figure 5.1: The (a) experimental mechanical lung apparatus with (b) a cross sectional view and descriptive numbers

The model developed for the experimental mechanical lung apparatus shown in Figure 5.1(a) is comprised of three functioning parts. In the first unit, a, the air passes through the conducting zone, where heat is transferred from the tube walls to the inhaled air, into the internal lung volume. The second unit, b, consists of the diaphragm movement, which controls the respiratory rate and breathing pattern of the inhaled air. The last unit, c, entails circulation of water at core temperature to enable heat transfer to inhaled air and to maintain core temperature in the internal lung volume.

Figure 5.1(b) is a cross sectional view of the experimental mechanical lung apparatus to indicate how this model functions to represent the respiratory system physiology. The numeric descriptions in Figure 5.1(b) are listed in Table 5.1 which contains a description on the represented physiological respiratory function.

Table 5.1: Experimental mechanical lung apparatus descriptions

1	Inhaled/Exhaled Air	5	Water inlet
2	Trachea	6	Water circulation
3	Internal lung volume	7	Water outlet
4	Diaphragm		

The conducting zone (Figure 5.1(a), a) consists of the oral and nasal cavity represented by 1 in Figure 5.1(b) where the air enters at the top of the experimental apparatus. These two channels follow into the laced tubing that

represents the trachea 2 where heat is transferred to the air. The tubing is lined with lace that is moist in order to also humidify the air while it is being warmed. Heat transferred to the inhaled air as well as humidification is not controlled and will occur naturally as in our respiratory system.

The internal lung volume 3 in Figure 5.1(b) represents the functional residual capacity, which is the amount of gas remaining in the lungs after normal tidal expiration. This air must always be at 37 °C and completely humidified. The diaphragm 4 is used to control the respiratory rate and the breathing pattern.

Lastly the water circulation, as shown by Figure 5.1(a) c, is used to keep the mechanical lung environment at the core body temperature of 37 °C. The detail of Figure 5.1(b) shows how water is pumped in at the bottom of the experimental apparatus 5 and circulates around the internal lung volume 6 and conducting zone to the top of the experimental apparatus where it exits 7 to be reheated.

5.1.2 Instrumentation and data capture

The set-up for the experimental mechanical lung is shown in Figure 5.2. The set-up includes the experimental mechanical lung apparatus as shown in Figure 5.1 as well as the electrical components used for control and data capture.

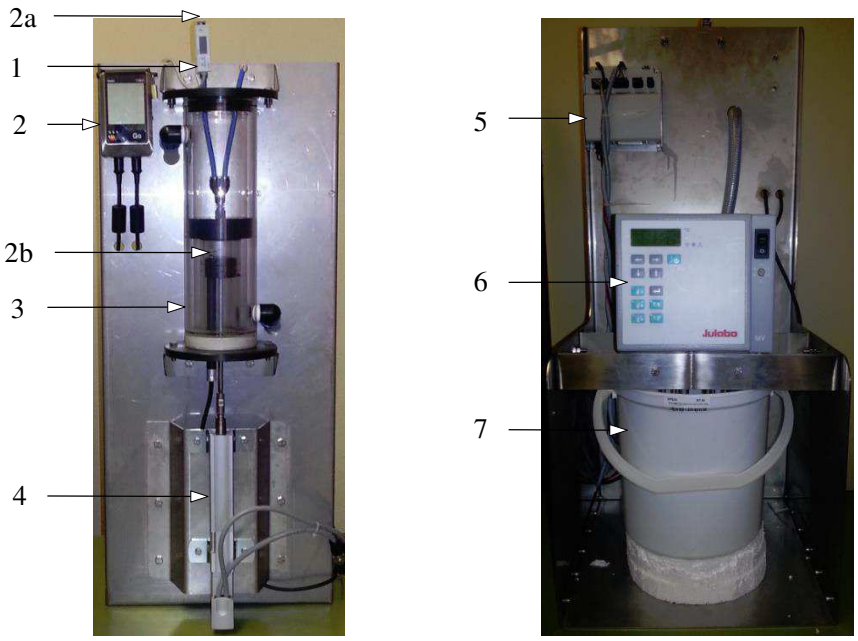

Figure 5.2: Experimental mechanical lung apparatus with electrical components

Figure 5.2(a) shows the front of the assembly while Figure 5.2(b) shows the rear of the assembly. All components used for operation and data capture, indicated by circled numbers, are listed in Table 5.2.

Table 5.2: Experimental mechanical lung apparatus electrical component list

1	FESTO flow sensor	4	EPCO electric cylinder with spindle drive
2	TESTO data logger	5	CMMO controller
2a	Temperature probe for inhaled/exhaled air monitoring	6	JUBALO water heater/circulator
2b	Temperature probe for internal lung air monitoring	7	Circulation water bucket
3	Experimental mechanical lung apparatus		

The FESTO flow sensor 1 is placed before the nasal or oral cavity. This device is used to measure the volumetric air flow rate of the inhaled and expired air caused by the movement of the diaphragm. This flow rate is calculated and based on tidal volume and breathing rate, where inhalation through the oral and nasal cavity can be simulated. The flow sensor operates on a 24 V input voltage and measures 0.1 to 1 litre/minute volumetric flow rate.

The TESTO data logger 2 comprises of two input channels for T-type thermocouples (able to measure temperature and relative humidity). The data logger can measure the input from the thermocouples on a cycling time of 1 reading per second to one reading every 24 hours. This device has an internal AA battery power supply of 3.6 V. The two input channels of the data logger will be used to monitor the temperature and relative humidity of the inhaled/exhaled air as well as the temperature and relative humidity of the air in the internal lung volume.

The EPCO electric cylinder drive 4 is a mechanical linear drive with piston rod and permanently attached motor. The driving motor consists of an electrically actuated spindle that converts the rotary motion of the motor into linear motion of the piston rod. This electric cylinder is attached to the piston in the experimental mechanical lung apparatus and is used to mimic the movement of the diaphragm during normal tidal volume respiration.

The EPCO electric cylinder drive 4 and the CMMO controller 5 form one operational unit. The breathing pattern (stroke length) and respiratory rate (frequency) is programmed from the computer into the CMMO controller which in turn sends the commands to the EPCO electric cylinder drive. This system is programmed from the computer but has its own 24 V power supply.

The JUBALO water heater/circulator 6 employs a circulator head and heating element submerged in a water reservoir tank 7. Electronic proportional temperature control adapts the heat supplied from the element to the water in the water reservoir tank according to thermal requirements. The thermal requirements for this set-up are to regulate the temperature of the water in the reservoir tank at

37 °C. This device also supplies the experimental mechanical lung apparatus with the heated water from the reservoir tank, which is also continuously circulated by the circulator head during operation of the experiment.

The operational diagram of the set-up for the experimental mechanical lung apparatus is shown in Figure 5.3. This operational diagram indicates how the measuring and electrical control components are integrated to form one functional unit that represents the mechanics of the respiratory system.

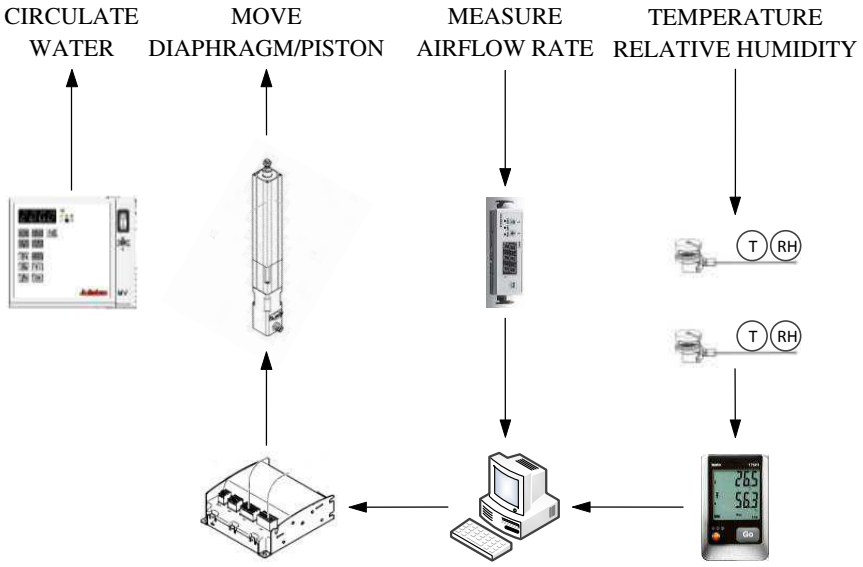

Figure 5.3: Operational diagram for the setup of the experimental mechanical lung apparatus

The theoretical simulation model for heat loss during the respiratory system suggests that the experimental mechanical lung apparatus will successfully mimic the thermo regulatory physiology and operation of the respiratory system. One limitation in this experiment is not being able to keep the lace in the trachea moist for continuous evaporation to inhaled air. The model can be further developed to simulate various breathing disorders in order to analyse and understand their effects better.

5.1.3 Heat transfer design of the experimental mechanical lung apparatus

The heat transfer design of the experimental mechanical lung apparatus involves calculating the surface area of the conducting zone needed for sufficient heating and humidification of inhaled air. This experimental set-up is used to validate the calculated surface area of the conducting zone in Section 3.3. This experiment will be conducted for varying respiratory rates and tidal volumes. The only variable that has to be determined for use in the experiment is the stroke length of the piston which is directly dependent on the volumetric flow rate, which is derived in this section.

The volumetric flow rate is dependent on the breathing rate (BR), tidal volume (TV) and weight (W) of the infant as described by equation (5.1). For the duration of the testing procedure for this experimental mechanical lung apparatus the weight will be considered constant at 3.3 kg, the growth chart average weight of a term infant.

$$\dot{V}_{inh} = BR(TV/10^3)W \tag{5.1}$$

Tidal volume for term infants varies from 5 to 7 ml/kg. This experiment will be conducted for different tidal volumes at a constant respiratory rate, to examine the effect that larger tidal volumes have on surface area needed for heat transfer to the inhaled air. Equation (5.2) is used to determine the total volume of air that enters the internal lung during one respiratory cycle and is dependent on the tidal volume.

$$V_{tidal} = (TV)(W)/10^6 \tag{5.2}$$

This volume of air can then be used to determine the stroke length of the piston for different tidal volumes. First the cross sectional area of the internal lung volume is determined according to equation (5.3). The diameter of the internal lung volume is fixed at 40 mm.

$$A_{l,c} = \pi(D_l/2)^2 \tag{5.3}$$

Finally the stroke length can be determined by division of the cross sectional area of the internal lung volume by the volume calculated by equation 4.2. From these equations it is clear that for larger tidal volumes the stroke length will increase.

$$SL = V_{tidal}/A_{l,c} \tag{5.4}$$

5.2 Operational Procedures and Safety

This section is devoted to instructions for operational procedures and safety of the set-up of the experimental lung apparatus. Operational procedures include the start-up instructions with a separate section on fault finding during the start-up procedure or during operation of the experimental set-up. Calibration is also briefly discussed as most of the components have calibration certificates. Safety instructions are also included for attention during operation of the experiment. The section ends of with instructions for the shut-down procedure and storage of the experimental set-up.

5.2.1 Start-up and operation procedure

The start-up and operation procedure comprises of attaching and configuring all the components (experimental mechanical lung apparatus, FESTO flow sensor, EPCO electric cylinder drive and CMMO controller, TESTO data logger and the JULABO water heater/circulator) needed for the completion of the experiment.

The steps are discussed with regards to each of the components of the experimental set-up outlined in Section 5.1.2.

Step 1: The FESTO flow sensor must be supplied with a 24V power supply. Attach the flow sensor to one of the tubes supplied for inhalation and exhalation. When the power supply is switched on ensure that the flow sensor is functioning correctly by blowing air through the tube and confirming that the sensor gives a relevant reading.

Step 2: This step involves setting up the TESTO data logger with the humidity/temperature probes. First insert the 3.6V AA battery into the TESTO data logger and wait for 'rST' to appear on the screen. Also connect the humidity/temperature probes onto channel 1 for monitoring of the internal lung volume and channel 2 for monitoring of the inhaled/exhaled air. Connect the data logger to the computer via a USB port and use the ComSoft Basic 5 Software to configure the data logger in order to log humidity and temperature on channel 1 and 2 and set the measurement cycle for 1 second intervals. Also check that both probes give the same readings when placed in the same environment to ensure that they are in working condition.

Step 3: The EPCO electric cylinder drive and CMMO controller will now be configured. Attach the shaft of the electric cylinder drive to the diaphragm piston of the experimental mechanical lung set-up. Supply the CMMO controller with 24 V external power supply and make sure that it is switched on. Connect the controller to the computer with an Ethernet cable and open the FESTO configuration tool. Configure the CMMO controller by setting the correct operating frequency and stroke length.

Step 4: Fill the water reservoir tank to the indicated level. Switch on the JULABO water heater/circulator. Program the operating temperatures, T1=36 °C and T2=37 °C. Also program the upper and lower temperature limits in order for the alarm to sound when malfunctioning occurs. The lower temperature limit is set to 15 °C and the upper temperature limit is set to 45 °C.

Step 5: A few instructions will happen simultaneously. First start logging the temperatures with the TESTO data logger. Next the JULABO water heater/circulator must be switched on to start heating and circulating the water through the experimental mechanical lung. The monitoring of the temperatures must be continued until the internal lung volume temperature reached 37 °C and approximately 100% relative humidity. The system is now in operation equilibrium and ready for the testing scenarios.

Step 6: This is the operation procedure. Enable the software connection for the CMMO controller, load configuration onto CMMO controller and check that the EPCO electric cylinder drive operates as instructed when it is software enabled. Also restart the TESTO data logger. This step can be repeated for different operating frequencies and stroke length. For correct functioning of the mechanical

lung a moist lace of specified area has to be inserted into one of the inhalation/exhalation tubes.

When using the water heater circulator remember that the volume of the water will increase due to thermal expansion when the water bucket temperature rises. Exercise caution when emptying hot bath liquids.

5.2.2 Shut-down procedure and storage instructions

The shut-down procedure is the reverse of the start-up procedure. This section enables the user to shut down and disassemble all components. It also provides further instructions regarding the storage of all the components. None of these components are especially sensitive but should be handled with care to avoid unnecessary damage.

Step 1: Shut down the JULABO water heater/circulator. Switch off at the button provided and then at the wall power supply. This will cause the experimental lung set-up to drain from the water. When that is finished empty the water reservoir for storage.

Step 2: Stop the EPCO electric drive cylinder procedure, disconnect the controller from the computer and switch off the power supply. Disassemble the cylinder drive from the diaphragm piston. Also switch off the power supply for the FESTO flow sensor, remove the flow sensor from the inhalation/exhalation channel and store in the provided container.

Step 3: Stop recording data with the TESTO data logger and remove the relative humidity/temperature probes from the experiment. Place the probes back in the storage containers provided. Remove the TESTO data logger from the main frame, remove the 3.6 V AA battery, and place both in the provided container.

All the main components are now switched off and removed from the main frame. Place the components in the provided containers and place the containers together with the main frame in a dry cool place. Ensure that all water is drained from the experimental mechanical lung apparatus before putting it in storage.

6 RESULTS

Thermal response of the neonate in the delivery room is one of the most important aspects to investigate with regards to neonate mortality. During the first few minutes of the neonate's life, adaptation to the extrauterine environment is crucial. The neonate is born at a core temperature of 0.5 °C (Adamsons & Towell, 1965), higher than the core temperature of the birth mother (±37 °C). The core temperature of the neonate will decrease as a result of the influence caused by the colder environment. The thermal regulation system of the neonate must now maintain a constant core body temperature in the colder extrauterine environment.

An average healthy neonate is born at 39 weeks gestation, with an average weight of 3.3 kg. According to the Fetal-Infant Growth chart (Fenton, 2003) the length and head circumference of the neonate is used as 0.50 m and 0.345 m, respectively. The core temperature is assumed as 37 °C. The information provided in this paragraph will be used as reference when evaluating the theoretical simulation model developed in Section 3.

The thermal response of the neonate in the delivery room is influenced by environmental elements as well as subject specific properties. The environmental elements that will be investigated include room temperatures and relative humidity as well as different air velocities. The subject specific properties that will be investigated include the metabolic heat producing ability, the skin surface area to weight ratio as well as the condition of the skin surface area (wet or dry).

In addition to the delivery room thermal response, this section also investigates the thermal response of the neonate in the neonatal ward. The neonate is placed in the neonatal ward during the first few days of life, depending on the maturity of the neonate. It is important to look at thermal response of the neonate in the neonatal ward in order to understand how the environmental elements influence the thermal regulation ability of the neonate. The thermal response of the neonate in a closed temperature and relative humidity controlled incubator versus an open bassinette in a temperature controlled room is evaluated. The effect of clothing on thermal regulation and heat loss will also be evaluated.

Verification of the theoretical simulation model, developed in Section 3 and discussed in Section 6.3, is accomplished by using the information acquired during the clinical trial as set out in Section 4. The acquired data will be used in the theoretical simulation model and the resulting skin temperature will be compared to measured data. The outcome of this comparison will indicate the accuracy of the theoretical simulation model.

Finally, in subsection 6.4, the experimental model used for simulating the temperature and humidification of the inhaled air is evaluated. The results obtained from the experimental procedure are given and the significance of this experimental mechanical lung model is discussed. This experiment is expected to represent some resemblance in mimicking the respiratory system with respect to heat transfer observations.

6.1 Thermal Response of the Neonate in the Delivery Room

The thermal response of the neonate, considered in this section, is dependent on environmental elements as well as some subject specific properties. The results are evaluated for the first 300 seconds (5 minutes) of the neonate‘s life.

The environmental elements that influence the thermal response of the neonate in the delivery room include the room temperature and relative humidity as well as air velocity. These environmental elements will be evaluated by assessing the skin temperature response of the neonate whilst looking at the time it takes for the neonate’s skin temperature to reach equilibrium.

The subject-specific properties that will be investigated include the functioning metabolic heat production ability, weight of the infant in comparison to the exposed skin surface area, as well as the surface area subject to evaporation during the delivery procedure. The latter will indicate the importance of drying the neonate immediately after birth. The effects of these properties will be discussed with respect to the skin temperature response of the neonate.

6.1.1 Thermal response in the delivery room as influenced by environmental elements

The environmental elements that influence the thermal response of the neonate in the delivery room include room temperature, relative humidity and air velocity. The effects of these environmental elements are evaluated in this section and the results are presented in Figure 6.1, graphs (a) through (d).

Figure 6.1(a) presents the neonate’s skin temperature distribution for the fat, inner skin and outer skin layer with an assumed constant blood temperature of 37 °C. The delivery room temperature was simulated as constant at 20 °C with wall temperatures also at 20 °C. The average relative humidity in Cape Town of 60% (Cedar Lake Ventures, 2014) was used with low air velocity simulated as 0.1 m/s.

The results presented in Figure 6.1(a) were simulated for a dried neonate (the ideal case). Figure 6.1(a) indicates that it takes 113 seconds to reach skin temperature equilibrium with temperature accuracy to 2 decimal places. The difference between core body temperature (37.00 °C) and outer skin layer temperature (34.66 °C) is 2.34 °C. In general there is a 4.00 °C temperature difference between core body temperature and outer skin layer temperature.

Delivery room temperatures depends on the type of delivery procedure that will be used (caesarean section or natural birth). Further the delivery room temperature also depends on the attending doctor’s preference, (Smith, 2014) and (Linde, 2014). Figure 6.1(b) presents the neonate’s outer skin layer temperature response after the delivery procedure at various delivery room temperatures. It can be seen from Figure 6.1(b) that a warmer environment results in a higher outer layer skin temperature. For a delivery room temperature of 18 °C, the outer skin layer temperature decreases to 34.43 °C compared to the outer skin layer temperature of

35.38 °C, for a delivery room temperature of 26 °C. These results implicate that lower metabolic heat production is needed for thermal regulation of the neonate at higher room temperatures.

The relative humidity in the delivery room is rarely adjusted or controlled, because of the limited influence it has on thermal regulation. Figure 6.1(c) presents the neonate's outer skin layer temperature response after the delivery procedure at various delivery room relative humidity values, with a constant delivery room temperature of 20 °C. For a delivery room relative humidity of 30%, the outer skin layer temperature decreases to 34.58 °C compared to the outer skin layer temperature of 34.69 °C, for a delivery room relative humidity of 70%. It is clear that the relative humidity does not have a big influence on the skin temperature and thus the thermal regulation of the infant. It only assists in limiting the evaporative heat losses of the neonate, as discussed in a later subsection.

The last environmental element evaluated in this section, is the influence of air velocity on the temperature response of the neonate. Figure 6.1(d) presents the outer skin layer temperature response of the neonate's skin after the delivery procedure at different air velocity values. These results were obtained for a constant delivery room temperature and relative humidity of 20 °C and 60%, respectively. From Figure 6.1(d) it can be seen that low air velocities do not significantly affect the temperature response of the outer skin layer. Standard maximum air velocities for indoor rooms are specified as 2.4 m/s (Stoecker & Jones, 1982). For a delivery room air velocity of 0.5 m/s, the outer skin layer temperature is 34.29 °C compared to the outer skin layer temperature of 32.51 °C, for an air velocity of 2.4 m/s. It is can be noted that the air velocity has a significant effect on the skin temperature response and thus the thermal regulation of the neonate. These results imply that more metabolic heat production is needed by the thermal regulation system of the neonate, at higher room air velocities.

Indicated by the results gleaned from the theoretical simulation model for the delivery room, presented in Figure 6.1, it is clear that the environmental effects have a large influence on thermal regulation and skin temperature response of the neonate. Not all environmental effects play as big a role when compared to each other. From the results, the room temperature and air velocity are the most important elements to keep in mind when evaluating the thermal regulation capabilities of the neonate.

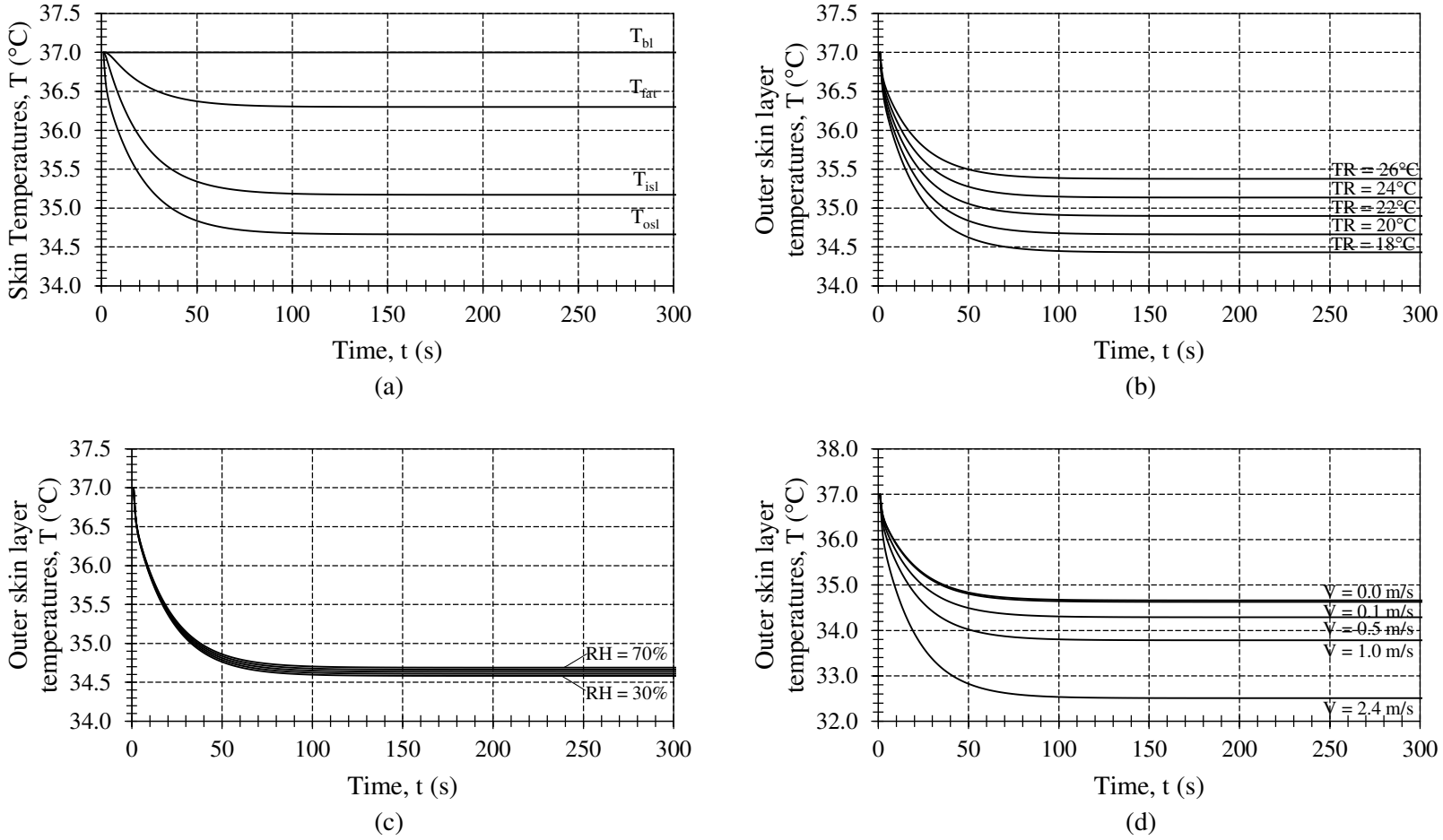

Figure 6.1: Outer skin layer temperature response of the infant after the delivery procedure in the delivery room with (a) different skin layer temperatures, (b) variable delivery room temperatures, (c) variable delivery room relative humidity, and (d) variable delivery room air velocity

6.1.2 Thermal response in the delivery room as influenced by subject specific properties

Subject-specific properties that influence the thermal response of a neonate in the delivery room include metabolic heat producing ability, weight to surface area ratio as well as the surface area subject to evaporation. The influence of these properties are presented in Figure 6.2, graphs (a) through (d), respectively.

Metabolic rate has an influence on the time it takes for the neonate's skin temperature to reach equilibrium. As seen in the previous subsection (Figure 6.1 (a)) it takes less than 150 seconds for an neonate's outer skin layer temperature to reach an equilibrium temperature of 34.66 °C in a 20 °C room temperature with 60% relative humidity and low air velocity (that is < 0.1 m/s).

From Figure 6.2(a), for an neonate with 75% metabolic capability temperature drops below 20 °C within 1227 seconds (20 minutes and 27 seconds) where 100% functioning metabolic capability allows the skin temperature to stabilise at 34.66 °C within the first 113 seconds (1 minute and 53 seconds). For lower metabolic heat producing capability percentiles, the time it takes to for the skin to reach room temperature decreases rapidly from 868 seconds for 50% functioning metabolic heat production, to 691 seconds for a non-responsive metabolic heat production system. These results emphasise the importance of monitoring the core temperature of the neonate. These results can also be used to determine whether the influence of environment elements are too great, and whether the neonate is capable of increasing its metabolic heat production rate in order to maintain a stable core body temperature.

The weight and exposed surface area are important neonate-specific properties to consider in evaluating the thermal regulation capability of the neonate, as highlighted in Section 2.2 of the literature study. Table 6.1 contains the Fetal-Infant growth chart (Fenton, 2003) values used for the weight and surface area evaluations.

Table 6.1: Fetal-Infant growth chart values used for subject-specific properties

	3%	**10%**	**50%**	**90%**	**97%**
Weight (kg)	2.4	2.7	3.3	4.0	4.3
Length (mm)	0.460	0.470	0.500	0.525	0.540
Head Circumference (mm)	0.315	0.325	0.345	0.360	0.370

First, for evaluation of the influence of weight, the average length (0.5 m) and average head circumference (0.345 m) of a neonate were used. The results gained by various input weights are presented in Figure 6.2(b). The weight varied from 2.4 kg (3rd percentile) to 4.3 kg (97th percentile), which resulted in an overall temperature difference of 0.0003 °C. It is thus clear that the weight does not play a big role in heat loss to the environment and a subsequent lowering in skin and core temperature.

For the evaluation of the influence of skin surface area, the weight was used as constant at 3.3 kg, and the length and head circumference were adjusted accordingly. The surface area varied between 0.191 m^2 and 0.215 m^2. The results for increased surface area and constant weight are presented in Figure 6.2(c). From the figure it can be seen that the surface area also does not have a significant influence on the skin temperature. Increasing the surface area resulted in an overall outer skin layer temperature difference of 0.0238 °C. Increased surface area has a larger effect on outer layer skin temperature than increased weight; but is also not a crucial property in evaluating the role of heat loss and subsequent temperature changes.

The last subject-specific property considered in evaluating the thermal regulation response of the neonate is the surface area subjected to evaporation. In considering the initial cool down period of a neonate, it is important whether the neonate is dried immediately after delivery, or left as wet. This was evaluated by changing the area subjected to evaporation. For the dried neonate, evaporation only takes place from the sweat glands in the outer skin layer, whereas for the wet neonate, evaporation takes place over the complete skin surface area. These results are indicated by Figure 6.2(d). From this figure, it can be noted that the time it takes for the skin to reach temperature equilibrium is equal for both scenarios. It can further be noted that the wet neonate will have a lower skin temperature of 31.36 °C in comparison to the dried infant with a skin temperature of 34.66 °C.

From the discussed results it can be seen that the metabolic heat production ability of a neonate is functional if a constant outer skin layer temperature or core temperature is maintained. Further, it can be noted that the influence of weight and surface area of a neonate is not an important property to be evaluated when ensuring a comfortable thermally neutral environment. In addition to the above mentioned subject specific properties it is important to consider whether, directly after birth, to dry the neonate, or not.

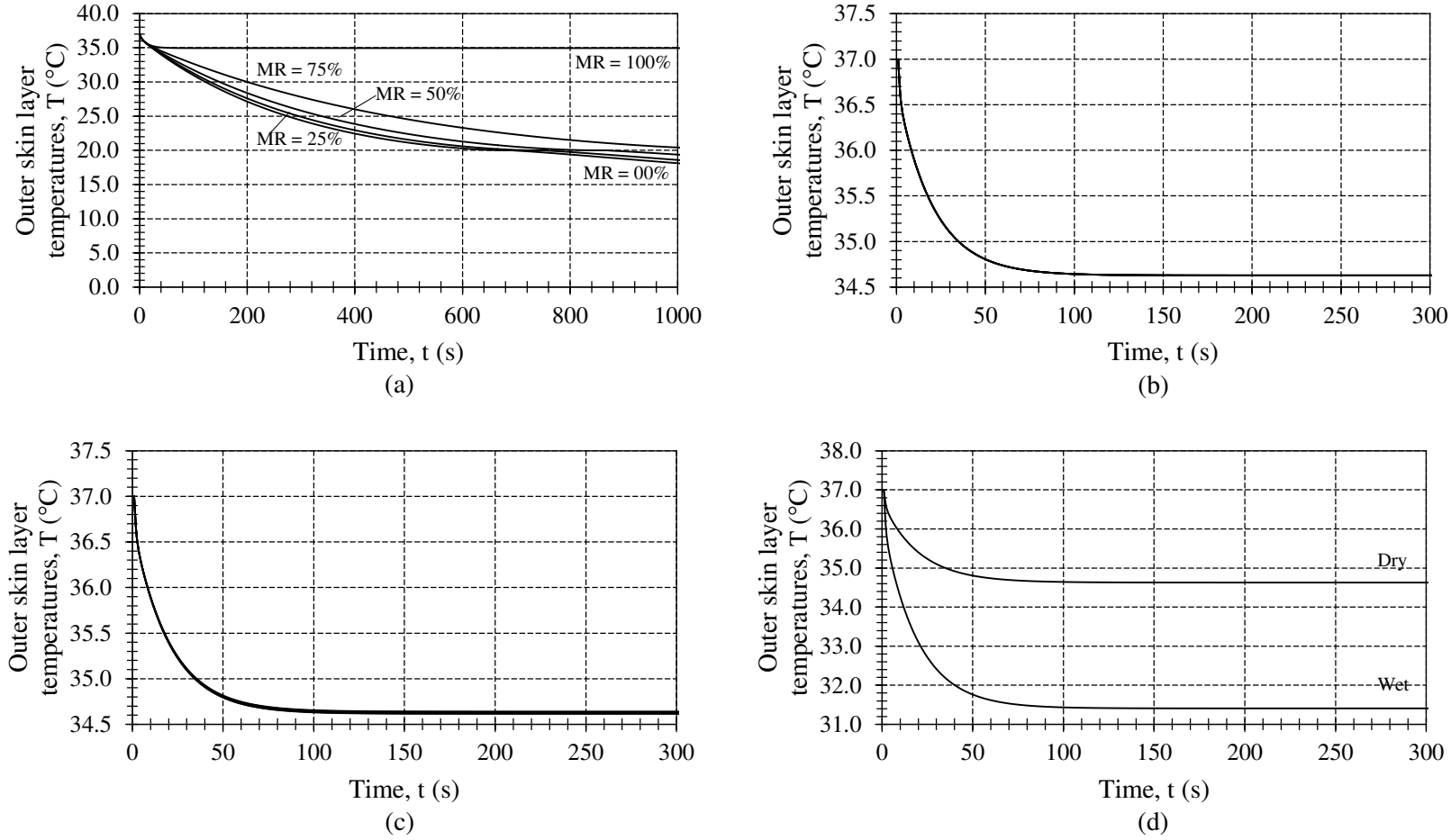

Figure 6.2: The outer skin layer temperature response as a result of the influence of various (a) metabolic heat production capability, (b) weights, (c) heat loss surface areas, and the (d) evaporation surface areas of a neonate

6.2 Thermal Response of the Neonate in the Neonatal Ward

Having evaluated the thermal response of the neonate in the delivery room, the thermal response of the neonate in the neonatal ward needs to be considered. The information gained from these results will assist in determining the important factors in maintaining a constant thermal neutral environment. The evaluations are given for the first 300 seconds (5 minutes) after birth, but when evaluating the thermal response only the equilibrium values are of importance.

The environmental effects that influence the thermal response of the neonate in the neonatal ward again include the temperature and relative humidity as well as air velocity. These environmental effects will be evaluated with respect to an open bassinette versus a closed temperature and relative humidity controlled incubator.

The effect of clothing on the thermal response of the neonate in the neonatal ward will also be evaluated. When evaluating the thermal insulation capacity of clothing the focus is placed on heat loss to the environment. These simulations will be done for a neonate placed in an open bassinette.

6.2.1 Thermal response of the neonate in a closed incubator compared to an open bassinette

Neonates are placed in incubators and open bassinettes, depending on the maturity and age of the neonate. The incubators provide a thermally neutral environment that assist in the thermal regulation of the neonate in order to maintain a constant core body temperature. In this subsection the immediate environment will be evaluated in order to determine if the surrounding air volume has any effect on the thermal regulation with respect to outer skin layer temperature, if the air is conditioned accordingly.

The first two graphs, Figure 6.3(a) and Figure 6.3(b), present the effect of various air temperature and relative humidity values on the outer skin layer temperature, for a neonate placed in a closed temperature and relative humidity controlled incubator. The room temperature is kept constant at 25 °C with a constant relative humidity of 60% at a low air velocity of 0.1 m/s.

From Figure 6.3(a) it is seen that different air temperatures in the incubator have a distinct effect on the outer skin layer temperature. For an incubator temperature of 25 °C, the outer skin layer temperature decreases to 35.22 °C compared to the outer skin layer temperature of 36.89 °C, for an extreme incubator temperature of 40 °C.

The results for variable relative humidity at constant incubator temperature of 30 °C are given in Figure 6.3(b). The relative humidity has less of an effect on the outer skin layer temperature of the neonate. For an incubator relative humidity of 40%, the outer skin layer temperature decreases to 35.75 °C compared to the outer skin layer temperature of 35.87 °C, for an incubator relative humidity of 70%.

The last two graphs, Figure 6.3(c) and Figure 6.3(d), present the outer skin layer temperature response obtained for a neonate placed in an open bassinette. The air in the room is conditioned by a standard air conditioning system and air velocity is kept minimal at 0.1 m/s.

Figure 6.3(c) indicates the outer skin layer temperatures obtained for a neonate placed in an open bassinette with variable room air temperature and constant relative humidity of 60%. For a room temperature of 25 °C, the outer skin layer temperature decreases to 35.22 °C compared to the outer skin layer temperature of 36.89 °C, for an extreme room temperature of 40 °C. These results correspond to the results obtained for the closed incubator at similar variable temperatures.

The results obtained for the outer skin layer temperature of a neonate placed in an open bassinette at various relative humidity values are indicated in Figure 6.3(d). For this simulation the room temperature was set to 25 °C. For an incubator relative humidity of 40%, the outer skin layer temperature decreases to 35.15 °C compared to the outer skin layer temperature of 35.25 °C, for an incubator relative humidity of 70%.

Again it is clear that increased air temperatures cause an increase in outer skin layer temperature. For a 1.00 °C increase in air temperature the outer skin temperature increases by 0.12 °C, provided the humidity is kept constant. As can be seen from the results as well the relative humidity has a decreased influence in increasing the outer skin layer temperature. For a 10% increase in relative humidity the outer skin layer temperature will increase with 0.03 °C. High relative humidity values can be used to assist in maintaining the moisture content of the skin.

From the results discussed in this subsection it is clear that the amount of air, with respect to different air temperatures or relative humidity, has no apparent influence on the outer skin layer temperature of the neonate. This means that the neonate can be placed in any type of incubator as long as the air temperature and relative humidity are controlled accurately. A neonate will maintain metabolic heat production ability in a thermally neutral environment.

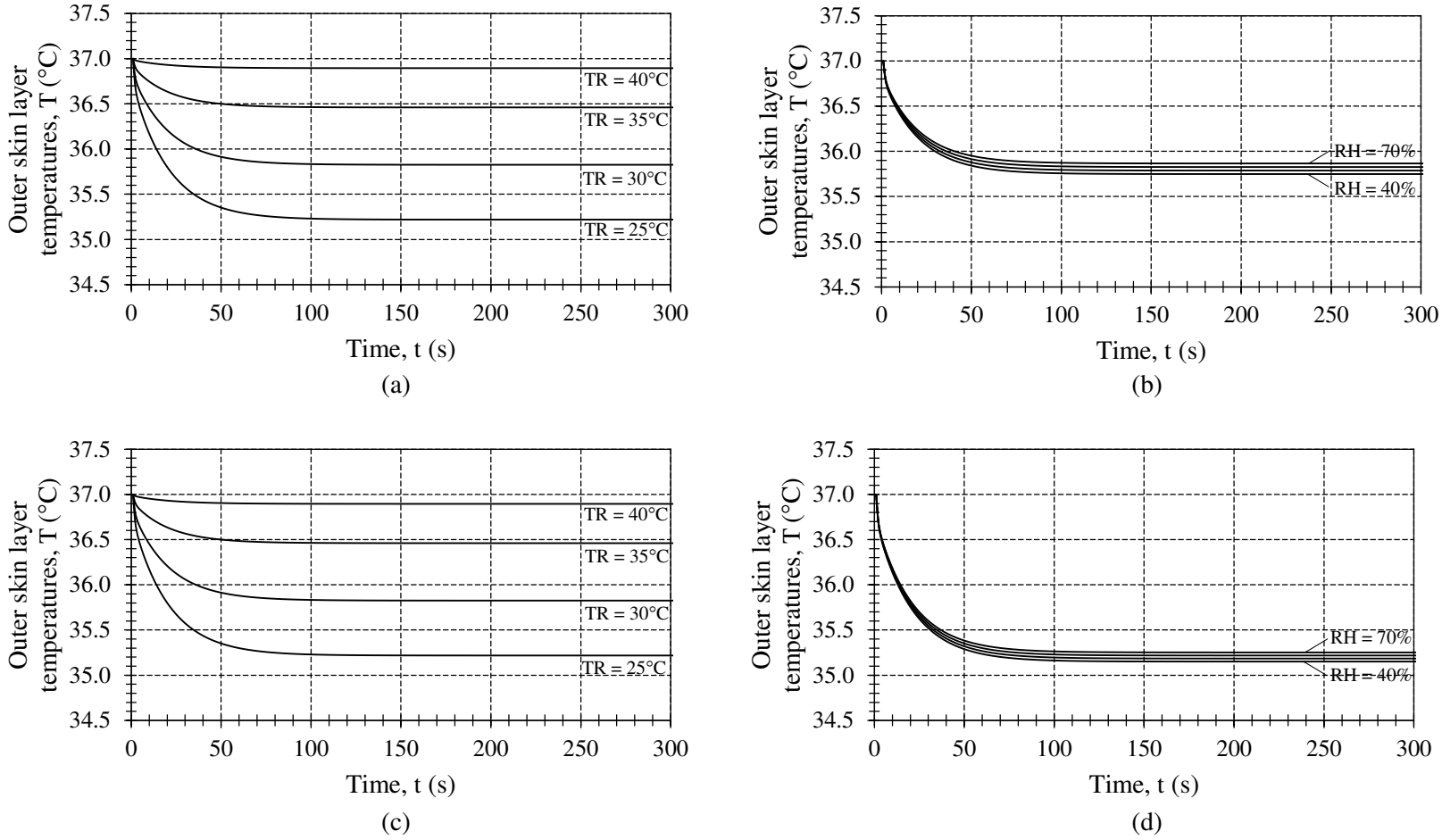

Figure 6.3: Outer skin layer temperature response for a neonate in the neonatal ward in a closed incubator at varying (a) incubator temperatures, (b) incubator relative humidity and for an open bassinette with (c) room air temperature and (d) room relative humidity

6.2.2 Thermal and heat loss response of the clothed versus unclothed neonate

The previous subsection examined the effect of environmental elements on the outer skin layer temperature of a neonate. The results presented in this section evaluated the thermal regulation response of the clothed neonate with that of the unclothed neonate with respect to temperature and heat loss. For this simulation the neonate was placed in an open bassinette in the neonatal ward, with the neonatal ward room conditions at a constant 25 °C room and wall temperature, 60% relative humidity and 0.5 m/s air velocity.

The clothing layer was simulated as pure cotton. The properties of cotton used for the simulation include an intrinsic clothing insulation factor of 0.094 W/m^2K and a permeability index of 0.34. Further, clothing factors had to be introduced. The clothing surface factor incorporates the surface area ratio covered by clothing. For the body, the clothing factor value of 0.5 and a clothing factor value of 0.5 were used for the head, because it was covered with a cotton hat, leaving the face and ears exposed to heat loss from bare skin.

The temperature response of the clothed neonate as opposed to the unclothed neonate is presented in Figure 6.4 with the value axis on the left side of the graph. From the figure it can be seen that the skin equilibrium temperature of the clothed neonate (35.94 °C) is 0.72 °C higher than that of the unclothed neonate (35.22 °C). This is not a large difference, but does not fail to indicate that clothing results in a higher outer skin layer temperature, resulting in less heat loss.

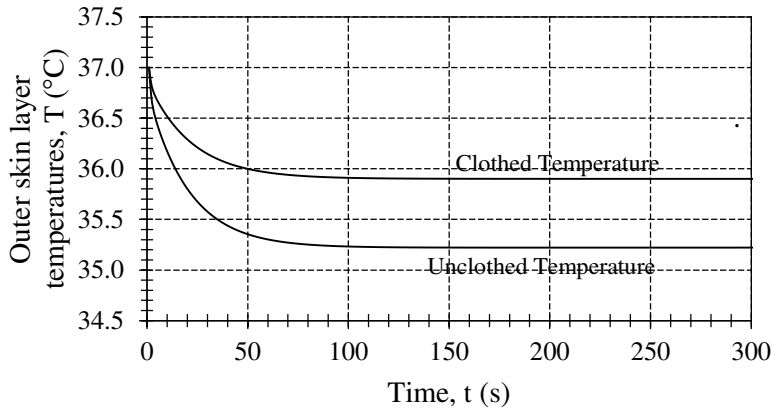

Figure 6.4: Temperature response of the clothed neonate against the unclothed neonate

Clothing is useful in fully developed, healthy term neonates (neonates older than 39 weeks gestation), due to the isolative capability restricting heat loss. The clothing reduces the effect that the environment has on the neonate's temperature regulation. The results suggest that no clothing should be used to assist in thermal regulation for a premature neonate. Controlling the environment with respect to

temperature, relative humidity and air velocity would provide more assistance than clothing insulation.

The results shown in Figure 6.5(a) and (b) indicate the heat loss from the body, head and respiratory system for the unclothed and clothed neonate, respectively. The results shown in Figure 6.5(a) and (b) are summarised in Table 6.2. Direct comparisons can be made for the contribution of the head, body and respiratory system with respect to heat loss. The percentage attributions for each of the body segments are also included in Table 6.2.

Table 6.2: Summarised heat loss results shown as shown in Figure 6.5(a) and (b) for the unclothed and clothed neonate

	Unclothed Neonate		**Clothed neonate**	
	Heat loss (W)	Heat loss (%)	Heat loss (W)	Heat loss (%)
Head	6.47	26.26	5.18	29.67
Body	14.98	67.75	11.64	66.67
Respiratory system	0.66	2.99	0.64	3.66

Figure 6.5(a) shows the heat loss from the head, body and respiratory system are 6.47 W, 14.98 W and 0.66 W respectively. The total heat loss for an unclothed neonate is 22.11 W. From these results it is clear that the respiratory system heat loss has a minimal effect compared to the heat loss from the body. The head is responsible for approximately 1/3 of the total heat loss whilst the body is responsible for approximately 2/3. This is due to the surface area ratio of the neonate; The head is large compared to the body. In adults this is no longer the issue. These results also illustrate why it is important to cover the head of the neonate when attempting to restrict heat loss in colder environments.

The results obtained by introducing a clothing layer in the theoretical simulation model are shown in Figure 6.5(b). Heat loss from the head, body and respiratory system are 5.18 W, 11.64 W and 0.64 W respectively. The total heat loss for the clothed neonate is 17.24 W, which is half the heat loss of the unclothed neonate in the same environment. A remark can be made regarding the heat loss from the head compared to the heat loss from the body: when clothing is introduced the majority of heat is lost from the body but the ratio of heat loss from the body (2/3) to the head (1/3) is still valid.

Figure 6.5(c) and (d) show the heat loss as contributed by convection, radiation and evaporation for the unclothed and clothed neonate. The results shown in Figure 6.5(a) and (b) are summarised in Table 6.3. Direct comparisons can be made for the contribution of the head, body and respiratory system with respect to heat loss. The percentage attribution for each of the heat loss mechanisms are also given in Table 6.3.

Table 6.3: Summarised heat loss results shown as shown in Figure 6.5(c) and (d)

	Unclothed Neonate		**Clothed neonate**	
	Heat loss (W)	Heat loss (%)	Heat loss (W)	Heat loss (%)
Convection	4.33	19.67	3.51	20.10
Radiation	7.77	35.21		
Evaporation	9.97	45.17	13.95	79.90

Figure 6.5(c) shows the heat loss for an unclothed neonate as a result of convection, radiation and evaporation of 4.33 W, 7.77 W and 9.97 W respectively. From these results it can be seen that evaporation heat loss has the highest influence on the total heat loss, it contributes a total of 50% toward the total heat loss from the outer skin layer. Due to the low air velocity used, convection heat loss contributed the least to the total heat loss of 22.11 W. Radiation has the second largest contribution toward the total heat loss and is dependent on the surrounding room wall temperature.

Heat loss for the clothed neonate is shown in Figure 6.5(d). These results indicate the effect that the intrinsic clothing insulation factor had on the three different heat loss mechanisms. Convection and radiation heat loss was combined in order to incorporate the intrinsic clothing insulation and resulted in a total heat loss of 3.51 W. The high evaporative heat loss of 13.95 W was caused by the low permeability factor of cotton. These results indicate that clothing reduces heat loss by convection and radiation significantly, whilst evaporation is not affected that much.

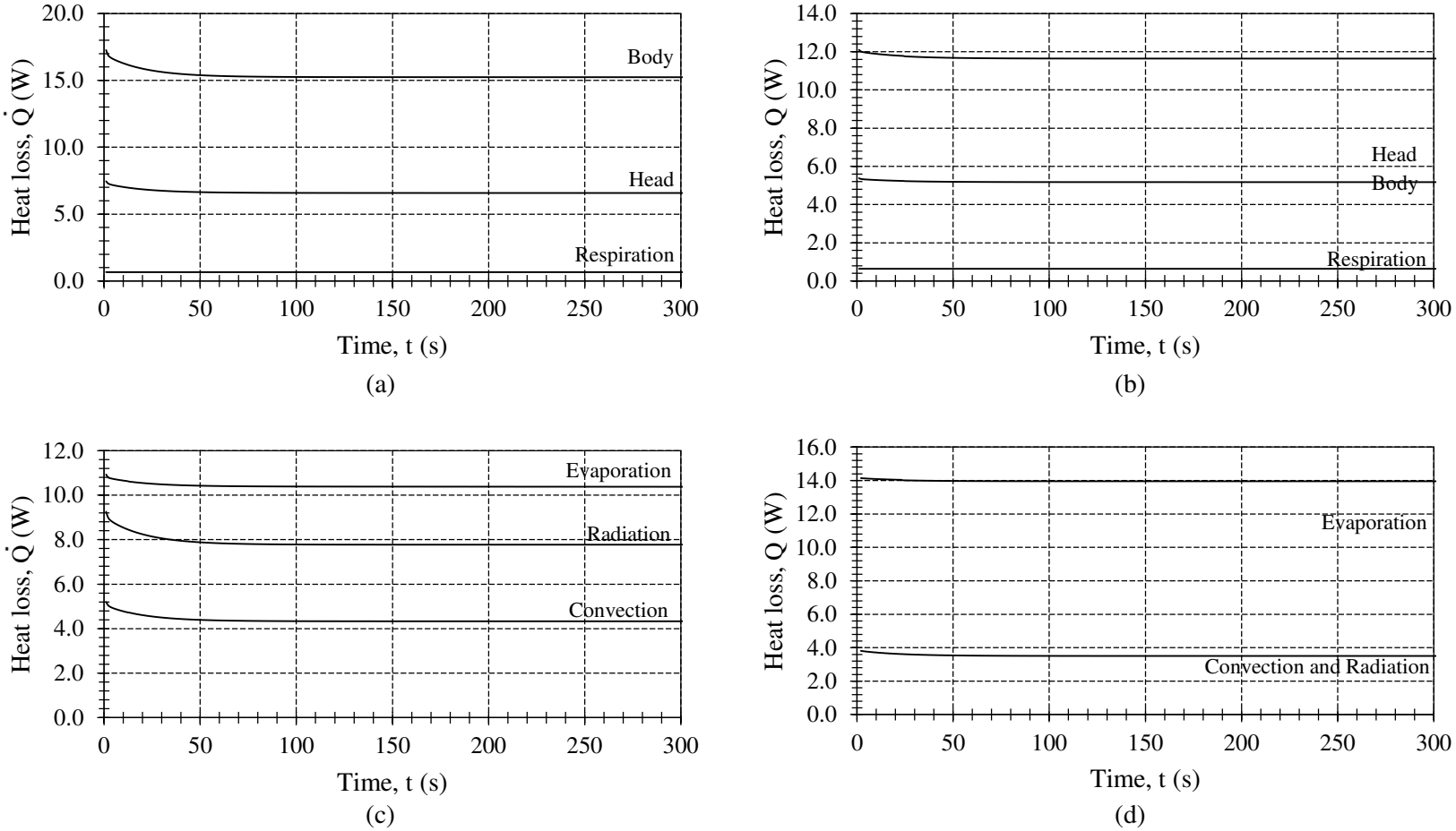

Figure 6.5: Heat loss response of the (a) body parts of an unclothed neonate, (b) body parts of a clothed neonate, (c) heat loss mechanisms of an unclothed neonate, (d) heat loss mechanisms of a clothed neonate

6.3 Verification of Combined Simulation Model

As discussed in Section 4, a clinical trial was undertaken to assist in understanding the maintaining of thermal stability in neonates. During the clinical trial data was acquired which will be used in this section to verify the theoretical simulation model for heat transfer in neonates that was developed in Section 3. The outcome of the verification, allowed simplifying the simulation model by developing an equation, by means of linear regression, to calculate the outer skin layer temperature with a single equation. The results obtained by the linear regression equation are presented in this section, while methods for development of the equation are discussed in Addendum A.

Table 6.4 provides the information acquired from 10 neonates during the clinical trial. The gender and ethnic group of the neonates was not important and did not prove to have an effect on the resulting outer skin layer temperatures. The information in Table 6.4 include all the neonate specific properties such as weight, length and head circumference which allows the calculation of the total surface area subjected to heat loss. The breathing rate was only measured once, because of the limiting influence on total heat loss as discussed in Section 6.2.2.

Table 6.4: Subject specific information acquired during the clinical trial for 10 neonates

	Weight (kg)	**Length (cm)**	**Head Circumference (cm)**	**Breathing Rate (breaths/min)**
1	2.60	40.0	36.5	56
2	2.19	45.5	31.0	56
3	3.07	48.0	35.0	56
4	3.28	44.0	35.7	56
5	2.57	50.0	35.0	56
6	3.67	49.0	39.0	56
7	1.76	38.0	36.8	56
8	2.56	40.0	36.7	60
9	2.265	40.0	36.6	60
10	1.98	49.0	36.0	54

Further information acquired during the clinical trial included the room temperature, relative humidity and the air velocity. This information is presented in Table 6.5 and constitutes the environmental elements that influence the outer skin layer temperature, as discussed in Section 6.1.1. The axillary temperature was measured in the neck folds due to uncomfortable methods used to measure the core temperature. The core temperature was calculated by adding 0.5 °C to the measured axillary temperature (Adamsons & Towell, 1965) and is given in Table 6.5. Table 6.5 also include the average outer skin layer temperature measurement. All the information presented in Table 6.5 is calculated average values for the measurements taken over the data acquiring period of 60 minutes. The calculated average values will be used to verify the accuracy of the simulation model.

Table 6.5: Measurements acquired during the clinical trial for the environmental elements that influence the outer skin layer temperature, as well as measured, simulated and calculated outer skin layer temperatures presented in Figure 6.6. * indicates standard deviation and [x] indicates difference in temperature with respect to the measured outer skin layer temperature.

	Room Temperature (°C)	**Room Relative Humidity (%)**	**Air Velocity (m/s)**	**Core Temperature (°C)**	**Outer Skin Layer Temperature (°C)**		
					Measured	Simulated	Calculated
1	26.46 (0.74)*	44.4 (0.55)*	0.25	37.12 (0.34)*	35.248	35.266 (-0.018)[x]	35.324 (-0.076)[x]
2	24.94 (0.09)*	44.8 (0.84)*	0.10	37.14 (0.36)*	35.408	35.262 (0.146)[x]	35.284 (0.124)[x]
3	24.80 (0.48)*	48.2 (3.49)*	0.50	36.08 (1.05)*	33.913	33.914 (-0.001)[x]	33.993 (-0.080)[x]
4	23.76 (0.99)*	45.2 (2.39)*	0.10	37.04 (0.63)*	35.144	35.033 (0.110)[x]	35.050 (0.094)[x]
5	24.90 (0.41)*	38.4 (3.97)*	0.10	37.00 (0.66)*	35.444	36.165 (0.279)[x]	35.210 (0.234)[x]
6	24.86 (0.34)*	37.9 (2.66)*	0.10	37.64 (0.66)*	36.155	35.724 (0.431)[x]	35.779 (0.375)[x]
7	35.42 (0.18)*	36.7 (0.91)*	0.10	37.40 (0.25)*	37.298	36.835 (0.462)[x]	36.785 (0.512)[x]
8	25.04 (0.36)*	50.2 (1.16)*	0.30	37.72 (0.49)*	35.571	35.556 (0.016)[x]	35.657 (-0.085)[x]
9	25.48 (0.13)*	48.8 (0.61)*	0.10	37.38 (0.37)*	35.592	35.585 (0.007)[x]	35.577 (0.015)[x]
10	25.46 (0.17)*	48.4 (0.70)*	0.50	34.86 (0.19)*	32.800	33.044 (-0.244)[x]	32.992 (-0.192)[x]

A total of 5 measurements were taken for each of the environmental elements, at intervals of 10 minutes. The average was calculated for every element together with the standard deviation, indicated by ()* in Table 6.5. From the data presented in Table 6.5 it can be seen that the room temperature stayed relatively constant with the largest temperature deviation being 0.99 °C for neonate 4. The relative humidity decreased when the environmental temperature increased and presented a maximum deviation of 3.97% for neonate 5. Air velocity was the most difficult to measure due to changes caused by movement of personnel in the vicinity of the air surrounding the neonate. The measured air velocity was found to be extremely low, never exceeding a value of 0.5 m/s.

Further, the axillary temperature was also measured 5 times at intervals of 10 minutes. The average calculated core temperature varied according to the weight, and exposed surface area of the individual neonate. The mothers were allowed to hold the neonates, but measurements were not taken during feeding times. All the neonates presented a core temperature warmer than 37.00 °C, except for neonate number 10, who had a very low birth weight compared to the exposed skin surface area. Neonate 7 also had a low birth weight, but were placed in an incubator, which assisted the neonate in maintaining a higher core temperature.

The last three columns in Table 6.5 present the outer skin layer temperature for each of the neonates obtained with three different methods. The outer skin layer temperatures are presented graphically in Figure 6.6. The three methods used to obtain the outer skin layer temperature include the measured average, theoretical simulation model results, and results obtained through use of linear regression analysis derived from the simulation model. A legend for the results obtained for each of the three methods is included in Figure 6.6.

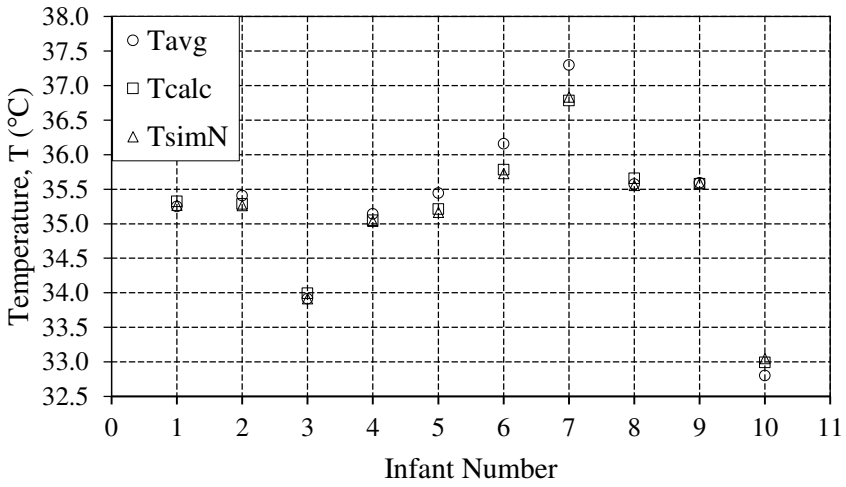

Figure 6.6: Results obtained for the outer skin layer temperature, based on the information gained during the clinical trial and data acquisition (also see Table 6.5)

The outer skin layer temperature was measured at various sites of the neonate's body which was not covered with a clothing layer. The sites measured include the head, neck, back or chest, left and right hand and arm. These measurements were used to calculate the average outer skin layer temperature. The calculated average outer skin layer temperature will now be used as reference temperature, to evaluate and verify the developed theoretical simulation model.

The information acquired from the clinical trial, presented in Table 6.4 and Table 6.5, was used to determine the resulting outer skin layer temperature by using the theoretical simulation model. The results obtained from the simulation program thus included the effects of subject specific properties and surrounding environmental elements. From Figure 6.6 it can be seen that the results obtained by using the developed simulation model, with the largest temperature difference of 0.46 °C for neonate 7, with respect to the average measured temperature. The smallest temperature difference with respect to the measured temperature was -0.001 °C for neonate 3. The standard deviation of simulated temperatures to the measured temperature was calculated as 0.22 °C. From these results it can be concluded that the developed theoretical mathematical simulation model was successful in predicting the outer skin layer temperature.

With successful verification of the theoretical mathematical simulation model, further analysis was attempted. Further analysis included developing a single equation by performing regression analysis on results obtained by the simulation model. The equation was developed based on the results discussed in Section 6.1 where the environmental elements of room temperature, relative humidity and air velocity had the largest influence on outer skin layer temperature. The subject specific property of core temperature also presented a large influence on the resulting outer skin layer temperature. The development of equation (6.1) is discussed in Addendum A.

$$T_{osl} = -0.830 + 0.887T_{core} + 0.124T_r + 0.336\phi_r - 0.861V_r \qquad (6.1)$$

The last column of Table 6.5 presents the outer skin layer temperature calculated with equation (6.1). From Figure 6.6 it can be seen that the results obtained by using equation (6.1), were fairly accurate as well. The largest and smallest temperature difference was 0.512 °C for neonate 7 and 0.015 °C for neonate 9, respectively, when compared to the average measured temperature. The average standard deviation of calculated temperatures to the measured temperature was calculated as 0.22 °C.

From these results it can be seen that the outer skin layer temperatures calculated by the developed simulation model and equation (6.1) proved accurate results with a possible maximum deviation of 0.22 °C. The results obtained by the last two methods proved to be accurate to the same standard deviation, thus any of the two methods can be used to predict the outer skin layer temperature, but the simulation model is preferred as it takes into account the exposed surface area as well as all the environmental elements.

6.4 Experimental Modelling Results

The experimental lung apparatus was designed to imitate the naturally occurring heat transfer mechanisms in the conducting zone of the respiratory system physiology. An experimental respiratory model was constructed accordingly, in order to observe the basic ventilation concepts of the respiratory system. The theoretical model for heat loss via the respiratory system suggested that the experimental mechanical lung apparatus would successfully mimic the thermal regulatory physiology and operation of the respiratory system. This subsection is dedicated to the response observed from the experimental model.

As discussed in Section 3.3 and Section 5, respectively, heat transfer during the respiratory process refers to the conditioning of the inhaled air. Conditioning of the inhaled air was accomplished by means of convection and evaporation heat transfer from the trachea walls to the inhaled air. Convection helped to raise the temperature of the inhaled air to 37 °C, whilst evaporation increased the relative humidity of the inhaled air to approximately 100%.

The inhaled air volume flow rate was the most important variable system input. Equation (6.2) was used to introduce the inhaled air volume flow rate and evaluate the heat transfer response of the experimental model accordingly. The biggest influence toward the inhaled air volume flow rate was caused by the tidal volume (TV), measured in ml/kg. The tidal volume indicates the amount of air that has to be conditioned during one inhalation phase. The average weight of 3.3 kg for a healthy 39 week gestation neonate was used in the calculations. Another important variable in equation (6.2) was the breathing rate (BR), measured in breaths per minute. The breathing rate indicates how regularly the amount of inhaled air needed to be conditioned.

$$\dot{V}_{inh} = BR(TV/10^3)W \tag{6.2}$$

The experiment had to determine what amount of area was needed by the conducting zone to successfully condition the inhaled air before it reached the internal lung volume. The conducting zone (trachea) was represented by a thoroughly moistened wick, through which the air was inhaled by mechanical means. The breathing rate was kept constant at 30 breaths per minute; the low breathing rate was used to accommodate the slow data logging time intervals of the equipment used. The minimum and maximum tidal volumes were used during completion of the experiment, 5.0 ml/kg and 7.5 ml/kg. The tidal volumes were introduced by using different piston stroke lengths of 13 mm and 20 mm, tagged (a) and (b) correspondingly in Figure 6.7.

Results obtained for the relative humidity response upon completion of the experiment is presented in Figure 6.7. Room conditions in the laboratory consisted of a 14 °C room temperature and 65% relative humidity. The probe used for data logging was situated in the internal lung volume. Water circulation was switched on and data logging was initiated as soon as the internal lung volume

temperature reached 37 °C. The initial relative humidity values, within the internal lung volume, varied between 50% and 72.5% as seen from Figure 6.7.

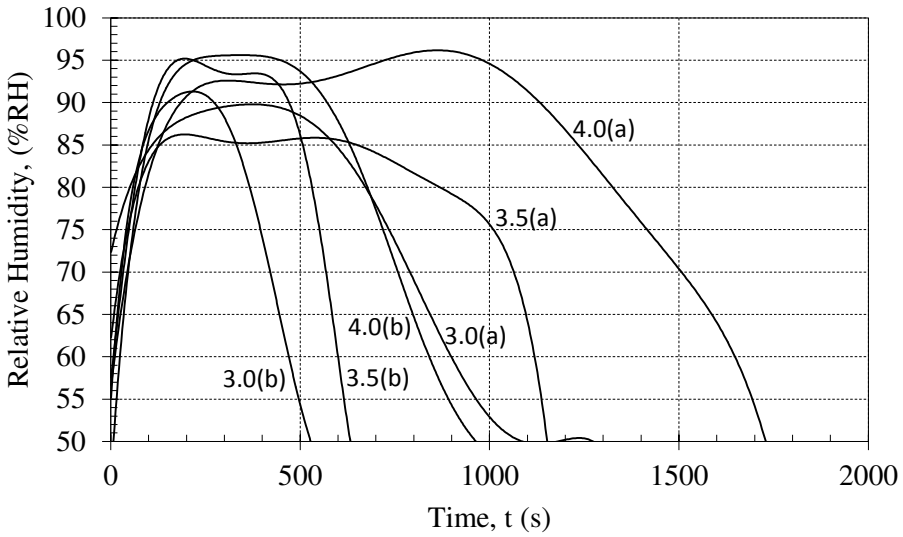

Figure 6.7: 13 mm stroke versus 20 mm stroke, relative humidity values obtained from experimental mechanical lung apparatus

The breathing simulation was also initiated when data logging started. The first phase of the experiment indicates the start of respiratory action, the relative humidity of the air in the lung increased to maximum value within the first 200 seconds. This is accomplished by the inhaled conditioned air, replacing the drier air in the lung. This phenomenon indicates that it is possible to completely humidify inhaled air, if the air is subject to a thoroughly moistened surface.

The second phase of the experiment, varied in length, but is indicated by the flat sections of each line on the graph, starting and ending at 80% relative humidity for reference purposes. The second phase of the experiment indicated that the moistened wick sustained the conditioning of the inhaled air as long as the wick contained enough moisture. The maximum and average values listed in Table 6.6 contain the values for relative humidity during the second phase of the experiment. The third phase of the experiment is indicated by the linear decrease of the relative humidity value. This is caused by the depletion of moisture in the wick, and thus resulted in dry air being inhaled again.

Table 6.6: Relative humidity values obtained during experiment

	3.0 cm (a)	**3.5 cm (a)**	**4.0 cm (a)**	**3.0 cm (b)**	**3.5 cm (b)**	**4.0 cm (b)**
Maximum	86.4%	89.9%	96.0%	90.9%	94.7%	95.6%
Average	84.4%	87.3%	91.1%	88.3%	92.1%	92.6%

From Table 6.6 it can be seen that the maximum relative humidity value increases for larger surface areas. For a wick length of 3.0 cm, the inner lung relative humidity increased to 86.4% compared to the inner lung relative humidity of

96.0%, for a wick length of 4.0 cm. The same result was experienced for the larger tidal volume where a wick length of 3.0 cm resulted in the inner lung relative humidity increasing to 90.9% compared to the inner lung relative humidity of 95.6%, for a wick length of 4.0 cm. The average relative humidity values showed the same results. During the completion of this experiment three different moistened wick areas were used. The diameter of the wick was measured as 3 mm, with varying lengths of 3.0, 3.5 and 4.0 cm. From Figure 6.7 it can be seen that the flat second phase of the experiment lasted longer for the larger surface area. This means that there is more moisture contained in a larger wick surface area, resulting in a longer period available for conditioning of the air.

The results obtained for the minimum and maximum tidal volumes used during completion of the experiment, 5.0 ml/kg and 7.5 ml/kg, are tagged (a) and (b) in Figure 6.7. When comparing the results obtain for corresponding values of (a) and (b) in Figure 6.7 it can be seen that for a smaller tidal volume (a), less air have to be conditioned during inhalation, resulting in a longer flat second phase in the experiment. The opposite is valid for the larger tidal volume (b), where more air has to be conditioned during inhalation and that results in a much shorter flat second phase in the experiment.

A larger evaporative area resulted in a longer period for conditioning of the air. During the exhalation phase of the respiratory cycle some of the vapour in the exhaled air was placed back into the wick because the air was exhaled at measured average of 80% relative humidity. For a larger stroke volume the time it took to dehumidify the wick was considerably less. Thus for larger tidal volumes more moisture must be sent to the trachea. In effect then it does not depend on the stroke volume but rather on the amount of air that has to be humidified for each inhalation.

The probe used for data logging of temperature was situated in the internal lung volume. Water circulation was switched on and data logging was initiated as soon as the internal lung volume temperature reached 37 °C. The initial temperature values were 37.0 °C ±0.6 °C. During the completion of the experiment the temperature stayed more or less within a ±0.7 °C temperature boundary. The minimum, maximum and average temperature values are given in Table 6.7. The designed experimental lung apparatus can be used to mimic the respiratory system to some extent with regards to heat transfer.

Table 6.7: Temperature values obtained during experiment

	3.0 cm (a)	**3.5 cm (a)**	**4.0 cm (a)**	**3.0 cm (b)**	**3.5 cm (b)**	**4.0 cm (b)**
Minimum	36.1 °C	36.6 °C	36.2 °C	36.5 °C	37.0 °C	37.0 °C
Maximum	37.3 °C	37.3 °C	37.8 °C	37.2 °C	37.9 °C	38.2 °C
Average	36.7 °C	37.0 °C	37.3 °C	36.8 °C	37.4 °C	37.5 °C

It shows that the trachea must be moistened continuously in order to condition inhaled air. Depending on the type of environment fluid control to the trachea will vary.

7 DISCUSSIONS AND CONCLUSION

In this section a number of conclusions, based on the findings of this thesis, are given. In particular the attainment of the thesis objectives is considered.

7.1 Literature Study

The first objective, stated in Section 1.4, was completed by undertaking a literature study that discussed topics regarding thermal regulation. The research done in fulfilment of this objective focused on infants.

The literature study discussed detailed information on background topics concerning the blood circulation system, skin tissue physiology and the respiratory system physiology. An understanding of thermal regulation mechanisms was gleaned and specified how heat transfer theory can be applied to analyse heat loss in neonates. This information lead to defining the thermal neutral environment, and indicated which elements were of concern when evaluating a thermal environment. Further an investigation was undertaken to determine the thermal heat transfer properties of skin tissue, which was later used in the development of the theoretical simulation model. Some focus was also placed on reviewing previously developed mathematical models.

The information gained upon completion of the literature study served as a physiologically based platform for the rest of the thesis project. The information gathered from background physiological topics helped to establish the link between biological theory and engineering application. Theoretical mathematical models developed by Pennes and Fiala, served as a good reference point, for heat transfer theory application, throughout the duration of this project.

7.2 Mathematical Modelling of Thermal Regulating Mechanisms

A theoretical thermal regulating system for the neonate was defined as required by the second objective, stated in Section 1.4. The theoretical simulation model was developed by using heat transfer equations based on energy conservation, and solved according to the explicit finite difference method as explained in Section 3.1. The theoretical simulation model consisted of heat loss through the skin (Section 3.2), heat loss through the respiratory system (Section 3.3) and included several thermal environmental elements (Section 3.4).

The development of the theoretical simulation model allowed evaluating different factors that influence the thermal regulation response of a neonate, as discussed in Section 6. The factors evaluated by using the theoretical simulation model in Section 6.1 included the influence of environmental elements as well as the influence of subject specific properties. The model was further used to evaluate the thermal response of a neonate in an incubator as opposed to a bassinette. The influence of clothing on skin temperature and heat loss was also evaluated and discussed in Section 6.2.

7.2.1 Environmental effects that influence thermal regulation

The environmental elements that influence thermal regulation and skin temperature distribution are air temperature, relative humidity and air velocity. These elements were evaluated in Section 6.1.1. From the results it was concluded that variation of air temperature had the most significant influence on the resulting skin temperature, where air temperature higher than 22 °C was considered comfortable. A difference of 40% relative humidity caused a small temperature change of 0.11 °C in skin temperature and can be neglected when evaluating the thermal environment, except in cases where water loss is of great concern. Air velocity presented no significant effects at low velocities, but caused a large decrease in skin temperature at the maximal accepted indoor air velocity of 2.4 m/s.

7.2.2 Subject specific properties that influence thermal regulation

The subject specific properties that influence thermal regulation of the neonate were evaluated in Section 6.1.2 and included the metabolic heat production ability, weight to surface area ratio and the surface area subject to evaporation. From the information gathered on thermal response in the literature study it became apparent that a neonate has sufficient metabolic heat production capability if the skin or core temperature stays constant. This fact was validated by the simulation model, where a neonate's temperature drops below 20 °C within 1227 seconds if the neonate had only 75% metabolic heat producing capability. Further it was found that the weight to surface area ratio of neonates do not have a great influence on the resulting heat loss. Results indicated no significant variance when the weight was kept constant while the surface area exposed to heat loss was increased. The same results were obtained when the surface area was kept constant with an increase in weight of the neonate. Evaluation of the final property, surface area subject to evaporation, did indicate that lower skin temperatures are induced if the neonate is covered in fluid.

7.2.3 Thermal response of the neonate in a closed incubator versus an open bassinette

The thermal response of a neonate in a closed temperature and relative humidity controlled incubator were evaluated and compared to the thermal response of a neonate in an open bassinette with room temperature and relative humidity controlled in Section 6.2.1. The thermal response was evaluated by varying temperature and relative humidity. The results indicated that a 1.00 °C increase in room temperature causes a 0.12 °C increase in outer skin layer temperature and a 10% increase in relative humidity results in a 0.03 °C increase in outer skin layer temperature. The results further indicated that the amount of air surrounding the neonate does not have an influence on thermal response of a neonate, with respect to outer skin layer temperature, when placed in an incubator compared to a bassinette, as long as the environmental conditions are controlled.

7.2.4 Clothed versus unclothed neonate

From the results evaluated in Section 6.2.2 it is realised that clothing has a significant effect on the resulting heat loss of a neonate. The total heat loss for a clothed neonate (11.94 W) is half as much as the total heat loss for the unclothed neonate (22.11 W). Clothing is useful due to the isolative capability restricting heat loss. The results suggest that no clothing should be used to assist in thermal regulation for a premature neonate. Controlling the environment elements such as temperature, relative humidity and air velocity would provide more assistance to thermal regulation of the neonate than clothing insulation.

Further evaluation for heat loss for the neonate indicated that 2/3 of heat loss occurs from the body while the remaining 1/3 is accounted for by the head. The respiratory system was found to have a low impact with regards to the total heat loss. These results were obtained and found to be similar regardless of clothing.

Evaluation of the heat loss mechanisms indicated that clothing reduces heat loss by convection and radiation significantly (12 W for the unclothed neonate compared to 2.56 W for the clothed neonate), whilst evaporation is not affected that much. Thus was concluded that evaporation is the most important mechanism to consider when evaluating the heat loss of a neonate.

7.2.5 Verification of the developed theoretical mathematical model

During the completion of a clinical trial information was acquired from 10 neonate's which included the weight, length and head circumference as well as the breathing rate. The gender and ethnic group of the neonates was not important and did not prove to have an effect on the resulting outer skin layer temperatures. Further information acquired during the clinical trial included the room temperature, relative humidity and the air velocity which was used to verify the theoretical simulation model.

The results provided by the theoretical simulation model were compared to the average outer skin layer temperature measured during the clinical trial. The simulated results presented an average deviation of 0.22 °C from the measured outer skin layer temperature. The theoretical simulation model was then used to develop a single equation that can be used to predict the outer skin layer temperature. The results obtained by evaluation of the equation also presented an average deviation of 0.22 °C from the measured outer skin layer temperature. Thus it can be concluded that any of the two methods can be used to predict the outer skin layer temperature, but the simulation model is preferred as it takes into account the exposed surface are as well as all the environmental elements.

7.3 Comparison of Simulation Results to other Models

As written in the literature study other mathematical models have been developed but each of them indicated limitations of their own. Pennes developed the bioheat

equation for blood perfusion through the skin and Fiala et.al. developed a model for human thermoregulation. Comparisons with other models could however not be done due to a few reasons. In the paper presented by Fiala they stated that it was not possible to validate the model by comparisons of field measurements because the model did not include thermoregulatory feedback mechanisms that exist in human beings.

The thesis presented the assumption for the temperature of blood to stay constant at the core body temperature. This assumption was introduced into the simulation model when the temperature of the fat layer beneath the skin was calculated; this assumption prevented me from comparing results to the results presented by the bioheat equation.

The Fiala model was validated by comparisons of predicted temperatures with derived analytically values for conductive cooling. The conduction cooling of tissue results was used to compare the accuracy of the Fiala model to the bioheat equation developed by Pennes. Fiala concluded that the model was capable of accurately predicting internal body temperatures. The results presented in the paper were not inclusive enough to compare with the simulation model presented in this thesis because the focus of the simulation model developed in this thesis was calculate and predict outer skin layer temperatures and not internal body temperatures.

7.4 Development of an Experimental Respiratory Model

The third objective, as stated in Section 1.4, required the development of a practical experimental model that had to simulate the respiratory system and illustrate the functioning thereof with regards to heat transfer. This objective was completed by designing an experimental mechanical lung apparatus as discussed in Section 5. This apparatus was designed to mimic the heat transfer mechanisms that take place during a respiratory cycle.

The experiment was used to determine the total surface area needed to successfully condition the inhaled air, for varying tidal volumes at a constant breathing rate. The results indicated that it was not the surface area subject to evaporation that had to be considered important, but rather the amount of moisture available for evaporation. The temperature of the inhaled air stayed relatively constant at 37 °C.

The results, as discussed in Section 6.4, indicated that the designed experimental mechanical lung apparatus was successful in mimicking the heat transfer that occurs during a respiratory cycle. There is, however, room for improvement as will be discussed in Section 8.

7.5 Conclusion

It can be concluded that this theoretical simulation model can be used with reasonable confidence and accuracy to predict the outer skin layer temperature of the neonate. The model presents two major applications:

- For the first application the theoretical simulation model can be used as a test tool for evaluating influences of different protocols in the transient temperature distribution of neonates.
- The second application would be to enable medical professionals to monitor and determine the influence of the thermal environment, including the temperature, relative humidity and air velocity, on the neonate's temperature regulation capability and allow for a speedier thermal intervention strategy.

Further it can be concluded that the experimental mechanical lung apparatus designed to mimic the heat transfer mechanisms that take place during a respiratory cycle was mimicked successfully. It was established that it was not the surface area subject to evaporation that had to be considered important, but rather the amount of moisture available for evaporation. The temperature of the inhaled air stayed relatively constant at 37 °C.

8 RECOMMONDATIONS AND FUTURE WORK

Energy balance during the first days of life for the neonate has not yet been measured directly due to the difficulty of determining the total daily expenditure in a nonintrusive manner. Insufficient information on metabolic heat production was found in the available published literature in the literature study undertaken in Section 2. It thus proved to be a challenge in developing the theoretical simulation model discussed in Section 3. Based on the limited knowledge available and referenced in the literature study on the topic of metabolism, it is recommended that a more detailed literature study has to be completed on the topic of metabolism in order to successfully understand how metabolic heat production functions as needed to assist thermal regulation in the neonate.

Based on the outcome of the theoretical simulation model for unclothed neonates, as developed in Section 3.2.1 to Section 3.2.3 and discussed in Section 6.1, it is recommended that the theoretical simulation model be extended to include the body structure as a number of cylindrical structures, rather than one cylindrical element. This will allow a more accurate theoretical simulation and provide a more detailed prediction of how thermal regulation is accomplished with regards to skin temperature distribution and heat loss for different parts of the body.

The results obtained and discussed in Section 6.2, for the thermal response of a clothed neonate, showed the relevance of including clothing properties when simulating heat loss and thermal regulation. It is recommended to develop a clothing specific simulation model; this will allow the researcher to ascertain calculating the type clothing that should best be worn in order to improve the clothing resistance theoretical simulation model developed in Section 3.2.4.

The three recommendations mentioned above will all help to improve the validity of the theoretical simulation model as developed in Section 3. The results gleaned from the improved model should then again be validated with information obtained from a clinical trial where the temperatures of neonates are measured. For the completion of the clinical trial it is recommended that the theoretical simulation model should be validated by the measured temperature of one body structure such as an arm or a leg, rather than using an average body temperature to validate the theoretical simulation model as discussed in Section 4.

It would be advantageous, based on the findings in Section 6.1 and Section 6.2, to develop a user friendly computer program enabling medical professionals to evaluate the effect of the thermal environment on the neonate's temperature regulation. This computer program can be used as a tool by medical professionals to predict the temperature outcome of a neonate if the environment is defined with respect to temperature, relative humidity and air velocity. This tool will help to provide the best environment, based on theory, rather than using the current suggestion or trial and error method.

Further, the user friendly computer program can be used in the education sector to aid the understanding of thermal regulation in humans as a result of the surrounding environment. This tool can provide an interactive educational platform.

With regards to the experimental mechanical lung model, discussed in Section 5, there are possibilities for improvement. It is recommended that a better theoretical understanding of the respiratory system mechanics is gained. This can be accomplished by the development of a more detailed experimental simulation model using computational fluid dynamics (CFD) to analyse the air flow during a respiratory cycle. The information gathered from these theoretical results can be used to design a more detailed experimental model that can incorporate the large suggested surface area of the lungs. This model may even be further developed in order to visually indicate how heat transfer takes place in the respiratory system with respect to convection and evaporation.

The relative success of the experimental respiratory model, discussed in Section 7.4, can be extended to the development of a 'dummy' used to illustrate the biomechanics of the respiratory system. This line of research can be extended to include the design of other organ systems such as the blood flow and circulation system. This tool can also provide an interactive educational platform.

9 REFERENCES

Adams, A. K., Neslon, R. A., Bell, E. F. & Eqoavil, C. A., 2000. Use of infrared thermographic calorimetry to determine energy expenditure in preterm infants. The American Journal of Clinical Nutrition, 71(4), pp. 969-977.

Adamsons, K. J., 1966. The Role of Thermal Factors in Fetal and Neonatal Life. The Pediatric Clinics of North America, 13(3), pp. 599-619.

Adamsons, K. & Towell, M. E., 1965. Thermal Homeostasis in the Fetus and Newborn. Anesthesiology, 26(4), pp. 531-548.

Asakura, H., 2004. Fetak and neonatal thermoregulation. Journal of Nippon Medical School, 71(6), pp. 360-370.

Blakemore, C. & Jennett, S., 2001. The Oxford Companion to the Body, London: s.n.

Bligh, J. & Johnson, K., 1973. Glossary of terms for thermal physiology. Journal of Applied Physiology, 35(6), pp. 941-961.

Bowman, F. H. & Balasubramaniam, T. A., 1976. A new technique utilising thermistor probes for the measurement of thermal properties of biomaterials. Cryobiology, Issue 13, pp. 572-580.

Cedar Lake Ventures, I., 2014. Weather Spark Beta. [Online] Available at: https://weatherspark.com/averages/29014/Cape-Town-Western-Cape-South-Africa
[Accessed 8 September 2014].

Cengel, Y. A. & Boles, M. A., 2007. Thermodynamics. In: An Engineering Approach. New York: McGraw-Hill, pp. 70-74.

Cengel, Y. A. & Ghajar, A. J., 2011. Heat and Mass Transfer: Fundamentals and Applications. 4th ed. New York: McGraw-Hill.

CES 2013 EDUPACK, n.d. Human Skin, s.l.: CES 2013 EDUPACK.

Chatson, K., 2003. Chapter 12: Temperature Control. In: J. P. Cloherty, A. Stark & E. Eichenwald, eds. Manual of Neonatal Care. s.l.:Lippincott Williams & Wilkins, pp. 143-146.

Cinar, N. & Filiz, T., 2006. Neonatal thermoregulation. Journal of Neonatal Nursing, 12(2), pp. 69-74.

Cohen, M. L., 1977. Measurement of the thermal properties of human skin. A review. The Journal of Investigative Dermatology, 69(3), pp. 333-338.

Communications, I. f. B. M., 2014. Skin Anatomy. [Online] Available at: http://en.wikipedia.org/wiki/Skin#mediaviewer/File:Blausen_0810_SkinAnatomy_01.png
[Accessed 25 June 2014].

Fenton, T. R., 2003. A new growth chart for preterm babies: Babson and Benda's chart updated with recent data and new format. BioMed Central, Volume 10, pp. 1-10.

Fiala, D., Lomas, K. J. & Stohrer, M., 1999. A computor model of human thermoregulation for a wide range of environmental conditions: the passive system. Modeling in Physiology, pp. 1957-1972.

Fox, S. I., 2009. Chapter 10: Blood and Circulation. In: Fundamentals of Human Physiology. Singapore: McGraw-Hill, pp. 240-241.

Fox, S. I., 2009. Chapter 12: Respiratory System. In: Fundamentals of Human Physiology. Singapore: McGraw-Hill, p. 299.

Geerligs, M., 2010. Skin layer mechanics, Eindhoven: Tegniese Universiteit Eindhoven.

Havenith, G., Holmer, I. & Parsons, K., 2002. Personal factors in thermal comfort assesment: clothing properties and metabolic heat production. Energy and Buildings, Volume 34, pp. 581-591.

Holmes, K. R., n.d. Thermal Properties, s.l.: s.n.

Kuramae, M., Maeda, T. & Yokoyama, S., 2007. A theoretical consideration of skin wettedness. Sapporo, Japan, Hokkaido University.

Le Rolle, V., Hernandez, A. & Carrault, G., 2008. A model of ventilation used to interperet newborn lamb respiratory signals, s.l.: s.n.

Linde, D. B., 2014. Incubator temperature management of new-born infants [Interview] (5 March 2014).

Lund, C. et al., 1999. Neonatal skin care: The scientific basis for practice. Neonatal Network, 18(4), pp. 15-27.

Merriam Webster, 2014. Merriam Webster. [Online] Available at: http://www.merriam-webster.com/ [Accessed 5 September 2014].

Pennes, H. H., 1998. Analysis of tissue and arterial blood temperatures in the resting forearm. Journal of applied physiology, 85(1), pp. 5-34.

Sharma, A., Ford, S. & Calvert, J., 2011. Adaptaion for life: a review of neonatal physiology. Anaesthesia and Intensive Care Medicine, 12(3), pp. 85-90.

Silverman, W. A., Fertig, J. W. & Berger, A. P., 1595. The influence of the thermal environment upon the survival of newly born premature infants. Pediatrics: Official Journal of the American Academy of Pediatrics, 22(5), pp. 876-886.

Sinclair, J. C., 1978. Temperature Regulation and Energy Metabolism. 1 ed. New York: Grune & Stratton, Inc..

Smith, P. J., 2014. Thermal regulation simulation of an infant [Interview] (February 2014).

Stoecker, W. F. & Jones, J. W., 1982. Chapter 4: Heating- and Cooling-Load Calculations. In: D. D. Heiberg & D. A. Damstra, eds. Refrigeration and Air Conditioning. Singapore: McGraw-Hill, pp. 59-63.

Swyer, P. R., 1978. Chapter 4: Heat loss after birth. In: H. C. Sinclair, ed. Temperature regulation and energy metabolism in the newborn. New York: Grune & Stratton, pp. 91-128.

Thomas, K., 1994. Thermoregulation in Neonates. Neonatal Network, 13(2), pp. 15-21.

Valvano, J. W., 2006. Bioheat Transfer, Austin: The University of Texas.

Waldron, S. & MacKinnon, R., 2007. Neonatal thermoregulation. Infant, 3(3), pp. 25-27.

Wheeler, D. S. et al., 2007. Assesment and Management of the Pediatric Airway, s.l.: Springer.

ADDENDUM A: REGRESSION ANALYSIS

The successful verification of the theoretical mathematical simulation model, allowed further analysis regarding simplification of the simulation model to a single equation that can be used to predict the outer skin layer temperature. The development of this equation will be explained in this addendum and will be completed by the use of regression analysis.

From the results explained in Section 6.1 it was seen that the variation of subject specific properties, such as weight and surface area, did not have a large influence on the resulting outer skin layer temperature. The most subject specific property was the metabolic heat producing capability, which is monitored by the core temperature. The environmental elements had a more significant effect on the resulting outer skin layer temperature; the room temperature and air velocity had the largest influence on the outer skin layer temperature, but relative humidity could not be ignored. From these results it was decided that the core temperature, room temperature, relative humidity and air velocity will be used for regression analysis.

Simulations were completed to calculate the outer skin layer temperature where one variable was changed in constant intervals while the other variables were held constant as indicated by Table A.1. This process was repeated for each of the particular variables as indicated in Table A.2, Table A.3 and Table A.4 respectively.

From the results for the simulated outer skin layer temperature it was seen that there is a constant linear increase in outer skin layer temperature as each of the variables were increased individually. This indicated the possibility of performing linear regression analysis in order to obtain a single equation, which uses all 4 variables to calculate the resulting outer skin layer temperature.

Table A.1: Results obtained from the developed simulation program for constant room temperature, relative humidity and air velocity and variable core temperature

T_{osl} (°C)	T_{core} (°C)	T_{room} (°C)	Φ_{room} (%)	V_{room} (m/s)
34.3302	36	25	0.6	0.1
34.419	36.1	25	0.6	0.1
34.5078	36.2	25	0.6	0.1
34.5967	36.3	25	0.6	0.1
34.6855	36.4	25	0.6	0.1
34.7743	36.5	25	0.6	0.1
34.8632	36.6	25	0.6	0.1
34.9519	36.7	25	0.6	0.1
35.0408	36.8	25	0.6	0.1

Table A.2: Results obtained from the developed simulation program for constant core temperature, relative humidity and air velocity and variable room temperature

T_{osl} (°C)	T_{core} (°C)	T_{room} (°C)	Φ_{room} (%)	V_{room} (m/s)
35.218	37	25	0.6	0.1
35.3394	37	26	0.6	0.1
35.4607	37	27	0.6	0.1
35.5822	37	28	0.6	0.1
35.7037	37	29	0.6	0.1
35.8254	37	30	0.6	0.1
35.9509	37	31	0.6	0.1
36.0761	37	32	0.6	0.1
36.2023	37	33	0.6	0.1

Table A.3: Results obtained from the developed simulation program for constant core temperature, room temperature and air velocity and variable relative humidity

T_{osl} (°C)	T_{core} (°C)	T_{room} (°C)	Φ_{room} (%)	V_{room} (m/s)
35.053	37	25	0.1	0.1
35.085	37	25	0.2	0.1
35.118	37	25	0.3	0.1
35.151	37	25	0.4	0.1
35.184	37	25	0.5	0.1
35.218	37	25	0.6	0.1
35.252	37	25	0.7	0.1
35.286	37	25	0.8	0.1
35.321	37	25	0.9	0.1

Table A.4: Results obtained from the developed simulation program for constant core temperature, room temperature and relative humidity and variable air velocity

T_{osl} (°C)	T_{core} (°C)	T_{room} (°C)	Φ_{room} (%)	V_{room} (m/s)
35.218	37	25	0.6	0.1
35.1509	37	25	0.6	0.2
35.0689	37	25	0.6	0.3
34.9803	37	25	0.6	0.4
34.8875	37	25	0.6	0.5
34.7936	37	25	0.6	0.6
34.6999	37	25	0.6	0.7
34.6072	37	25	0.6	0.8
34.5158	37	25	0.6	0.9
34.4259	37	25	0.6	1
34.3377	37	25	0.6	1.1
34.251	37	25	0.6	1.2
34.1659	37	25	0.6	1.3
34.0841	37	25	0.6	1.4
34.0025	37	25	0.6	1.5
33.9218	37	25	0.6	1.6
33.8425	37	25	0.6	1.7

A linear regression analysis was completed in order to determine how the outer skin layer temperature is affected by core temperature, room temperature, relative humidity and air velocity. These results are used to predict the outer skin layer temperature as a result of change in environmental conditions and core temperature. Linear regression was completed on the individual data as given in Table A.1, Table A.2, Table A.3 and Table A.4 respectively. Linear regression analysis provides coefficients a and b for equation (A.1), where X_n is the coefficient that was changed with constant intervals.

$$T_{osl} = a + bX_n \quad \text{(A.1)}$$

The coefficients obtained for individual evaluation of the core temperature, room temperature, relative humidity and air velocity is given in Table A.5, where the R^2 values are also presented. From the R^2 values given in Table A.5 it can be seen that the core temperature has the greatest effect on predicting the outer skin layer temperature.

Table A.5: Linear regression analysis coefficients for separate evaluated environmental influences

	a	**b**	**R^2**
Core Temperature	2.366	0.888	0.999999799
Room Temperature	32.085	0.125	0.999766877
Room Relative Humidity	35.017	0.337	0.999833648
Air Velocity	35.308	-0.864	0.999021899

In order to combine the effects of core temperature, room temperature, relative humidity and air velocity to develop one equation, combined linear regression analysis was completed. The equation obtained by performing combined linear regression can be described by (A.2). The values obtained for equation (A.2) are presented in Table A.6. Combined model was used with R^2=0.999794182.

$$T_{osl} = a + bX_1 + cX_2 + dX_3 + eX_4 \quad \text{(A.2)}$$

Table A.6: Linear regression analysis coefficients for combined environmental conditions

Variable	**Variable Description**	**Coefficient**	**Coefficient Value**
_	_	a	-0.830077751
X_1	Core Temperature	b	0.887466581
X_2	Room Temperature	c	0.123849736
X_3	Room Relative Humidity	d	0.335931159
X_4	Air Velocity	e	-0.861048844

ADDENDUM B: ETHICAL APPROVAL

B.1 Protocol Synopsis

Thermal regulation is a critical physiological function that is closely related to the transition and survival of the infant. An understanding of transitional events and the physiological adaptations that the new-born term-infants must make is essential to helping medical professionals provide an appropriate thermal-neutral-environment to help assist the infants in maintaining thermal stability.

This protocol is a summary of a bigger thesis project of which one objective involves measurements on healthy live term new-born infants. This protocol synopsis will be undertaken to gain information on neonates for further processing and comparisons to computer simulated information in order to build a neonatal temperature prediction model for future improvement of neonatal care.

B.1.1 Research Question or Hypothesis

According to literature reviews done in the respective field of thermal regulation, an infant gains heat by metabolism as well as using brown adipose fat tissue. This heat is lost to the environment through the skin via conduction, convection, radiation and evaporation and the respiratory heat loss must also be taken into account. This research poses the question to what relationship these different heat loss mechanisms interact with each other in a well-defined environment and how does it influence the neonate. The research will help to predict what the outcome of a neonate will be when the respective environment is defined.

B.1.2 Aims and Objectives

The hypothesis states that a term infant of 39 weeks gestation or older has an appropriate metabolism to thermally regulate the core body temperature if the environment conditions are in a respectable range. This will be tested with the developed computer simulation completed in the larger scope of this project. The validity of the developed simulation model will be established by comparison with information gleaned from the measurements stipulated in the summery of methodology.

The relationship of body to head heat loss will be evaluated, with respect to all heat transfer mechanisms. Further the respiratory heat loss will be weighed against the head and body heat loss with respect to convection and evaporation heat transfer mechanisms.

B.1.3 Summary of Methodology

The methodology of this protocol is based on the standard procedures of data collection at birth, with the exception that the room temperatures will also be

recorded for data simulation purposes. No invasive methods will be used to obtain the data needed for this protocol.

Data that will be recorded for this protocol includes delivery room temperature and relative humidity as well as the birth mother's (participant) temperature before the delivery procedure. The weight, length, head circumference and skin thickness of infant after delivery procedure must be recorded as well as the skin and axillary temperature.

Further the breathing rate, skin and axillary temperature of the infant for the first 4-6 hours of life with corresponding room air temperature and relative humidity will be recorded. This information is recorded every 10 minutes from the time that the neonate is placed in a bassinette in the post natal ward. Temperatures will be recorded in the post natal ward at every measurement interval as noted in the protocol data collection form. A change of room must be noted on the protocol data collection form (eg. Move from delivery room to post natal ward), it must also be indicated whether a measurement is taken whilst the mother is holding the neonate.

The length of the neonate will be measured using a sterilised plastic tape measure. The infant must be placed on a flat surface without a diaper to provide free movement of the legs. With the legs held flat the length is measured by placing the tape measure on the surface at the same position as the crown of the head and measuring the length to the ball of the foot. The measurement of the length is taken using the centimetre scale on the plastic tape measure. The accuracy is good enough for protocol data collection purposes.

The head circumference is measured using the same plastic tape measure. A paper tape is not used because it has too much variability in printed measurement intervals. A metal tape would also not be used due to the increased risk of lacerations on the neonate during the measurement procedure.

The neonatal waist/abdomen skinfold thickness measurement recorded using a skinfold calliper. A measurement will be taken by gently pulling the fold of skin out and holding it while applying the calliper. This measurement will be repeated three times for average results.

The breathing rate will be taken once every hour with all the other measurements, as this is not as important of a measurement and an average will be used in the calculations. This is done only to get an idea of the breathing rate for healthy term infants.

No pain or discomfort is associated with the measurements undertaken for the protocol data collection. The baby can be with the mother although this should be indicated in the protocol data form. Also feeding times can be indicated but will not have a great effect on the outcome of the research because the metabolic rate is not monitored or used as critical input to the simulation. Feeding times is non-

relevant to the research project. An example of the form that will be filled in for the duration of this protocol is attached at the end of this protocol Synopsis.

B.1.4 Description of Subject Population

A number of 15 boys and 15 girls will be needed for this medical research. The age must be 39 weeks gestation and older. Race or ethical group is of no relevance to the project. The infants must be regarded as "healthy" by the residing paediatrician or doctor doing the delivery. Healthy implies that that the infant is not growth restricted or small for gestational age. Method of birth is not of critical importance for this protocol synopsis. The infants that will be used for the research must be healthy enough to be placed in a bassinette after the delivery procedure.

B.1.5 Anticipated Risks

This protocol only requires standard information from the participants. The protocol involves no discomfort. If a participant, at any time, feels like removing their information, they are free to do so. Any participant case that presents complications of any sort will not partake in this protocol. This will in no way disadvantage the participant in any way.

B.1.6 Anticipated Benefits

There will be no direct medical or financial benefit accruing from participating in this project.

B.1.7 Ethical Considerations

Ethical considerations include the general consent form. This will be given to the mother prior to the anticipated delivery date. Any information recorded during this protocol will be treated as strictly confidential. The information will be recorded by a registered nurse residing at the relevant hospital. No participant's names will be recorded in the thesis or in any publications or journals. The participant's identity is not of importance to this protocol but rather the data recorded of the participant. The information gathered during tests will not be specific to any person but rather be related to averaged statistics.

B.2 Participant Information Leaflet and Consent Form

PARTICIPANT INFORMATION LEAFLET AND CONSENT FORM

TITLE OF THE RESEARCH PROJECT: Develop a simulation model of the human thermoregulatory response relative to the immediate environment; with the objective of gaining a better understanding of the thermo-control mechanisms of new-born infants in a thermally controlled environment.

REFERENCE NUMBER: S14/04/089
PRINCIPAL INVESTIGATOR: Alida Fanfoni, Masters Student
SUPERVISOR: Mr RT Dobson
ADDRESS: University of Stellenbosch, Department of Mechanical and Mechatronic engineering, Corner of Banghoek and Joubert Street, Stellenbosch, Room 308
CONTACT NUMBER: 072 536 7808 (alida.fanfoni@gmail.com) or 021 808 4208 (rtd@sun.ac.za)

You are being invited to take part in a research project. Please take some time to read the information presented here, which will explain the details of this project. Please ask the study staff or doctor any questions about any part of this project that you do not fully understand. It is very important that you are fully satisfied that you clearly understand what this research entails and how you could be involved. Also, your participation is **entirely voluntary** and you are free to decline to participate. If you say no, this will not affect you negatively in any way whatsoever. You are also free to withdraw from the study at any point, even if you do agree to take part.

This study has been approved by the **Health Research Ethics Committee at Stellenbosch University** and will be conducted according to the ethical guidelines and principles of the international Declaration of Helsinki, South African Guidelines for Good Clinical Practice and the Medical Research Council (MRC) Ethical Guidelines for Research.

What is this research study all about?

- The study will take place at the Tygerberg Hospital in the Western Cape Province. This will be the only site used for the study duration. A total of 30 babies will be needed to successfully obtain enough information for the proposed project. All the babies used for this research must be declared as healthy by the doctor.

- For this study some information will be recorded after the delivery procedure in the delivery room as well as in the post natal ward. This study is done to mainly collect temperature measurements of your baby and the temperature of the surrounding room. These measurements will be used in a computer

program done to better understand how the temperature of babies change during the first hours of life.

- The methods which are used to get these measurements are based on standard procedures for data collection at birth. After the delivery has taken place the length, head circumference, weight and skin fold thickness of your baby will be measured by the nurse on duty. This information will be filled out on a form. These measurements are usually taken when any baby is born, therefor they will not disturb the normal delivery procedure or cause any discomfort for you, the mother.

- A temperature measurement of the axillary temperature of the mother will be recorded before the delivery procedure. This will allow us to calculate/determine the temperature of your unborn baby. The axillary temperature is a temperature taken underneath your armpit or by measuring the temperature in your ear. This depends on the thermometer the nurse will use

- Immediately after birth the axillary and skin temperature of your baby will be measured with a standard thermometer. This will allow us to determine how *quickly your baby's temperature* drops after the delivery procedure.

- When you and your baby are moved to the post natal ward, after the delivery procedure, the temperature of your baby will be recorded every 10 minutes as well as the temperature of the post natal ward by the nurse. This will allow us *to see how your baby's temperature adapts with respect to the surrounding* room temperature. The breathing rate of your baby will also be recorded every 10 minutes.

- Further you, the mother, are allowed to handle your baby. This will not interfere with the temperature measurements, although the nurse should just note on the information form when a measurement was taken whilst you were holding the baby.

Why have you been invited to participate?

- Because your new-born baby is of the right age and in good health to meet the criteria set out for this study.

What will your responsibilities be?

- Your only responsibility is to provide us with consent so that data may be collected from your new-born baby. This information will be used on an anonymous basis.

Will you benefit from taking part in this research?

- There will be no direct medical or financial benefit accruing from participating in this project.

Are there any risks involved in your taking part in this research?

- This protocol only requires that you provide us with some standard information about yourself and your new-born baby. The protocol involves no discomfort. As a participant, if at any time, you feel like you wish to withdraw your information, then you are free to do so. Also if you or your baby present any complications of any sort then you will not be required to partake in this protocol. This will in no way disadvantage you in any way.

Who will have access to your medical records?

- Any information recorded during this protocol will be treated as strictly *confidential. Neither you nor your baby's names will be recorded in this thesis* or in any publications or journals. Your identity is not of importance to this study but rather the data being recorded. Only the investigator, doctor and supervisor will have access to the information.

Will you be paid to take part in this study and are there any costs involved?

No you will not be paid to take part in the study. There will be no costs involved for you, if you do take part.

Is there anything else that you should know or do?

- You should inform your family practitioner or usual doctor that you are taking part in a research study.

- You can contact **Prof Johan Smith**. at tel **021 938 4835** if you have any further queries or encounter any problems.

- You can contact the Health Research Ethics Committee at 021-938 9207 if you have any concerns or complaints that have not been adequately addressed by your study doctor.

- You will receive a copy of this participant information leaflet and consent form for your own records.

Declaration by participant

By signing below, I ……..……. agree to take part in a research study entitled "Develop a simulation model of the human thermoregulatory response relative to the immediate environment".

I declare that:

- I have read or had read to me this information and consent form and it is written in a language with which I am fluent and comfortable.
- I have had a chance to ask questions and all my questions have been adequately answered.
- I understand that taking part in this study is **voluntary** and I have not been pressurised to take part.
- I may choose to leave the study at any time and will not be penalised or prejudiced in any way.

Signed at (place) .....…..…….. on (date) …….. 2014.

……. ..... ……..

Signature of participant **Signature of witness**

Declaration by investigator

I (name) ……..…… declare that:

- I explained the information in this document to ……..
- I encouraged him/her to ask questions and took adequate time to answer them.
- I am satisfied that he/she adequately understands all aspects of the research, as discussed above
- I did/did not use a interpreter. (If a interpreter is used then the interpreter must sign the declaration below.

Signed at (place) .....…..…….. on (date) …….. 2014.

……. ..... ……..

Signature of participant **Signature of witness**

B.3 Ethical Approval Letter

UNIVERSITEIT·STELLENBOSCH·UNIVERSITY
jou kennisvennoot · your knowledge partner

Approved with Stipulations
Response to Modifications- (New Application)

18-Aug-2014
Fanfoni, Alida A

Ethics Reference #: S14/04/089

Title: **Develop a simulation of the human thermoregulatory response relative to the immediate environment; with the objective of gaining a better understandingof the thermo-control mechanisms of new-born infants in a thermally controlled environment.**

Dear Miss Alida Fanfoni,

The **Response to Modifications** - ***(New Application)*** received on **15-Jul-2014**, was reviewed by members of **Health Research Ethics Committee 2** via Expedited review procedures on **25-Jul-2014**.

Please note the following information about your approved research protocol:

Protocol Approval Period: **04-Aug-2014 -04-Aug-2015**

The Stipulations of your ethics approval are as follows:
1. Application form: no budget supplied.

2. In the informed consent form (ICF) it is stated that "The methods which are used to get these measurements are based on standard procedures for data collection at birth. After the delivery has taken place the length, head circumference, weight and skin fold thickness of your baby will be measured by the nurse on duty" . Skin fold thickness is not a standard observation in healthy newborns and the ICF should be changed to reflect this.

Please remember to use your **protocol number** (**S14/04/089**) on any documents or correspondence with the HREC concerning your research protocol.

Please note that the HREC has the prerogative and authority to ask further questions, seek additional information, require further modifications, or monitor the conduct of your research and the consent process.

After Ethical Review:
Please note a template of the progress report is obtainable on www.sun.ac.za/rds and should be submitted to the Committee before the year has expired. The Committee will then consider the continuation of the project for a further year (if necessary). Annually a number of projects may be selected randomly for an external audit.
Translation of the consent document to the language applicable to the study participants should be submitted.

Federal Wide Assurance Number: 00001372
Institutional Review Board (IRB) Number: IRB0005239

The Health Research Ethics Committee complies with the SA National Health Act No.61 2003 as it pertains to health research and the United States Code of Federal Regulations Title 45 Part 46. This committee abides by the ethical norms and principles for research, established by the Declaration of Helsinki, the South African Medical Research Council Guidelines as well as the Guidelines for Ethical Research: Principles Structures and Processes 2004 (Department of Health).

Provincial and City of Cape Town Approval

Please note that for research at a primary or secondary healthcare facility permission must still be obtained from the relevant authorities (Western Cape Department of Health and/or City Health) to conduct the research as stated in the protocol. Contact persons are Ms Claudette Abrahams at Western Cape Department of Health (healthres@pgwc.gov.za Tel: +27 21 483 9907) and Dr Helene Visser at City Health (Helene.Visser@capetown.gov.za Tel: +27 21 400 3981). Research that will be conducted at any tertiary academic institution requires approval from the relevant hospital manager. Ethics approval is required BEFORE approval can be obtained from these health authorities.

We wish you the best as you conduct your research.
For standard HREC forms and documents please visit: www.sun.ac.za/rds

If you have any questions or need further assistance, please contact the HREC office at 0219389207.

Included Documents:
Investigator declaration
HREC Checklist
Investigator CV
MOD_Protocol synopsis revised
MOD_Protocol
MOD_Investigator Declaration (Dobson)
Protocol
Supervisor CV
Synopsis
MOD_Consent form
Consent form
Supervisor declaration
MOD_Investigator declaration (Fanfoni)
Application form
MOD_Investigator CV (Smith)
MOD_Investigator CV (Fanfoni)
MOD_Investigator CV (Dobson)
MOD_Protocol information sheet

Sincerely,

Mertrude Davids
HREC Coordinator
Health Research Ethics Committee 2

Investigator Responsibilities

Protection of Human Research Participants

Some of the responsibilities investigators have when conducting research involving human participants are listed below:

1. Conducting the Research. You are responsible for making sure that the research is conducted according to the HREC approved research protocol. You are also responsible for the actions of all your co-investigators and research staff involved with this research.

2. Participant Enrolment. You may not recruit or enrol participants prior to the HREC approval date or after the expiration date of HREC approval. All recruitment materials for any form of media must be approved by the HREC prior to their use. If you need to recruit more participants than was noted in your HREC approval letter, you must submit an amendment requesting an increase in the number of participants.

3. Informed Consent. You are responsible for obtaining and documenting effective informed consent using **only** the HREC-approved consent documents, and for ensuring that no human participants are involved in research prior to obtaining their informed consent. Please give all participants copies of the signed informed consent documents. Keep the originals in your secured research files for at least fifteen (15) years.

4. Continuing Review. The HREC must review and approve all HREC-approved research protocols at intervals appropriate to the degree of risk but not less than once per year. There is **no grace period**. Prior to the date on which the HREC approval of the research expires, **it is your responsibility to submit the continuing review report in a timely fashion to ensure a lapse in HREC approval does not occur**. If HREC approval of your research lapses, you must stop new participant enrolment, and contact the HREC office immediately.

5. Amendments and Changes. If you wish to amend or change any aspect of your research (such as research design, interventions or procedures, number of participants, participant population, informed consent document, instruments, surveys or recruiting material), you must submit the amendment to the HREC for review using the current Amendment Form. You **may not initiate** any amendments or changes to your research without first obtaining written HREC review and approval. The **only exception** is when it is necessary to eliminate apparent immediate hazards to participants and the HREC should be immediately informed of this necessity.

6. Adverse or Unanticipated Events. Any serious adverse events, participant complaints, and all unanticipated problems that involve risks to participants or others, as well as any research-related injuries, occurring at this institution or at other performance sites must be reported to the HREC within **five (5) days** of discovery of the incident. You must also report any instances of serious or continuing problems, or non-compliance with the HRECs requirements for protecting human research participants. The only exception to this policy is that the death of a research participant must be reported in accordance with the Stellenbosch Universtiy Health Research Ethics Committee Standard Operating Procedures www.sun025.sun.ac.za/portal/page/portal/Health_Sciences/English/Centres%20and%20Institutions/Research_Development_Support/Ethics/Application_package All reportable events should be submitted to the HREC using the Serious Adverse Event Report Form.

7. Research Record Keeping. You must keep the following research-related records, at a minimum, in a secure location for a minimum of fifteen years: the HREC approved research protocol and all amendments; all informed consent documents; recruiting materials; continuing review reports; adverse or unanticipated events; and all correspondence from the HREC

8. Reports to the MCC and Sponsor. When you submit the required annual report to the MCC or you submit required reports to your sponsor, you must provide a copy of that report to the HREC. You may submit the report at the time of continuing HREC review.

9. Provision of Emergency Medical Care. When a physician provides emergency medical care to a participant without prior HREC review and approval, to the extent permitted by law, such activities will not be recognised as research nor will the data obtained by any such activities should it be used in support of research.

10. Final reports. When you have completed (no further participant enrolment, interactions, interventions or data analysis) or stopped work on your research, you must submit a Final Report to the HREC.

11. On-Site Evaluations, MCC Inspections, or Audits. If you are notified that your research will be reviewed or audited by the MCC, the sponsor, any other external agency or any internal group, you must inform the HREC immediately of the impending audit/evaluation.

ADDENDUM C: COST ANALYSIS

The information presented below consists of an outline of the costs incurred for the completion of this project. The costs consist of components and equipment used in the design and building of the experimental mechanical lung apparatus.

Material	Part Number/Dscription	Amount	Cost	Company
Electro-cylinder	EPCO-16-50-3P-A-ST-E+1.5E+C5DIOP	1	R 13,952.70	FESTO
Y-Fitting	QSY-6	1	R 60.07	FESTO
I-Fitting	QS-1/8-6	4	R 83.68	FESTO
tubing	PUN-6X1-BL		R 38.25	FESTO
			R 16,113.56	
Temperature Logger	testo 176-H1	1	R 6,767.27	RS COMPONENTS
Humidity/Temp Probe	12 mm @ R 2 735.79	4	R 10,943.16	RS COMPONENTS
			R 20,189.89	
Perspex tube	Thickness 5 mm		R 196.99	Maisy Plastics
Perspex tube	Thickness 5 mm		R 329.99	Maisy Plastics
Polyethelene sheet	Thickness 25 mm		R 156.06	Maisy Plastics
			R 778.67	
electric cylinder bracket	Thickness 2 mm	1	R 135.56	Fabrinox
main frame	Thickness 2 mm	1	R 106.14	Fabrinox
cylinder cap bracket	Thickness 2 mm	2	R 697.30	Fabrinox
controler bracket	Thickness 2 mm	1	R 94.98	Fabrinox
			R 1,178.74	
wick	Diameter 3 mm		R 3.05	Fabric Centre
Piping elbows		2	R 48.00	Loxton Irregation
PVC clear hose		1	R 34.00	Builders Warehouse
O-rings		4	R 31.50	BMG Somerset
			R 132.87	
Total			**R 38,393.72**	

ADDENDUM D: SAFETY REPORT FOR EXPERIMENTAL LUNG SETUP

This addendum provides the drafted safety report, which was signed and filed with the laboratory manager, as required by the department of mechanical and mechatronic engineering for experimental procedures and tests completed in laboratories.

Risk	**Design Impact**	**Operating Instructions**
Falling Objects	• The experimental setup can tilt due to an unstable working surface.	• Ensure that the experiment is set up on a fixed work bench that cannot be bumped. • Indicate safety area away from experiment to prevent people from getting close to operating area
Moving Equipment	• If moving equipment is mismanaged, harm can be done to the experimental set-up.	• Ensure that warning signs indicate that no touching of moving parts is allowed.
Sensitive Instruments	• If there is tampering with the instruments the data obtained may occur faulty without reason.	• Ensure that warning signs indicate no touching or operating of instruments are allowed.
Water Circulator Heat Element	• The heating element may injure a person touching it.	• Ensure that the heating element is fully submerged in the water and that a no touching sign is visible
High Temperatures	• Prevent people from accidentally accessing the warm area • Conduct warm water to area where there is restricted access	• Ensure that warning signs are in position
Electrical Shock	• If water is spilled from the water circulator bucket it may reach the electric power supply source and cause electrical shock.	• Ensure that electrical equipment are not placed near any immediate water sources as this might cause electric shock • Ensure that warning signs are in position • Ensure that emergency off switch is easily accessible

ADDENDUM E: CALIBRATION CERTIFICATE

The Testo Data Logger with temperature and relative humidity probes do not have a calibration procedure, but was supplied with the calibration certificate presented in Figure E.1.

testo

Kalibrier-Protokoll
Certificate of conformity • Protocole d'étalonnage
Protocollo di collaudo • Informe de calibración

Gerät / Module type / Modèle / Modelo:	**testo 176 H1**
Messbereich / Measuring range / Etendue de mesure / Rango de medición :	**Temperature: -20...70°C** **Humidity: 0...100%rF%rH**
Serien-Nr. / Serial no. / N°. de série / Número de serie:	**40801182** Date: 44347
Segmenttest / Display test / Test d'affichage / Test del visualizador:	☑ **OK**

Messwerte / Measured values / Valeurs mesurées / Valores medidos:		
Sollwert / Reference / Référence / Referencia:	Zulässige Toleranz / Permissible tolerance / Tolérance admise / Tolerancia permitida :	Istwert / Actual Value / Valeur réelle / Valor medido :
Temperature :		
25.0 °C	**±0.2 °C**	**25.0 °C**
Humidity:		
12.0 %rH	**±1 Digit**	**12.0 %rH**

J. Young
Prüfer / Inspector / Responsable / Verificador

Figure E.1: Calibration certificate for the temperature and humidity probes used with the Testo data logger

ADDENDUM F: FETAL INFANT GROWTH CHART

The Fetal-Infant Growth chart used in Section 6 in evaluation of the theoretical simulation model is given in Figure F.1 (Fenton, 2003).

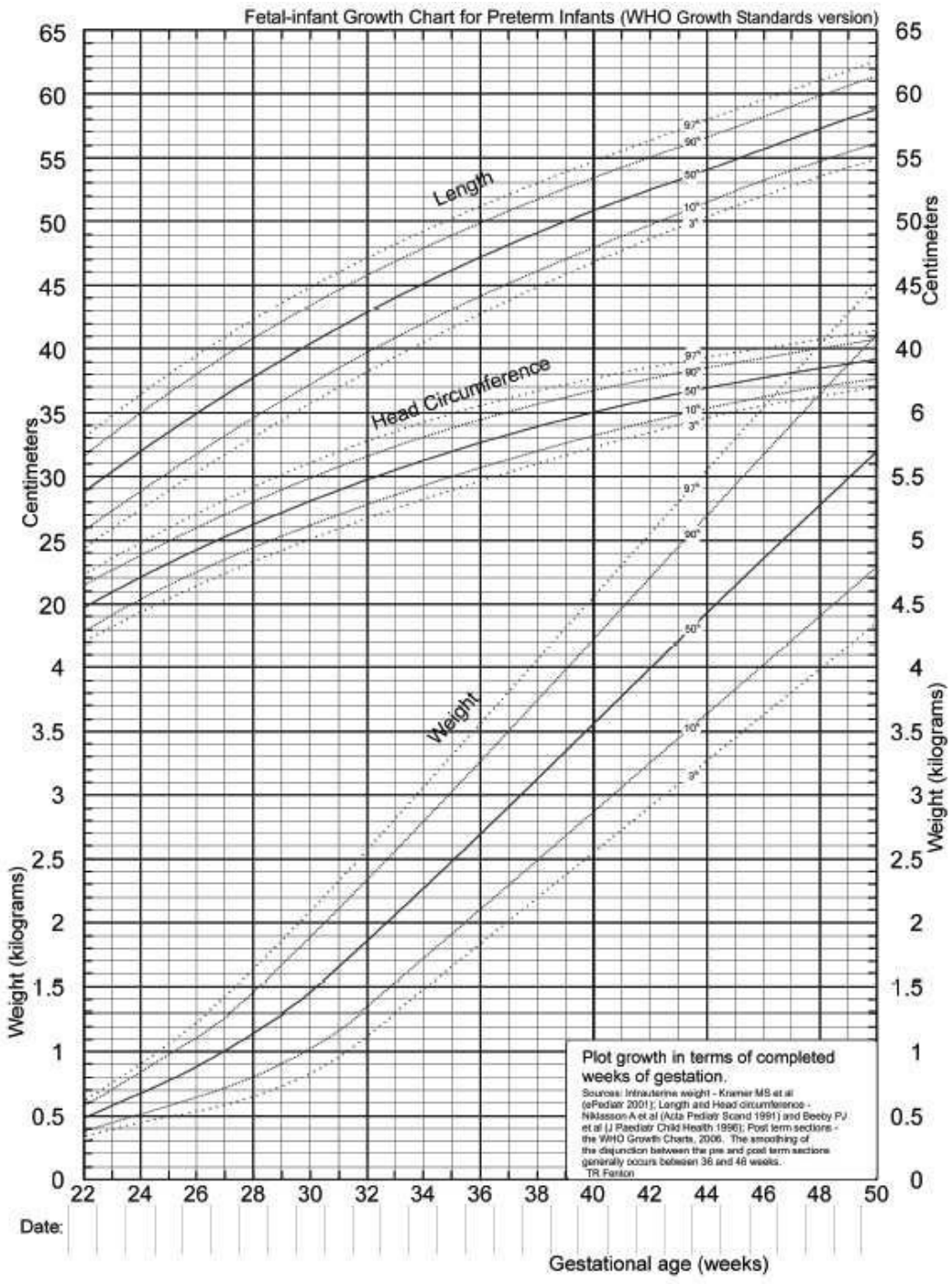

Figure F.1: Fetal-Infant Growth chart used during evaluation of the theoretical simulation model in Section 6